REPORT NO. DOT-TSC-OST-73-2

DESCRIPTION OF A GROUND FACILITY FOR CONDUCTING IONOSPHERIC SCINTILLATION MEASUREMENTS WITH THE ATS-5 SPACECRAFT

W.E. Brown, III
G.G. Haroules
W.I. Thompson, III

JULY 1974
INTERIM REPORT

Prepared by
U.S. DEPARTMENT OF TRANSPORTATION
OFFICE OF THE SECRETARY
Office of the Assistant Secretary for
Systems Development and Technology
Washington DC 20590

Technical Report Documentation Page

1. Report No.	2. Government Accession No.	3. Recipient's Catalog No.
DOT-TSC-OST-73-2		

4. Title and Subtitle	5. Report Date
DESCRIPTION OF A GROUND FACILITY FOR CONDUCTING IONOSPHERIC SCINTILLATION MEASUREMENTS WITH THE ATS-5 SPACECRAFT	July 1974
	6. Performing Organization Code
7. Author(s) W.E. Brown, III, G.G. Haroules, and W.I. Thompson, III	8. Performing Organization Report No. DOT-TSC-OST-73-2
9. Performing Organization Name and Address U.S. Department of Transportation Transportation Systems Center Kendall Square Cambridge MA 02142	10. Work Unit No. (TRAIS) OS334/R5003 11. Contract or Grant No.
12. Sponsoring Agency Name and Address U.S. Department of Transportation Office of the Secretary Office of the Assistant Secretary for Systems Development and Technology Washington DC 20590	13. Type of Report and Period Covered Interim Report June 1971-June 1972 14. Sponsoring Agency Code

15. Supplementary Notes

16. Abstract

Some of the capabilities of the DOT/TSC/Westford Propagation Facility located in Westford, Massachusetts (Latitude: 42.60° N; Longitude: 71.50° W) as they relate to ionospheric scintillation measurements will be described. In particular the following systems will be detailed:

a) A two-element coherent L-band interferometer comprised of 10-foot (3.05 m) diameter antennas spaced 130 feet (39.6 m) on an east-west baseline.

b) An L-band receiving system with a 10-foot (3.05 m) diameter antenna.

c) An L-band transmitting system with 225 watts of radio frequency power and a 15-foot (4.75 m) diameter antenna.

d) A VHF (135.6 MHz) receiving system with a 6 element Yagi array antenna.

e) An automatic data processing system which includes a minicomputer, a magnetic tape system and a disc system.

A detailed bibliography with over 400 citations is also included.

17. Key Words	18. Distribution Statement
Amplitude scintillation measurements, L-band (1550 MHz) ATS-5 geostationary satellite, Aeronautical Satellite (AEROSAT), Ionospheric scintillation, bibliography	DOCUMENT IS AVAILABLE TO THE PUBLIC THROUGH THE NATIONAL TECHNICAL INFORMATION SERVICE, SPRINGFIELD, VIRGINIA 22151.

19. Security Classif. (of this report)	20. Security Classif. (of this page)	21. No. of Pages	22. Price
Unclassified	Unclassified	166	

Form DOT F 1700.7 (8-72) Reproduction of completed page authorized

PREFACE

This report describes experimental apparatus for measuring ionospheric scintillation at the DOT/TSC/Westford Propagation Facility in Westford, Massachusetts. The measurements are made using the L-band (1550 MHz) transmissions from the NASA Applications Technology Satellite 5 (ATS-5) which is in a geostationary orbit. Details of equipment configurations and data analysis procedures are given.

The authors would like to acknowledge the support of and the constructive criticism offered by Mr. Richard Beam of the Office of the Assistant Secretary for Systems Development and Technology, DOT and Mr. Joseph Gutwein of the Transportation Systems Center, Cambridge, Massachusetts.

Specifically the authors would like to acknowledge Messrs Herbert Whitney, John Mullen and Richard Allen of the Radio Astronomy Branch, Ionospheric Physics Laboratory of the Air Force Cambridge Research Laboratories for their critique of the manuscript of this report.

In addition, we would like to acknowledge Mr. Fredric Kissel of the ATS Operations Control Center at NASA Goddard Space Flight Center for numerous discussions and helpful comments.

TABLE OF CONTENTS

LIST OF ILLUSTRATIONS

LIST OF ILLUSTRATIONS (CONT.)

LIST OF ILLUSTRATIONS (CONT.)

LIST OF ILLUSTRATIONS (CONT.)

LIST OF TABLES

LIST OF ABBREIVATIONS

AC	alternating currents
ADCF	automatic data collection facility
ADPE	automatic data processing equipment
AEROSAT	aeronautical satellite
AFAL	Air Force Avionics Laboratory
AFCRL	Air Force Cambridge Research Laboratories
AGARD	Advisory Group for Aerospace Research and Development
AGC	automatic gain control
ALSEP	Apollo Lunar Surface Experiment Package
AM	amplitude modulation
AMP	amplifier
ASCII	American Standard Code for Information Interchange
ASTRA	Application of Space Techniques Relating to Aeration
ATS	Applications Technology Satellite
ATSOCC	ATS Operations Control Center
A/D	analog-to-digital
BPF	bandpass filter
BW	bandwidth
calb.	calibration
cdf	cumulative distribution function
cm	centimeter
CIRC	circulator
COMSAT	Communications Satellite Corporation
COSPAR	COmmittee on SPAce Research
CPU	central processing unit
CRT	cathode ray tube
CW	continuous wave
C-band	the portion of the radio frequency spectrum between 4,000 MHz and 8,000 MHz (Wavelengths between 7.5 and 3.75 cm)
d	a distance

LIST OF ABBREVIATIONS (CONTINUED)

dB	decibel
dBm	power relative to a milliwatt expressed in dB
DC	direct current
DEI	Defense Electroncis Industries
DET	detector
DISC	discriminator
DIV	divider
div.	division
DOC	U.S. Department of Commerce
DOT	U.S. Department of Transportation
D/A	digital-to-analog
E	East
EDP	electronic data processing
EIRP	equivalent isotropic radiated power
EOT	end of transmission
ESSA	Environmental Science Services Administration
f	frequency
f_c	center frequency
f_o	fundamental frequency
F	radius of a Fresnel zone
ft.	foot
FFT	Fast Fourier Transformation
FLT	filter
FM	frequency modulation
FT	frequency translation mode
F2	a region of the ionosphere
Geograph.	geographic coordinates
Geomag.	geomagnetic coordinates
GE	General Electric Co.
GHz	Gigahertz = 10^9 Hz
GMT	Greenwich Mean Time
hr	hour
h_m	height of peak electron concentration
Hz	Hertz = 1 cycle per second
HP	Hewlett-Packard Co.

LIST OF ABBREVIATIONS (CONTINUED)

HR	hour
in.	inch
ICAO	International Civil Aviation Organization
IF	intermediate frequency
Intelsat	names of satellites sponsored by INTELSAT
INTELSAT	International Telecommunication Satellite Consortium
IR	infrared
ITOS	Improved TIROS Operational Satellite (ESSA)
I/O	input-output
JSSG	Joint Satellite Study Group
km	kilometer
KHz	kilohertz = 10^3 Hz
k_o	a constant
kW	kilowatt = 10^3 W
LES-6	Lincoln Experimental Satellite-6
LHCP	left-hand circular polarization
LIM	limiter
LO	local oscillator
LPF	low pass filter
LT	local time
L-band	the portion of the radio frequency spectrum between 1,000 MHz and 2,000 MHz (wavelengths between 30 and 15 cm)
m	meter
min/Min	minute
ms	millisecond
mA	milliamp = 10^{-3} ampere
mW	milliwatt = 10^{-3} W
MA	multiple access mode
MHz	megahertz = 10^6 Hz
MIT	Massachusetts Institute of Technology
MIX	mixer

LIST OF ABBREVIATIONS (CONTINUED)

MMW	millimeter wave
MO	master oscillator
MT	magnetic tape
ns	nanosecond = 10^{-9}s
N_m	peak electron concentration
N	north, electron number density
NASA	National Aeronautics and Space Administration
NATO	North Atlantic Treaty Organization
NB	narrow-band
NBFT	narrow-band frequency translation mode
NBS	National Bureau of Standards
NELC	Naval Electronics Laboratory Center
NF	noise figure
NIMBUS	a NASA meteorological satellite series
NOAA	National Oceanic and Atmospheric Administration
NPD	noise power density
OGO	Orbiting Geophysical Observatory
OMNI	omnidirectional
PCM	pulse-code modulation
PFM	pulse-frequency modulation
PLACE	Position Location and Aircraft Communications Experiment
PM	phase modulation
PREAMP	preamplifier
PREDET	predetection
PWR	power
$\vec{r}$	a distance vector
rms	root-mean-square
rpm	revolutions per minute
R	a height to the ionosphere from the earth's surface
RC	resistance, capacitance
RCVE	receive
RF	radio frequency

LIST OF ABBREVIATIONS (CONTINUED)

RFI	radio frequency interference
RHCP	right-hand circular polarization
RPTR	repeater
s	second, distance
S	south
SAMSO	Space & Missile System Organization (USAF)
SATCOM	Satellite Communications Agency (Army)
SHF band	Super-high frequencies. The portion of the radio frequency spectrum between 3 GHz and 30 GHz (wavelength between 10 and 1 cm)
S.I.	scintillation index
SIG	signal
SSB	single sideband
STADAN	Space Tracking and Data Acquisition Network
SUM	summer
SW	switch
SYNC	sychronization
S/C	spacecraft
S/N	signal-to-noise ratio
TACSAT	Tactical Satellite
TC	time constant
TSC	Transportation Systems Center
TV	television
TWT	traveling wave tube
TWTA	traveling wave tube amplifier
UT	universal time
USAF	United States Air Force
VCO	voltage controlled oscillator
VCXO	voltage controlled crystal oscillator
VDC	direct current voltage
VHF	Very high frequencies. The portion of the radio frequency spectrum between 30 and 300 MHz (wavelengths between 10 and 1 m)
VLBI	very long baseline interferometry
VSWR	voltage standing-wave ratio

LIST OF ABBREVIATIONS (CONTINUED)

W	watt, west
WBFT	wide-band frequency translation mode
x2,x3	multiplier (by 2, by 3, etc.)
XMIT	transmit
XTAL	crystal
α	constant = 80.5
Δ	a differential
ΔP	phase path difference
ε	dielectric constant
η	scintillation index
λ	wavelength
μ	refractive index
μs	microsecond = 10^{-6}s
σ_D	standard deviation
ψ	wave function
<>	average

1. INTRODUCTION

The ground facility described herein was established for conducting ionospheric scintillation measurements with the Applications Technology Satellite (ATS) 5 spacecraft. The objective of the experimental program being conducted at this facility is to enlarge upon the electromagnetic wave propagation data existing in the L-band (1,000 - 2,000 MHz) region of the radio spectrum. Specifically, this work is being done in support of the proposed AERO-nautical SATellite (AEROSAT) system which will rely heavily on the use of the radio spectrum around 1550 MHz (electromagnetic wavelength of 19.4 cm) for transmission of voice and digital data.

Ionospheric scintillation is produced by the presence of small-scale irregularities within the ionosphere which introduce random phase changes in the wave front of a traversing electromagnetic wave. As a result, the phase of a radio wave emitted by a geostationary satellite transmitter will not be constant over the ground but will form an irregular pattern. This pattern will, in general, appear to move because of ionospheric winds moving the irregularities and also because of the motion of the mobile receiving platform. The result is that the phase and amplitude of the received signal will appear to fluctuate or scintillate.

Amplitude scintillations caused by ionospheric irregularities have been recorded at electromagnetic frequencies ranging from 20 MHz (15 m) to 6 GHz (5 cm). (Rufenach, 1971A,B; Skinner, et al., 1971 Taur, 1973). Many of these measurements will be described in the following sections along with some relevant theoretical considerations.

2. REVIEW OF IONOSPHERIC SCINTILLATION THEORY*

Electron density irregularities have been discovered to exist throughout the ionosphere, from the D region (approximately 70 km altitude) to the magnetosphere (approximately 1500 km altitude) and beyond (Al'pert et al. 1971; Chivers and Davies, 1962).

When a wave propagates through the ionosphere, its amplitude and phase are sensitive to changes in the refractive index of the medium. Since electron density irregularities near the peak of the F region present largest percentage change in refractive index, a reasonably simplified model can be assumed in connection with space communication problems (Liu and Yeh, 1970). This is the problem of propagation through a slab of irregularities situated at the F region peak. Rough values of several pertinent F region parameters are presented in Table 2-1.

TABLE 2-1. ROUGH VALUES OF F REGION PARAMETERS (ADAPTED FROM RISHBETH AND GARRIOTT, 1969, p. 171)

Quality and Symbol	Sunspot Minimum	Sunspot Maximum	Units(c.g.s.)	Units(m.k.s.)
F2 layer (noon)				
Züruch sunspot number	0	180	-	-
Peak electron concentration N_m	4	16	10^5 cm^{-3}	10^{11} m^{-3}
Height of peak h_m	240	320	km	km
Total electron content $\int N\,dh$	2	7	10^{13} cm^{-2}	10^{17} m^{-2}
F2 layer (midnight)				
Peak electron concentration N_m	1	5	10^5 cm^{-3}	10^{11} m^{-3}
Height of peak h_m	320	380	km	km

*A very complete report on the theory of ionsphoric scintillation by Wernick et al. (1973) was received after this report was finalized.

The fading of radio waves was first detected by Hey, Parsons and Phillips (1946). Since they used radio stars as sources, it was thought at the time that the scintillation indicated the possibility that the sources were variable in power output. Subsequent spaced-receiver experiments demonstrated that the cause was in the ionosphere (Smith, 1950; Little and Lovell, 1950). Reviews of the early radio star studies have been prepared by Nupen (1963) and Meyer-Arendt and Emmanuel (1965).

To properly interpret the scintillation, it is desirable to study the behavior of waves in a medium with irregularities. Such a theoretical study depends on our ability to solve the stochastic wave equation of the form

$$\nabla^2\psi + k_o^2 \left[\varepsilon(\vec{r},t)/\varepsilon_o\right]\psi = 0 \qquad (2\text{-}1)$$

or some other perhaps more complex wave equations (Yeh and Liu, 1972A,B). The dielectric constant ε of Equation (2-1) is a random process and enters as a coefficient of the equation. Since we do not know how to solve exactly the stochastic equation (2-1), some approximate methods must be used. The most popular approximation is the single-scatter theory, also known as the Born approximation. Under this approximation, the dielectric constant is written in the form

$$\varepsilon(\vec{r}) = \langle\varepsilon\rangle + \Delta\varepsilon(\vec{r}) \ , \qquad (2\text{-}2)$$

and the stochastic part $\Delta\varepsilon$ is assumed to be small in comparison with the average part $\langle\varepsilon\rangle$, i.e., a weakly random medium. Many authors have worked on problems of this nature with differences in geometry, the type of wave, the statistical properties of irregularities, etc. (e.g. Chernov, 1961; Tatarski, 1961; Yeh, 1962; de Wolf, 1965; Budden, 1965; Liu, 1966; Salpeter, 1967; Ichimaru, 1969; Lovelace, 1970).

These authors considered amplitude, phase, autocorrelations of amplitude and phase and cross correlations of amplitude and phase. A comprehensive theoretical review of the subject has been

recently published by Barabanenkov et al. (1971), which includes 542 references.

In considering the fluctuations imposed on a wave in its passage through an irregular medium, there are two possible approaches. First is the diffraction method in which the medium is considered to be equivalent to a thin diffracting screen. Because the absorption in the ionosphere is negligible for the frequencies normally used for the observations of scintillations, this screen will produce across the emerging wave front variations of phase only, with no variations of amplitude. Figure 2-1 illustrates such a case where a plane wave is incident on a relatively thin slab in which the optical, or phase, thickness is a function of position and in which no power is absorbed from the wave. For simplicity, the slab thickness is shown to vary periodically, but this is not necessary to the argument. Immediately below the slab, the surface of constant phase, that is, the wave front, will be corrugated because the time delay in passing through the slab varies along the wave front. The amplitude distribution along the wave front will, however, still be uniform because no power has been absorbed.

As shown in Figure 2-1, different parts of the wave front are traveling in different directions. Hence, as we move away from the screen, various parts of the wave will interfere with each other, and there will be a redistribution of amplitude. The amplitude will have maxima where the various wavelets reinforce and minima where they tend to interfere destructively. Therefore, as the wave front leaves the screen, the relative phases of the various wavelets will change owing to the different directions of propagation. The amplitude variations along the entire wave front will increase in magnitude as the distance from the screen increases. It has been shown by Hewish (1951) that the amplitude variation across the wave front becomes fully developed at a distance R from the screen where an average ionospheric irregularity occupies the size of the first Fresnel zone. The Fresnel zone is shown in Figure 2-2 and the radius F is given by

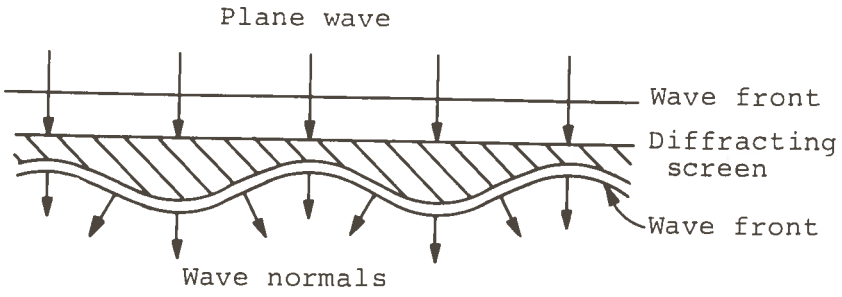

Figure 2-1. Passage of a Plane Radio Wave Through a Corrugated Phase Changing Screen. On Emerging from the Screen, the Wave Front is Corrugated.

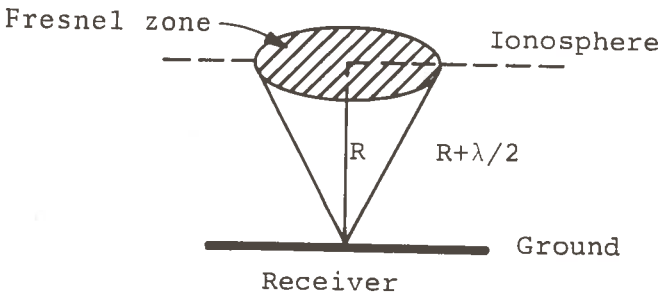

Figure 2-2. The Fresnel Zone in the Ionosphere as Seen from the Ground.

$$F = \left(\left(R+\frac{\lambda}{2}\right)^2 - R^2\right)^{1/2} \approx \sqrt{R\lambda} \quad . \qquad (2\text{-}3)$$

Here R is the height of the ionospheric irregularity and λ is the wavelength of the radiation. Figure 2-3 is a plot of the Fresnel diameter versus electromagnetic frequency for several assumed layer heights.*

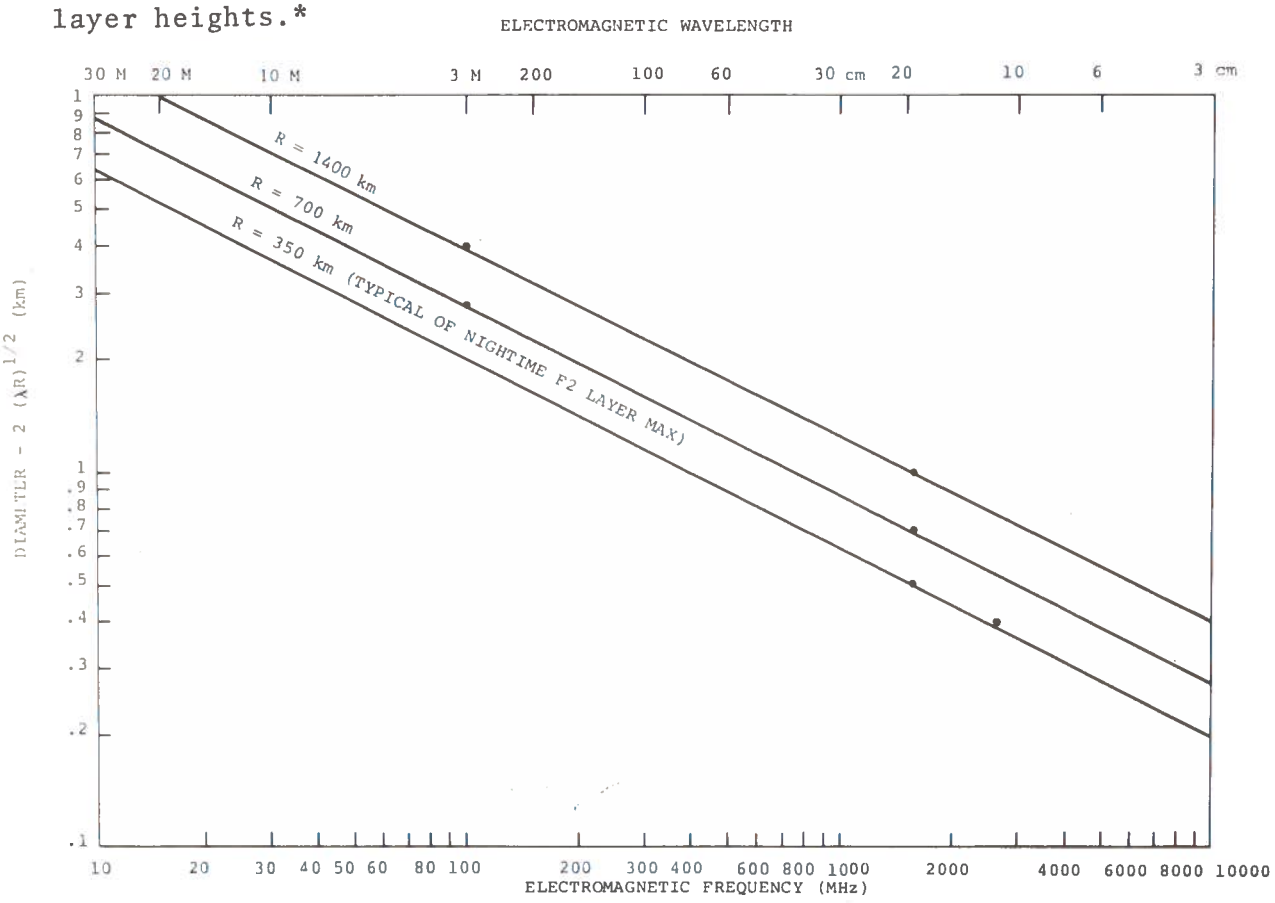

Figure 2-3. Graph of Fresnel Diameter (Twice the Fresnel Radius) Versus Electromagnetic Frequency for Several Layer Heights

The alternative approach is called the scattering method and the wave at the observing point is considered to be the sum of the unscattered wave and the waves scattered by the irregularities in the medium. This type of theory has been well advanced by Booker

*A complete analysis of this problem is inappropriate here and the interested reader is referred to the paper by Ratcliffe (1956).

and Gordon (1950), Wheelon (1959), Muchmore and Wheelon (1963), and Lawrence, Little and Chivers (1964). It is reasonably simple so long as the scattering is weak*, but becomes complicated when the scattering is strong. Both methods are equally valid and give identical results, as has been shown for a simple case by Booker (1958).

According to Booker, essentially two processes can be distinguished: (1) Single scattering is due to a thin layer of irregularities in the atmosphere. In this case, the scale of the irregularities at ground level is a projection of the irregularity sturcture in the atmosphere. (2) Multiple scattering occurs when the mean-square phase deviation is greater than one radian. In this case the correlation distance on the ground is less than the scale of the atmospheric irregularities by a factor equal in magnitude to the average phase change in radians.

The theories of ionospheric scintillation have been used to deduce various parameters connected with ionospheric irregularities. An example presented below estimates the magnitude of the ionospheric electron density variations required to produce scintillations. We shall compute the fractional variation of phase path ΔP that will result in phase differences of the order of one radian (weak scattering) in waves emerging at places separated by the Fresnel zone radius $F \approx \sqrt{R\lambda}$.

The differences in phase path without and with the ionization is given by

$$\Delta P = \int ds - \int \mu ds \qquad (2\text{-}4)$$

where μ is the refractive index and s represents a path.

For very high frequencies, on which the effect of the magnetic field is small, the refractive index is given by

*The scattering is considered weak when the scintillation amplitude is small compared to the unscattered amplitude of when the phase fluctuation over twice the Fresnel radius is much less than 1 radian (57.3°).

$$\mu \approx \left(1 - \frac{\alpha N}{f^2}\right)^{1/2} \qquad (2\text{-}5)$$

where $\alpha = 80.5$ if N (the electron density) is expressed in electrons per cubic meter and f is the electromagnetic wave frequency expressed in Hz. Equation (2-5) can be expanded to

$$\mu \approx 1 - \frac{\alpha N}{2f^2} \quad . \qquad (2\text{-}6)$$

Thus

$$\Delta P = \int ds - \int \left(1 - \frac{\alpha N}{2f^2}\right) ds \qquad (2\text{-}7)$$

or

$$\Delta P = - \frac{\alpha}{2f^2} \int N \, ds. \qquad (2\text{-}8)$$

Taking typical values of $\int N \, ds = 10^{17}$ m^{-2} column (Table 2-1) and $f = 4.0 \times 10^7$ Hz (40 MHz or 7.5 m), we get $P \approx 2.5$ km, which corresponds to about 2000 radians at a frequency of 40 MHz. For a distance R of 350 km* from screen to observer, the Fresnel zone radius $\sqrt{R\lambda}$ is 1.62 km (Figure 2-3). Since a relative change of about 1 radian in phase path over a Fresnel zone is required for strong scintillations, it follows that there must be differences in electron density of about 1 part in 2000 over distances of about 1.6 km. Since strong scintillations are observed at 40 MHz, it is concluded that such variations in electron density do, in fact, exist.

For other examples, Hewish (1952) attempted to get the height of ionospheric irregularities by comparing phase and amplitude scintillations, Spencer (1955) measured the size of irregularities, McClure and Swenson (1964) estimated the thickness of the region

*Published observations all suggest that the scattering layer is located, on the average, at about 350 km altitude (Fremouw and Rino, 1971; See also Table 2-1).

of irregularities and Rufenach (1971, 1972A,B) used spectral analysis of amplitude scintillations to show a power-law variation in wavenumber for the power spectrum of irregularities.

The experimental scintillation studies have also been concerned with obtaining a synoptic picture on a world-wide scale. The results have been reviewed periodically as more and more data become available (e.g. Booker, 1958; Briggs, 1958; Lawrence, et al., 1964; Yeh and Swenson, 1964; Newman, 1966; Special Issue, 1966; Aarons, et al., 1969, 1971, 1972; Fremouw and Bates, 1971; Hartmann, 1971). On a global basis it has been found that there are essentially three zones of intense scintillations: the equatorial zone ($\pm$ 20° N-S) and the northern and southern auroral zones.

Prediction of phase and amplitude scintillation has been modeled by Fremouw and Bates (1971), Fremouw and Rino (1971) and Smith (1967A). Fremouw and Rino utilize the model of Briggs and Parkin (1963) and the empirical model of Fremouw and Bates to estimate the amplitude distribution of signal level for VHF and UHF signals. Smith modeled the phase distortion impressed on the radio wave signal in the range 1 - 15 GHz (2-30 cm) by the earth's atmosphere. One of his results is presented in Figure 3-1.

The radio frequency dependence of the magnitudes of the scintillations is helpful in determining their cause. For instance, if turbulence in the troposphere is responsible, then the scintillation magnitude should be nearly independent of frequency (Yokoi, Yamada and Satoh, 1970B). On the other hand, if turbulence in a plasma is the cause, then the magnitudes should scale in the range between frequency independence and variations proportional to the wavelength squared. The latter relationship should hold for weak scattering in a "nearby" thin plasma layer (Salpeter, 1967; Lovelace, 1970). Equation (2-8) which was derived under these conditions does indeed predict an inverse frequency squared relationship. As the scintillation becomes stronger, the magnitude should approach frequency independence. Another factor is irregularity size. Fremouw and Rino found that during the course of their modeling that the scale-size of the irregularities was

found to be more important than anticipated. It was particularly so for predicting frequency dependence of scintillation (Fremouw and Rino, 1971, p. 14).

The present understanding of the physics associated with ionospheric scintillation is far from complete. For example, the conventional diffraction model proposed by Hewish usually considers weak scattering and assumes a Gaussian spectrum for the irregularities. This spectrum appears to given reasonable results for weak scattering over a limited radio freuqnecy range but seriously underestimates the scintillation level when extrapolated to much higher frequencies. The OGO-6 in-situ measurements and spectral analysis of scintillation observations (Rufenach, 1972A) suggest that on many occasions the spectrum of the irregularities is power-law with an index near 2. The power-law spectrum does not decrease with smaller irregularity sizes as rapidly as the Gaussian spectrum. This means that the Gaussian spectrum will give smaller scintillation levels than the power-law spectrum. In fact, Rufenach (1972B) states that the Gaussian spectrum will not explain both VHF and SHF radio frequency scintillation observations.

The Gaussian model usually assumes weak scattering and uses a scale size deduced from either spaced site observations, the reciprocal scintillation spectral width, or some other means to describe the irregularities. It has been shown for weak scattering that the scale size is approximately proportional to $\lambda^{1/2}$ where λ is the radio wavelength (See Equation 2-3 and Eq. 17 of Lovelace, Salpeter and Sharp, 1970). Therefore, the scale size changes slowly with radio frequency. However, if the radio frequency changes by a significant amount, say two orders of magnitude or for the sake of discussion from 15 MHz (20 m) to 1.5 GHz (20 cm), then the scale size changes by one order of magnitude assuming, of course, that the weak scattering approximation is valid over the entire range. One intuitive way to consider this scale size dependence, which some workers have assumed as constant, is to consider two receiving sites, separated by a distance d. The scintillation will be sensitive to structure sizes smaller than about

Twice the Fresnel radius (the Fresnel diameter as plotted in Figure 2-3). This works out to be 5 km assuming F-layer scattering (350 km) at 15 MHz (20 m) and a near vertical path. Therefore, the scintillations will be correlated for d < 5 km. However, for an observing frequency of 1.5 GHz (20 cm) twice the Fresnel radius is about 500 m (from Figure 2-3) and the scintillations will be correlated for d < 500 m. These two radio frequency observations give significantly different scale sizes from spaced site observations assuming, of course, that the scattering is weak at both frequencies (Golden, 1970A).

The problem of developing a realistic theory of radio scattering is more than a significant effort. The relationship between the irregularities and the scintillation and phase fluctuations are fairly well defined for weak scattering. The phase coherence bandwidth for weak scattering can be derived using standard techniques. However, the amplitude fluctuations, phase fluctuations and phase coherence bandwidth relationships for strong scattering are difficult to handle and probably can be derived only for special cases using numerical methods. However, even if all the above models were available, realistic input parameters for the irregularities would be required for equatorial through polar latitudes.

3. REVIEW OF SCINTILLATION DATA

3.1 BACKGROUND

The VHF frequency of 136 MHz is heavily used in the satellite telemetry band. There exists as a result an abundance of signal amplitude data from earth satellites including synchronous satellites. However, most of the amplitude data is in the form of scintillation indexes. Some of this scintillation index data has been converted to cumulative amplitude probability distributions and has been made available in the literature.

This literature includes Aarons, Whitney and Allen (1971), Fremouw and Bates (1971) and Whitney, Aarons and Seemanns (1971). Most of the available data is in the form of amplitude distributions, seasonal dependences and fade depth-duration information. There is very little information on phase effects in transatmospheric propagation except for the work of Porcello and Hughes (1968) and Smith (1967A; See Figure 3-1).

Knowledge at 1550 MHz has been reported by several researchers: Golden (1970A,B,C), Maynard and Selin (1971), Wernlein (1970), Kissel (1970) and Crampton and Sessions (1971). The most comprehensive measurement program reported to date is the work of Crampton and Sessions.

Observations were taken at a large number of sites throughout the world. Table 3-1 lists the sites where scintillation observations have been made. Also included in the table are such items as the geographic and geomagnetic coordinates as well as the names of the researchers involved in the work. Appendix A defines several coordinate systems used in Table 3-1. A definition of scintillation indexes is given in Appendix C.

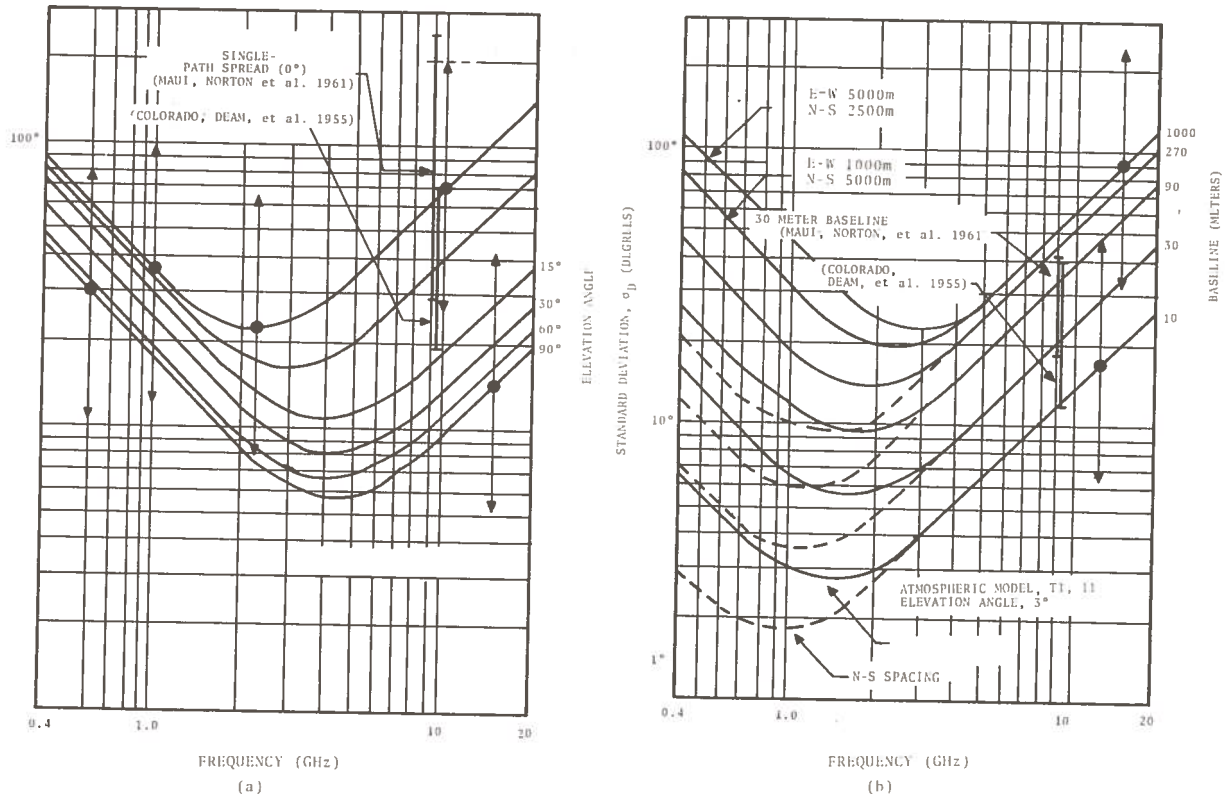

Courtesy: Holden-Day, Inc., 500 Sansome Street, San Francisco CA 94111

Figure 3-1. (a) Phasefront distortion versus frequency and elevation angle computed by Smith, 1967A.
(b) Phasefront distortion versus frequency and baseline spacing. Curves are average values, arrows show approximate spreads. Elevation angle of 3°.

TABLE 3-1 LOCATIONS WHERE IONOSPHERIC SCINTILLATIONS HAVE BEEN OR ARE BEING MEASURED -- EMPHASIS ON 136 MHz AND 1550 MHz

Location	Investigator(s)	Comments
Huancayo, Peru Geomag: 02°N; 06°W Geograp: 13.5°S; 75°W	Mueller, 1970A, B Whitney, Aarons et al 1971	ATS-3; Scintillation Index(S.I.) 20% - 90%
Lima, Peru (Ancón, Peru) Geomag: 0°; 8°W Geograp: 11.6°S; 77.1W	Wernlein, 1970 Crampton & Sessions, 1971; Pomalaza, et al 1970	Fig. 9 Geophysical Institute of Peru
Accra, Ghana Geomag: 10°N; Geograp: 0°; 6°N	Allen, 1969 Koster, 1968B	
Quito, Ecuador Geomag: 11N; Geograp: 0°; 78°W	Golden, 1970B	136.47 MHz; 1550 MHz
Hamilton, Mass. USA Geomag: 53.5°N Geograp: 43°N; 71°W	Mullen, et al 1969 NASA, 1970B	Sagamore Hill Radio Observatory
Schenectady, NY, USA Geomag: 54°N Geograp: 42°50'53"N 74°05'15"W	General Electric, 1971A, C	General Electric Radio & Optical Observatory
Westford, Mass. USA Geomag: 53°N; 2°W Geograp: 42.5°N 71.3°W	Brown, Haroules and Thompson, 1973, 1974	DOT/TSC/Westford Propagation Facility; using ATS-5
Thule, Greenland Geomag: 35.8°W; 89°N Geograp: 77°N; 69°W	Aarons, Whitney and Allen, 1971	
Narssarssuaq, Greenland Geomag: 36.6°W; 71°N Geograp: 61.2°N; 45°W	Aarons, Whitney and Allen, 1971	20° elevation angle to ATS-3
Gilmore Creek, Alaska, USA Geomag: 63°N; 270°W Geograp: 65°N; 147.5°W	Pope and Fritz, 1970	NOAA Control and Data Acquisition Station (20 km NE of College)
Churchill, Manitoba Canada Geomag: 69°N Geograph: 58°45'N 94°4' W Invariant Lat: 72°N	Rudin	L-Band 254.14 MHz Canada Dept. of Transport Dept. of Communication Research 6 ft diam parabola, BW = 30 kHz
Ottawa, Ontario Canada Geomag: 56°N Geograph: 45°N; 76°W Invariant Latitude: 58°N	Maynard	L-Band 30 ft diameter parabola BW = 100 kHz

3.2 AMPLITUDE DATA FROM RADIO STARS AT FREQUENCIES FROM 60 TO 400 MHz

Aarons, Allen and Elkins (1967) reported on the frequency dependence of radio star scintillation at the frequencies 30, 63, 113, 228 and 400 MHz. Their conclusions were:

a. With only a few exceptions, the exponent of the frequency dependence of scintillation index lies in the range 0-2.

b. Under conditions of weak scattering, and at high frequencies (113-400 MHz), the exponent of the frequency dependence of scintillation index η is close to 2, which is the expected theoretical value for Fresnel zone observations.

c. At the lower frequencies studied (30-113 MHz) frequent examples were found that were apparently characterized by strong scattering. For these conditions, the value of η was generally observed to be lower, and usually in the range 0-1.

d. In the portion of the spectrum between 30 and 63 MHz, for observations looking through the auroral zone, η was found to be centered about the value 1.

e. For some cases of very intense scintillation, the frequency dependence exponent approached zero, and on occasion became negative (i.e. scintillation index increased with frequency instead of the converse, which is normally the case).

f. Irregularity scale size of the order of 1 - 2 km are consistent with most of the measurements.

Chivers (1960) also discussed various aspects of the phenomenon of the scintillation of a radio star covering the frequency range 26 MHz to 408 MHz. His conclusions are:

g. The mean scintillation amplitude varies as the inverse square of the observing wavelength up to the point where the lower frequency index saturates at 100 percent (the scintillation index used). For zenithal observations on

26 MHz at the latitude of Jodrell Band (Geographic Latitude 53°N), a scintillation index of 100 percent is commonly obtained.

h. The rate of scintillations is independent of observing wavelength under weak scattering conditions, and for strong scattering, the rate increases with wavelength.

i. The probability amplitude distribution of small scintillations is a displaced Gaussian curve, and larger amplitudes have a Rayleigh distribution. Very intense scintillations have an irregular amplitude indicating the occurrence of non-statistical focusing and defocusing of the incident wave.

j. There is no significant cross-correlation between records of scintillations obtained simultaneously on frequencies differing in the ratio 3:1. Combining this with the results of other workers, it is clear that the fall in cross correlation with frequency separation is at least at a linear rate.

Table 3-2 summarizes most of the available data on the frequency dependence of ionospheric scintillation. As can be seen from the table, the data to date has not been conclusive as to the exponent of the frequency factor, if in fact one exists for all possible conditions.

Crampton and Sessions (1971) show a scatter diagram of the exponent of frequency dependence as a function of depth of VHF scintillation fading for each test run. These results show that the exponent of the frequency dependence decreases as the fading increases which is contradictory to the relationship experienced at high and mid-latitudes by Mullen et al (1969) and Allen (1968). Crampton and Sessions discuss the possible reasons for this departure from other measurements, however, a similar finding is indicated in the high latitudes by the study of Pope and Fritz (1970).

TABLE 3-2 COMPARISON OF FREQUENCY-DEPENDENCE RELATIONSHIPS OF IONOSPHERIC SCINTILLATION

Frequency Range	Scintillation Amplitude	Scintillation Rate	Comments and Citation
26 MHz - 408 MHz	$1/f^2$	independent of wavelength	See conclusions (vii) - (x) in section 2.3.2 from Chivers, (1960) Mid latitude
254; 1550 MHz	$1/f^2$	-	Maynard and Selin (1971) Ref. 5 in Golden, (1970B), auroral region
136; 1695 MHz	$1/f$	-	Pope and Fritz (1970), auroral. In general the S-band scintillation amplitudes were about 1/10 of the VHF scintillation amplitudes.
4; 6 GHz	$1/f^2$	-	Craft and Westerlund (1972), Hong Kong
?	$1/f$	-	Allen, (1968)
30; 63; 113;	$1/f^2$	-	Weak scintillations higher radio frequencies
228; 400 MHz	$1/f$	-	High levels of ionospheric activity and lower frequencies, Aarons, Allen and Elkins (1967) Mid-latitudes
136; 1550 MHz	$1/f^{0.78}$	-	Crampton and Sessions, (1971), equatorial
136; 1550 MHz	$1/f$ $1/f^{0.5}$	- -	Summer solstice, equatorial autumnal equinox, equatorial Golden (1970B)

The real problem in trying to estimate frequency dependence over such a wide frequency region (136 - 1550 MHz) is that there is usually saturation of the lower frequency scintillation index before scintillation commences at the higher frequency. In other words, strong scattering occurs at 136 MHz and weak scattering occurs at 1550 MHz.

It thus may be concluded that frequency scaling of VHF data does not provide a reliable estimate for scintillation at L-band. Extensive measurements at 1550 MHz are urgently needed in order to provide useful system design information for aeronautical satellite systems.

3.3 AMPLITUDE SCINTILLATION DATA AT 136 MHz

A summary of available amplitude scintillation data at 136 MHz is presented in Table 3-3. Much of the amplitude-time information has been sponsored and reported by the Air Force Cambridge Research Laboratories and presented in cumulative form by Whitney, Aarons and Seemann (1971).

Data was collected at three different latitudes. The mid-latitude site was Hamilton, Massachusetts, the auroral site was Narssarssuaq, Greenland, and the equatorial site was Huancayo, Peru. The data collected at these sites was converted from scintillation index measurements over the indicated periods of measurement. Thus, to date there is only one source of digitized data at 136 MHz which has been converted into amplitude probability density distributions. This is item 4d at Hamilton, Mass. in Table 3-3.

Cumulative amplitude distribution of ATS-5 (1550 MHz) and INTELSAT I (136 MHz) signals were collected at Ancón, Peru. This data was reduced from strip chart data manually. The conclusion to be drawn from the 23 hours of data reported to date is that a proper physical interpretation of scintillation cannot be deduced from these data due to the restricted sample size (Crampton and Session, 1971). The relative severity of microwave scintillation

TABLE 3-3 SUMMARY OF PROPAGATION DATA AVAILABLE AT 136 MHz -- EMPHASIS ON SYNCHRONOUS SATELLITE DATA

Location Name	Type(s) of Data	Satellite	Reference(s)
Huancayo, Peru	1. S.I. 20% to 90%, Fig. 8	ATS-3	Mueller, 1970
	2. S.I. - cumulative distribution function (cdf), Fig. 9	ATS-3	Whitney, Aarons, and Seemann 1971
	3. 9381 hrs. Fig. 11, S.I. cdf (6 Jan. 1968 - 30 Apr. 1970)	"	"
	4. S.I. - cdf (5 Jan. 1968 - 30 Apr. 1969)	"	"
	5. S.I. - cdf (5 Jan. 1968 - 30 Apr. 1969) Day - Night - All hours, Fig. 14	"	"
	6. Fading Range vs month, Fig. 15 (1 Jan. 1968 - 30 Apr. 1970; 9245 hrs)	"	"
Lima, Peru (Ancón) Ancón Satellite Tracking Station	1. cdf from manual data reduction of strip chart data Elevation Angle: 49-52°	INTELSAT I (Early Bird)	Crampton and Sessions, 1971 Pomalaza, et al, 1970
	2. cdf for runs on 29 Sept., 6, 8, 10, Oct. 1970, Figs. A-1 - A-5		
Hamilton, Mass. USA Sagamore Hill Radio Observatory	1. S.I. - cdf (11 May 1967 - 30 Apr. 1968) Day - Night - All Hours	INTELSAT II F3 F3 (Canary Bird)	Whitney, Aarons and Seemann, 1971
	2a. S.I. - cdf; 1745 hrs (11 May 1967 - 9 Aug. 1967)	"	Whitney, 1969, Fig. 7 NASA, 1970, Fig. 6-1 Aarons, 1970
	2b. Fade depths; Distribution of 3 and 6 dB fades, Fig. 8	"	Whitney, 1969

TABLE 3-3 (CONTINUED)

Location Name	Type(s) of Data	Satellite	Reference(s)
Hamilton, Mass. USA (Continued)	3. Strip chart recording; 1 1/2 hrs 7 Aug. 1965, Fig. 4-11	INTELSAT I (Early Bird)	Allen, 1969
	4. 37° Elevation Angle over a propagation path intersecting an invariant latitude of approximately 54°	ATS-3	
	4a. 15 minute sample of strip chart and a corresponding amplitude distribution. Fig. 2	"	Aarons, Whitney, and Allen, 1971
	4b. 16 May 1970; 0130 - 0630 UT "Worst Case", Fig. 5	"	"
	4c. 15,750 hrs S.I. - cdf 9 Nov. 1967 - 31 Oct. 1969, Fig. 4	"	"
	4d. 35.5 hrs digitized - cdf, Fig. 7	"	Whitney, Aarons and Seemann, 1971
	4e. 1296 hrs - S.I. -cdf, Fig. 6	"	"
	4f. strip chart, 15 Oct, 1970 (412; 137.35; 136.47 MHz) 0300-0600 GMT; Figs. 11-37	"	General Electric, 1971
Schenectady, NY USA General Electric Radio & Optical Observatory	1. Experimental VHF satellite-to-aircraft comm. link with a jet over the N. Atlantic. A strip chart for the entire flight is included in the reference.	ATS-3	General Electric, (1970) Note: there is also a tape recording to go along with the strip chart

TABLE 3-3 (CONTINUED)

Location Name	Type(s)	Satellite	Reference(s)
Thule, Greenland	1. Fading period and amplitude for 21, 22, 23 Oct. 1968, See Fig. 7 of the present report	ATS-3	Aarons, Whitney and Allen, 1971
Narssarssuaq, Greenland	1. 20° Elevation Angle Intersection with invariant latitude at 350 km level was 63° on the average; Fig. 13	ATS-3	Aarons, Whitney and Allen, 1971
	2. S.I. - cdf; Fig. 8 Mean Distributions	ATS-3	Whitney, Aarons and Seemann, 1971
	3. S.I.- cdf; Fig. 13 17 Sept. 1968 - 14 Aug. 1969 All Hours - Day Hours - Night Hours	"	"
	4. 7635 hrs (Sept. 1968 - Apr. 1970) S.I. - cdf; Fig. 10	"	"
Gillmore Creek, Alaska, USA	1. 1700 MHz too. 22 Feb. 1970; three times; strip chart data	ESSA-9 ITOS	Golden, 1970C
NOAA Control & Data Acquisition Station	2. Description of amplitude scintillations	TIROS-9 NIMBUS	Fremouw, 1967
	3. S.I., 137 MHz and 1695 MHz	ITOS-1	Pope and Fritz, 1970

effects points out again the urgent need for further experimentation in this area.

It was found that the equatorial VHF fade duration statistics generally were about the same as those observed at higher latitude stations. One significant finding in the equatorial data was that at low fade depths (2 dB or less), the durations are about the same at L-band. However, as the depth of fade increases, the VHF fades tended to be considerably longer than L-band fades for the same length of time.

4. DESCRIPTION OF EXPERIMENTAL INSTRUMENTATION

4.1 INTRODUCTION

The experimental instrumentation used to perform amplitude measurements at 136 and 1550 MHz is depicted in the photograph of the DOT/TSC/Westford Propagation Facility which is presented in Figure 4-1. The two large antennas in the foreground (A,B) are 10 feet (3.05 m) in diameter. Figure 4-2 shows a close-up view of the antenna mounted on the modified Nike-Ajax mount. The basic receiving system employs a two element phase coherent interferometer which is completely operated under computer control. The elements of the interferometer are the modified Nike-Ajax mounts with 10-foot diameter antennas mentioned above. The data processing, analysis and display is accomplished in real-time while the interferometer is being operated.

The 15-foot (4.58 m) diameter antenna (C) mounted on the flatbed trailer shown in the left side of Figure 4-1 is used for transmitting and receiving at 1650 and 1550 MHz respectively. A 225 watt transmitter is housed in the air-conditioned enclosure at the back of the flatbed trailer and the radio frequency portion of the receiving equipment is housed in the canister at the focus. The 15-foot diameter antenna is also used for receiving signals at 4200 MHz.

An additional 10-foot diameter antenna (D) is mounted atop a 30-foot high tower. This antenna is used for transmitting and receiving at 1650 and 1550 MHz respectively. This antenna has its own receiving equipment mounted behind the reflector. The transmitter on the flatbed trailer may also be connected to this 10-foot diameter antenna.

The array of six crossed Yagi antennas mounted on the 40-foot high tower (E) at the left of Figure 4-1 is used to receive 136 MHz signals. A 1.5 dB noise figure preamplifier and calibration side coupler are mounted in the center of the array.

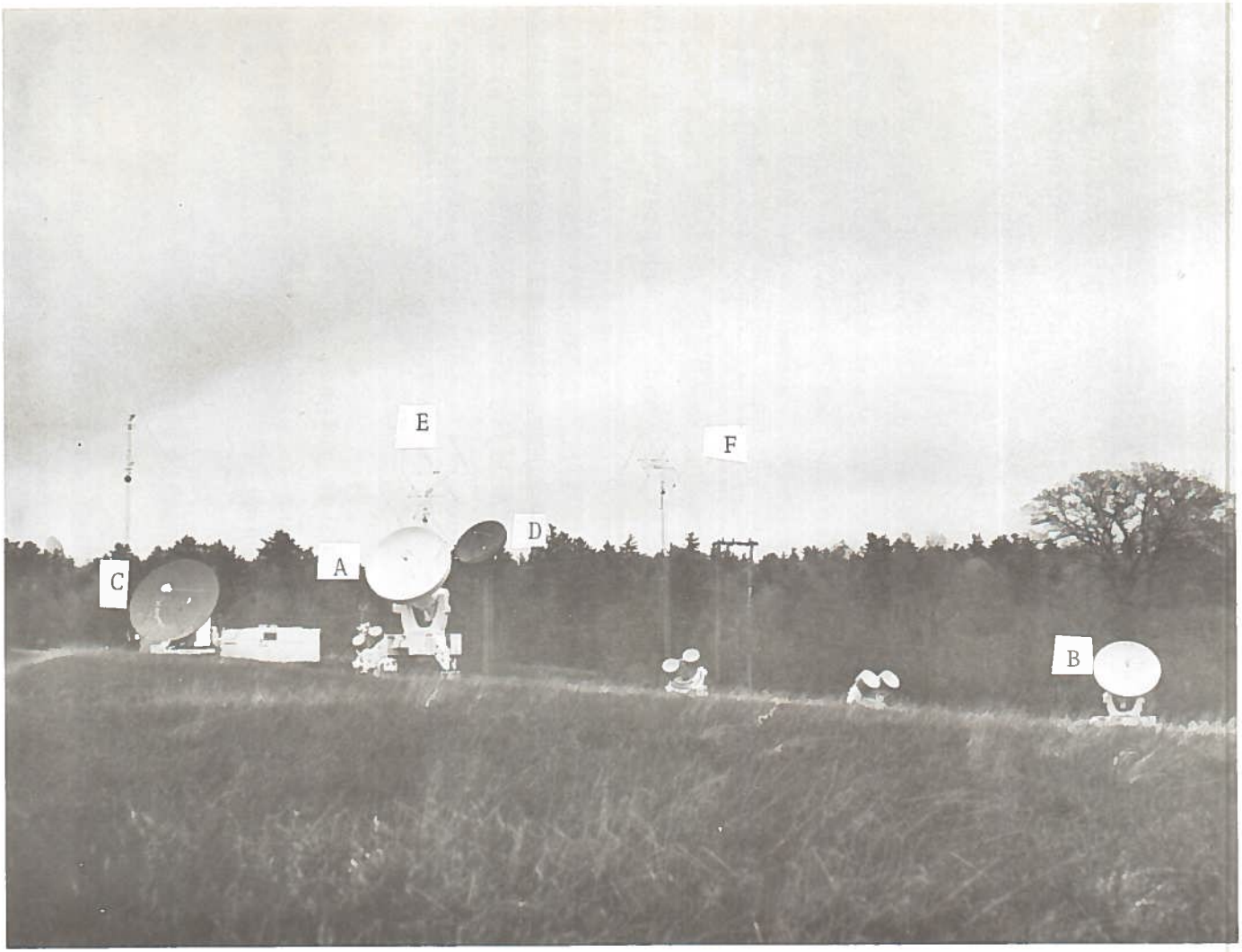

Figure 4-1 Photograph of the DOT/TSC/Westford Propagation Facility, Westford, Massachusetts (Looking North)

Figure 4-2 A Single Element of the Interferometer

The array of 4 crossed Yagi antennas mounted on the 50-foot tower (F) on the right-hand side of Figure 4-1 is used for transmitting at 149.2 MHz.

4.2 L-BAND INTERFEROMETER SYSTEM

4.2.1 System Description

A functional block diagram of the L-band interferometer system is shown in Figure 4-3. The figure shows the overall organization of the receiving systems. The central processing unit controls the antenna pointing through the antenna control station. The receiver electronics are also under computer control such that automatic calibration can be made. The major portion of the computer control is devoted to data acquisition and processing. Preliminary analysis of the data is also performed continually in order to assure the data is of acceptable quality.

A detailed block diagram of the telemetry data receivers used in the interferometer system is also included without discussion (Figure 4-4) so that the exact details of the intermediate signal processing may be examined.

The interferometer receiving system is capable of making several different measurements simultaneously. These measurements may be categorized as incoherent and coherent (phase locked, or synchronous) in various combinations with the two antennas.

Incoherent measurements consist of signal amplitudes as measured by a square-law detector in the second or third intermediate frequency amplifier. The intermediate frequency detector in the telemetry receivers can be preceded by a series of narrow-band filters ranging from 1 kHz to 100 kHz. The square-law detected voltage is then directly coupled to a stabilized operational amplifier with a 1 kHz bandwidth. This provides an output voltage proportional to the input power. With this detector it is possible to obtain a dynamic range of 20 dB with a 0.1 dB error.

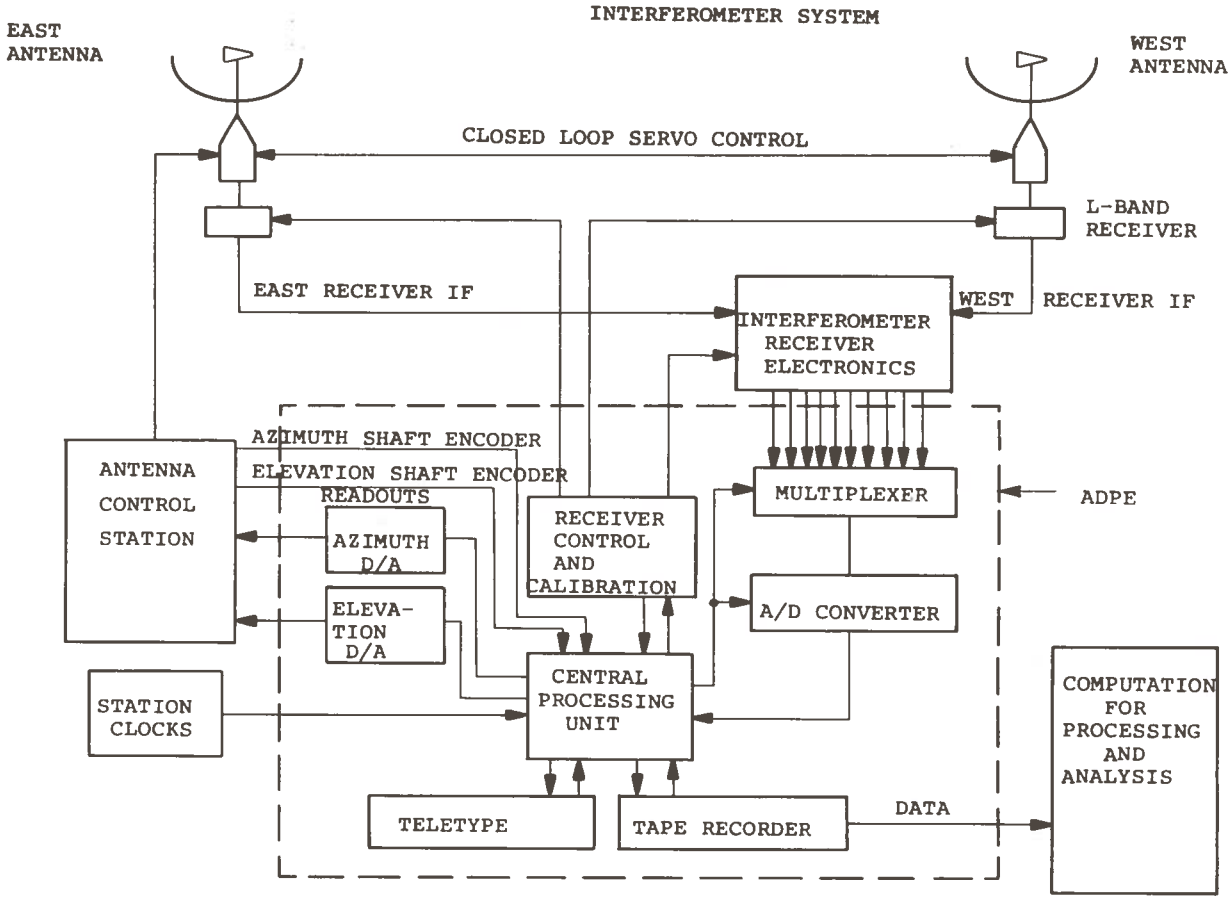

Figure 4-3 Functional Block Diagram of the L-Band Interferometer System

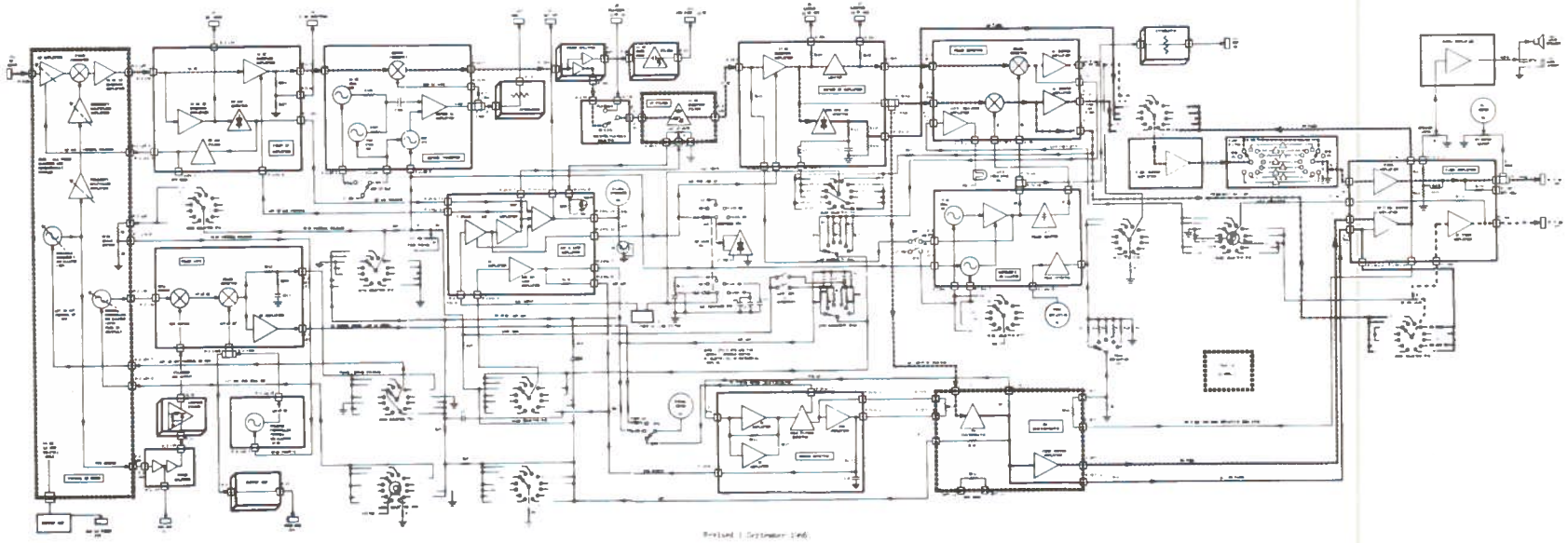

Figure 4-4 Schematic Diagram of Resdel Telemetry Receiver as Used in the L-Band Interferometer System

The linear 10 MHz signal from the interferometer telemetry receivers is also fed to a combination of vector voltmeters. The vector voltmeters down convert the signal to 20 kHz and square-law detect. The radio frequency bandwidth at 20 kHz is 1 kHz. The vector voltmeters provide a direct current output voltage (2 ms rise time) over a 12 dB dynamic range with an 0.1 dB error.

The 10 MHz output from each of the telemetry receivers is split, and one output from each receiver is then fed to an individual vector voltmeter. This provides a measure of the signal strength as received at each antenna. Other equal portions of the individual receiver's 10 MHz outputs are added together and fed to a third vector voltmeter. This provides a means of calculating the correlation between the signals received by the two antennas.

The 10 MHz reference frequency for the vector voltmeters is provided by the station standard. Another portion of the 10 MHz output from the telemetry receivers is fed to two additional vector voltmeters. In the latter configuration, however, the reference frequency for one vector voltmeter comes from a frequency synthesizer operating at 9,999,500 Hz and the frequency reference for the other vector voltmeter comes from another frequency synthesizer operating at 10,000,500 Hz. This provides a continuous set of receivers for determining the frequency stability of the received signal.

A delay cable is used in the West antenna's receiver. The cable is inserted in the 30 MHz intermediate frequency line to compensate for differences in cable length between the two antennas. Also the proper length of delay cable is added to compensate for the fact that the West antenna is 98 feet closer to the ATS-5 than the East antenna. The first local oscillators, at 1520 MHz, are also phased in such a way that the phase of the local oscillator's signal injected at each antenna is the same with respect to each other.

Coherent measurements can be conducted using these telemetry receivers. This is accomplished by allowing each receiver to phase lock to the carrier at the second intermediate frequency (the two

receivers share a common second local oscillator) and provide coherent detection of the carrier amplitude. The detected coherent carrier amplitude is then direct coupled to a stabilized operational amplifier with a bandwidth of 1 kHz. This coherent detection of the carrier amplitude has a 12 dB dynamic range with a 0.1 dB error from the loop lock threshold. The coherent carrier amplitude and the incoherent carrier detection previously discussed operate with the receiver's automatic gain control turned off in order to insure true linearity.

4.2.2 Antenna Pointing System

A functional block diagram of the interferometer pointing system is presented in Figure 4-5. The central processing unit provides closed loop, digital, ephemeris tracking for the West antenna mount. The East antenna mount follows the West antenna through a two-speed 400 Hz servo loop. The two antennas have a separation of 127.50 feet (38.86 m) with the West antenna being 13.55 feet (4.13 m) above the East antenna. The baseline is in a near East - West direction within $\pm$ 2.0 arc seconds.

The azimuth and elevation of the West antenna are encoded with 18 track optical shaft encoders providing 0.01 degree accuracy. The azimuth and elevation angles from the mount are compared with the calculated ephemerides of the target based upon the time and orbit parameters. The error between calculated and actual antenna position is sent to the digital-to-analog converters to reposition the antennas. The error detection resolution is 0.001 degree (velocity and acceleration interpolation is employed with the readings from the shaft encoders to obtain a more accurate estimation of the antenna position). The digital error signal is converted to an analog signal for control of the West antenna mount. The digital-to-analog converter has a possible resolution of 0.0002 degrees with the noise level about 0.1 of that.

The velocity tracking error of the overall system is approximately 0.003 degrees for velocities up to 1 degree per second. For

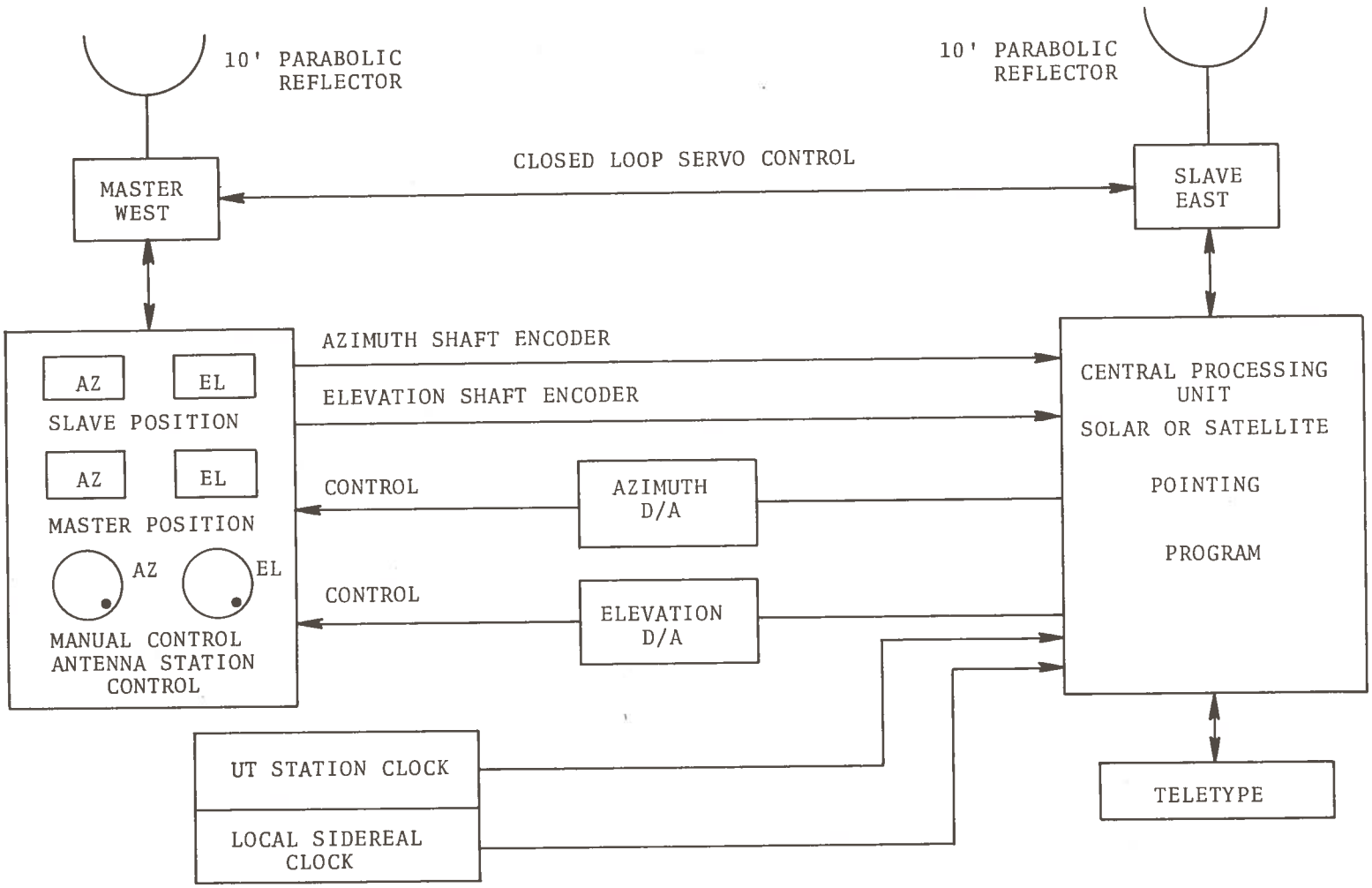

Figure 4-5 Functional Block Diagram of the Interferometer Pointing System

slower velocities the error is approximately 0.001 degree for velocities on the order of 0.1 degree per second. The closed loop static pointing error is approximately 0.001 degree (less than 4 seconds of arc).

4.2.3 System Configuration with the ATS-5 Signal

Figure 4-6 presents a functional block diagram of the L-band interferometer system used in conjunction with the ATS-5 for making propagation measurements. The first conversion is performed at each antenna and the signal is returned at 30 MHz to the East and West antennas' 30 MHz intermediate frequency telemetry receivers. A local oscillator reference signal of 250 MHz is sent to each antenna's radio frequency package. Control functions are also sent to the radio frequency package. The control functions may be performed automatically or manually. A switchable set of delay lines is incorporated into the West antenna's intermediate frequency cable. This unit compensates for differences in intermediate frequency cable length as well as the path differences across the interferometer aperture. Consequently, when the intermediate frequency signals from the East and West antennas are combined they have each traveled through the same overall path length (i.e. they have experienced the same time delay).

A more detailed figure of the receiver's intermediate frequency section is shown in Figure 4-3, however, Figure 4-6 illustrates how receiver outputs are interfaced with the computer. The various outputs of each 30 MHz telemetry receivers are digitized and the digital word from the East antenna's analog-to-digital converter is combined with the West antenna's analog-to-digital converter to form a computer word. The 10 MHz receivers (vector voltmeters) are multiplexed into one analog-to-digital converter (each reading is a computer word). The multiplexer is twenty channels and may also be used to sample data from the telemetry receivers. The low speed analog-to-digital converter works at a 500 Hz rate and the high speed converter works at a 250 kHz rate.

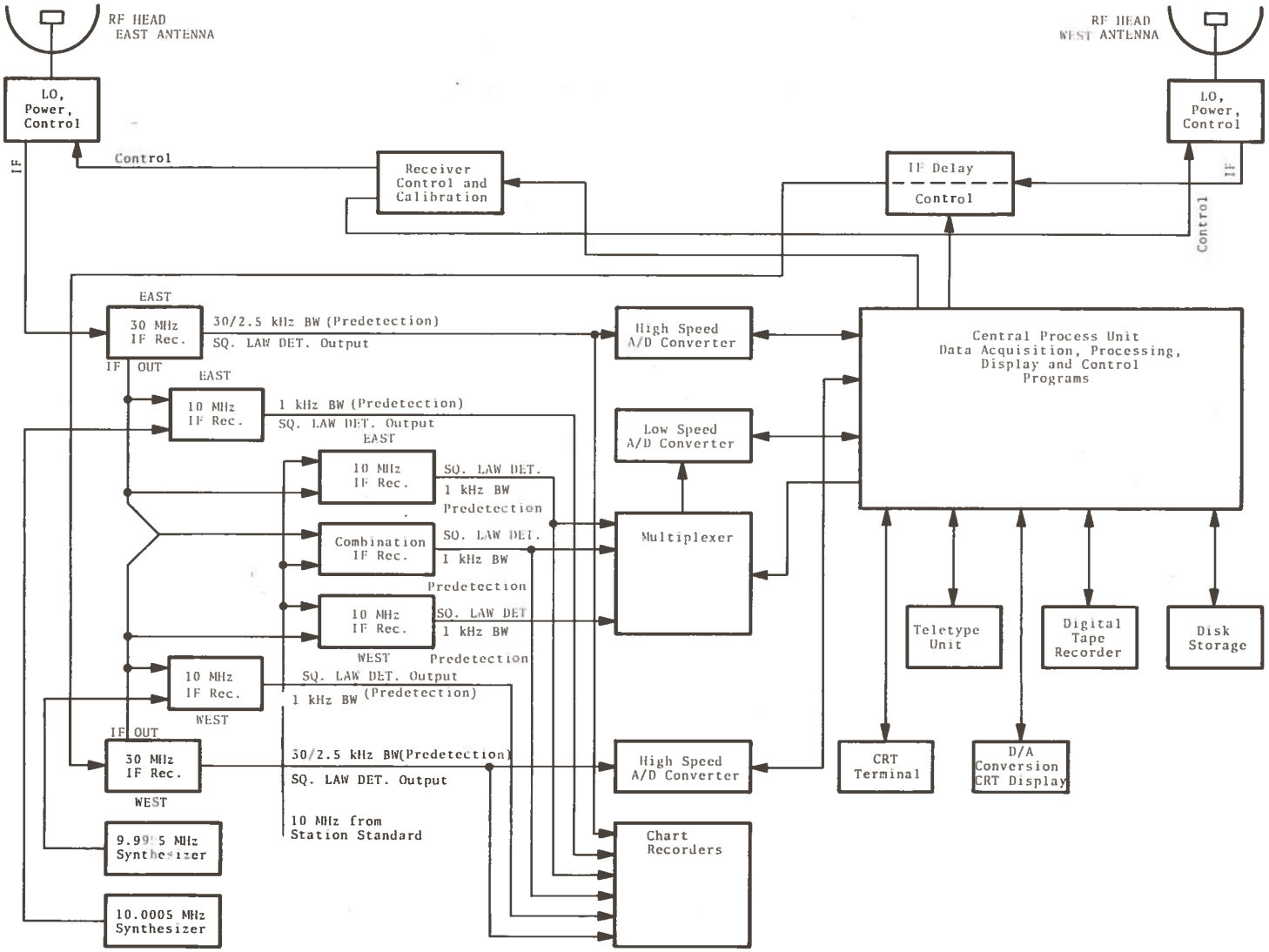

Figure 4-6 Functional Block Diagram of the L-Band Interferometer for Use with the ATS-5 Spacecraft

The first local oscillator is controlled by a frequency synthesizer at 60.222 MHz to provide a 1520 MHz local oscillator signal. A common 250 MHz signal is generated, split and sent to the individual antenna's radio frequency electronics for final multiplication to 1520 MHz. The second local oscillator is a crystal oscillator unit serving both telemetry receivers. The third local oscillator is common to the three vector voltmeters operating at 10 MHz. Tuning the third local oscillator allows the narrow-band third intermediate frequency to be tuned within the wider bandwidth of the telemetry receivers.

4.2.4 System Configuration with Solar Source

A functional block diagram of the L-band solar interferometer is shown in Figure 4-7. The electronics in the radio frequency package at each antenna is identical to that used with the ATS-5 measurements. The intermediate frequency signals are fed into intermediate frequency amplifiers which operate over the entire intermediate frequency bandwidth of the interferometer, 29 to 49 MHz. The intermediate frequency signals from each antenna are amplified, filtered (29 to 39 MHz) and split in half. One half of the split signal from each intermediate frequency amplifier is combined, amplified and detected. The other half of the signal from each intermediate frequency is combined also except that it is passed through 180° additional length of line before being recombined, amplified and detected. The detected outputs are digitized and processed by the computer.

The use of two receivers permits the operation with two sets of interferometer fringes. The fringes are placed such that when one fringe is maximum the other is minimum. This simplifies the data processing since the ratio of the amplitudes of the two receiver outputs is the tangent (or cotangent) of the angle between the target and the main fringe (or displaced fringe).

4.2.5 L-Band Equipment Located at Each Antenna

Figure 4-8 presents a functional block diagram of the L-band equipment located at each antenna. The feed antenna is connected

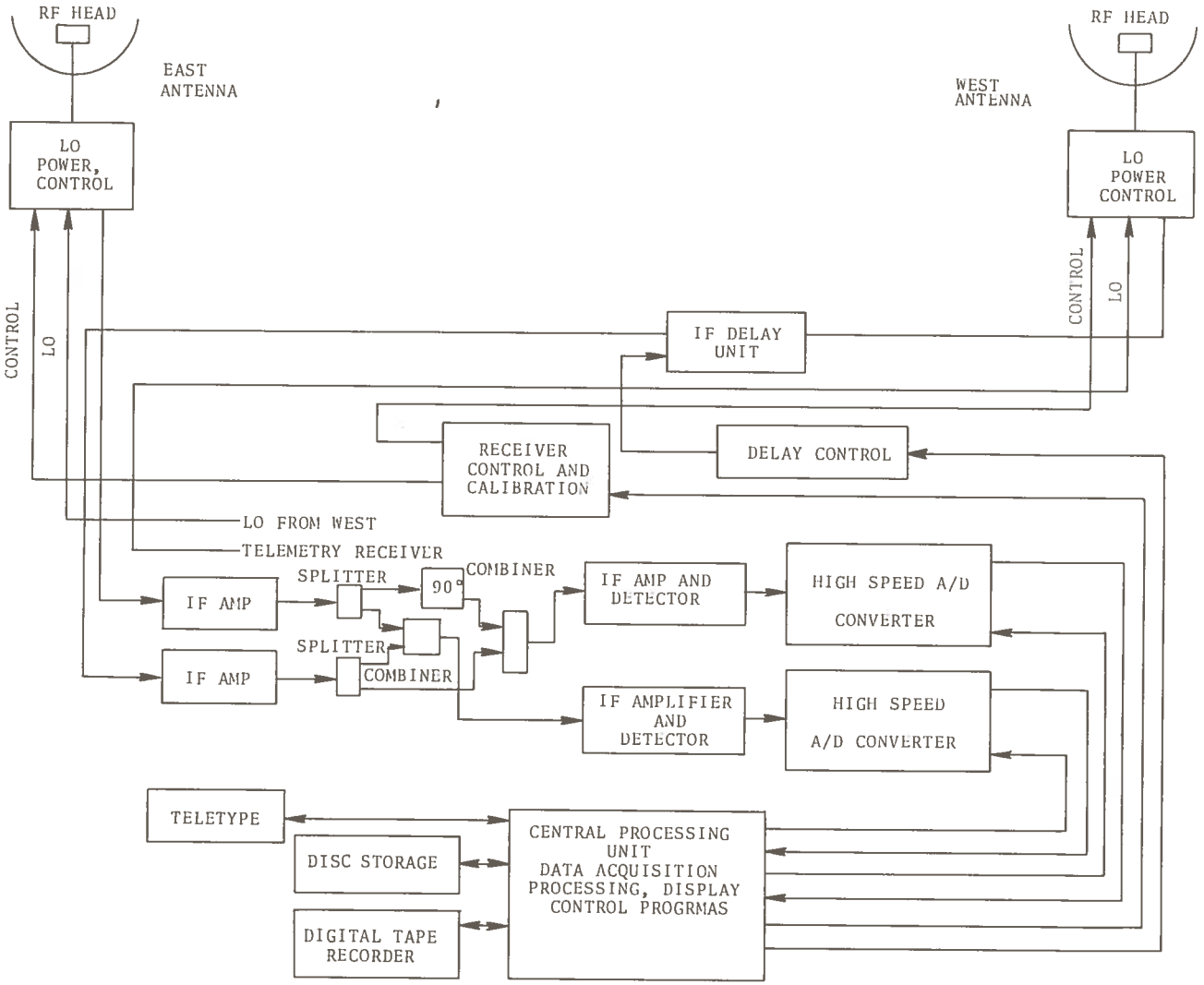

Figure 4-7 Functional Block Diagram of the L-Band Solar Interferometer

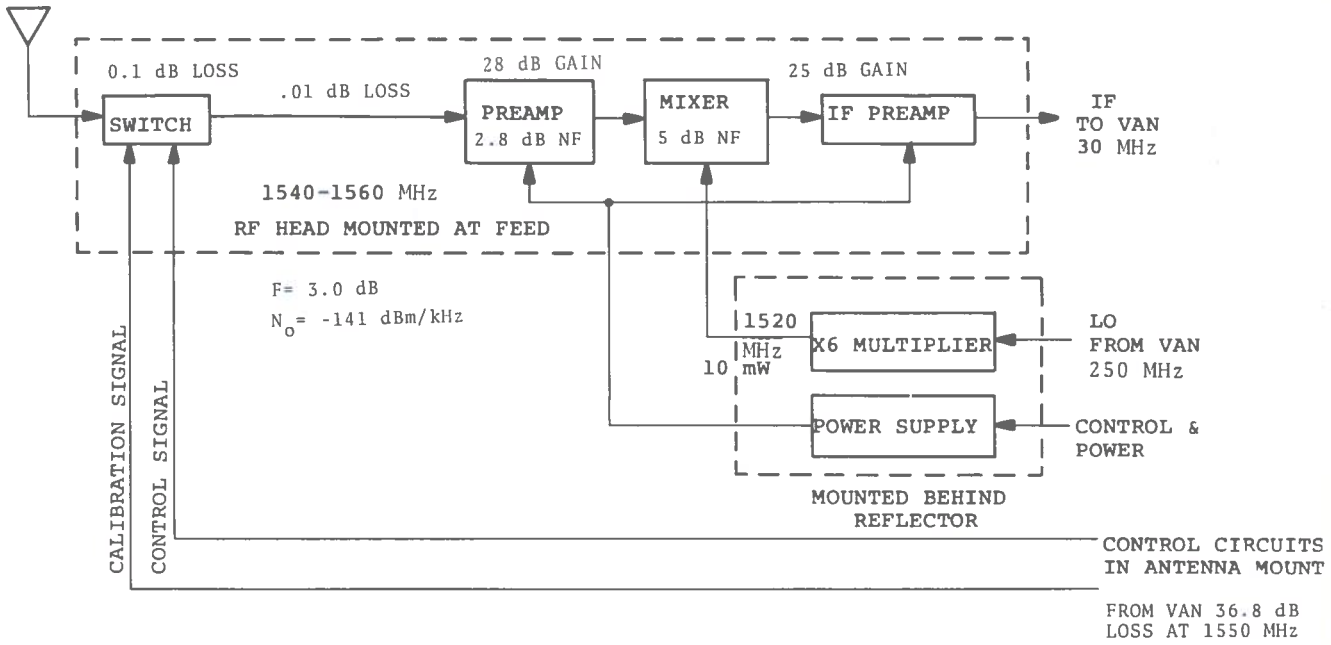

Figure 4-8. Functional Block Diagram of L-Band Equipment Located at Each Antenna

directly to the radio frequency electronics through 3 inches (7.62 cm) of 0.141 rigid coax cable. The radio frequency feed package consists of radio frequency switch and a transistor preamplifier. The amplifier signal is fed to the mixer-intermediate frequency preamplifier located behind the main reflector. The radio frequency switch directly at the input allows a calibration signal to be substituted for the antenna's signal. The calibration signal is generated by a signal generator located in the electronics van and fed to each antenna through a cable whose loss is accurately measured. A noise source is also introduced in the calibration port of the switch when the interferometer is used for broadband solar measurements. The transistor amplifier has a gain of 28 dB and a single sideband noise figure of 2.8 dB. The measured insertion loss of the switch and cables is 0.2 dB. The measured single-sideband noise figure of the system is 3.0 dB for both radio frequency units. This computes out to a sensitivity of -171 dBm in a 1 Hz bandwidth. The measured sensitivity in a 1 kHz bandwidth is -141 dBm.

The mixer is a double balanced unit with conversion loss of 5 dB and the preamplifier has a gain of 30 dB with a 1.5 dB noise figure. The intermediate frequency passband is flat from 29 MHz to 49 MHz. This allows operation over the bandpass of the ATS-5 as well as operation near 1550 MHz and also at the beacon frequency of 1565.814 MHz. The operating bandwidth of the local oscillator multiplier allows operation from 1520 to 1540 MHz.

4.2.6 L-Band Intermediate Frequency Receivers

A simplified block diagram of the L-band telemetry receiver used in the interferometer is shown in Figure 4-9. The receiver is a double conversion receiver with provisions for various types of coherent and incoherent demodulation. A third conversion to 20 kHz is also included to permit narrow-band operation at 1 kHz. The linear 10 MHz is also fed to a spectrum analyzer for display. When the automatic gain control amplifier is in the manual position it provides manual radio frequency gain control. The gain of the

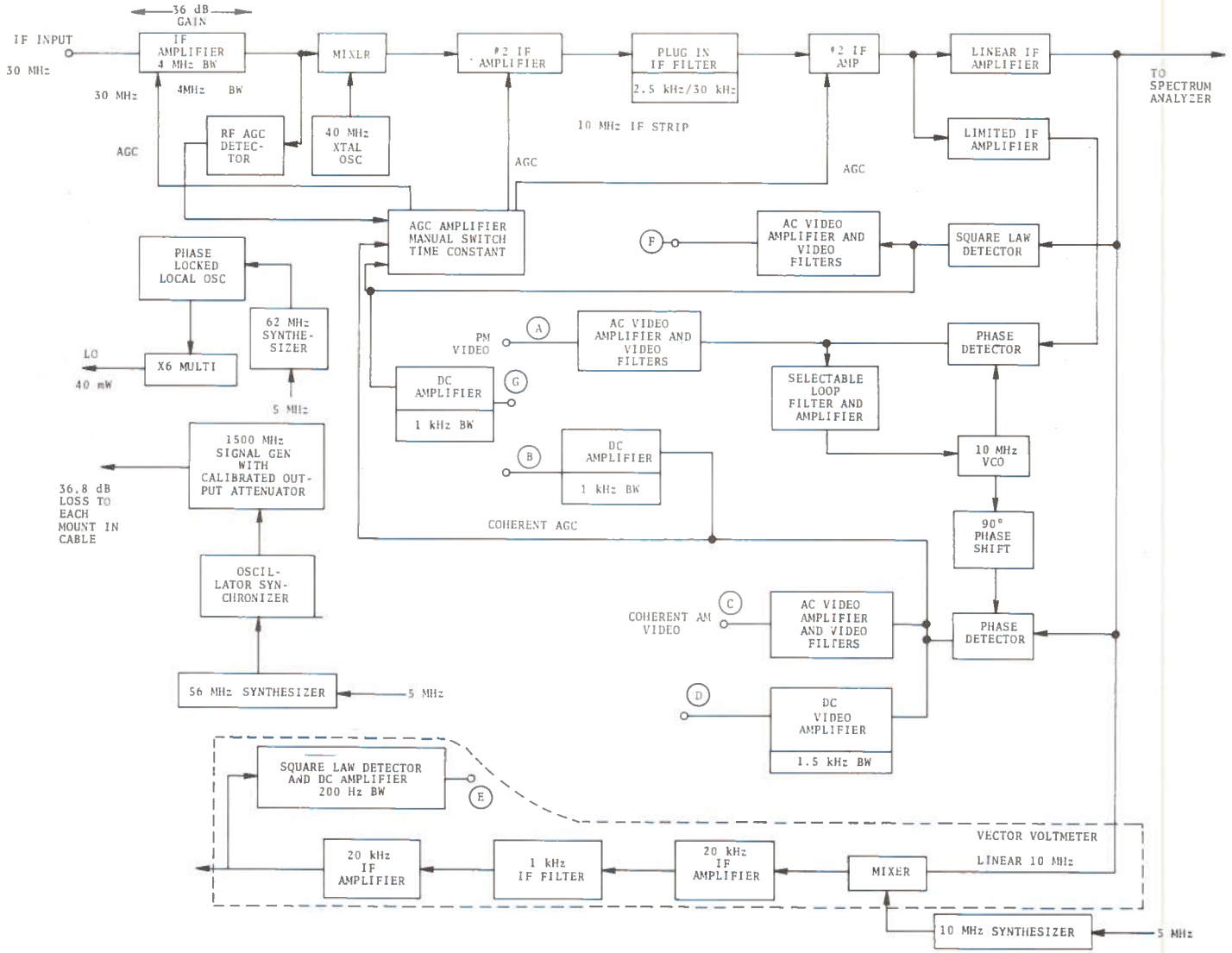

Figure 4-9. Block Diagram of L-Band Intermediate Frequency Receiver for Each Element of the Interferometer

first intermediate frequency amplifier may also be independently controlled. This allows almost perfectly linear operation over any 20 dB signal range. When the receiver is under automatic gain control, the operation is linear within 3 dB over a 90 dB dynamic range from threshold.

Figure 4-10 is a plot of the square-law detector for the East receiver and Figure 4-11 is a plot of the square-law detector of the West receiver using 2.5 kHz or 30 kHz predetection bandwidths. Figure 4-12 shows the 30 MHz to 10 MHz conversion response of the two telemetry receivers. Figure 4-13 is the measured bandpass characteristics typical of the vector voltmeters.

Either 2.5 kHz or 30 kHz crystal filters may be plugged into the 10 MHz intermediate frequency. Outputs A, C, and F (Figure 4-9) provide video demodulation signals. The lower frequency half power point may be selected as 6.25 kHz, 12.5 kHz, 25 kHz, 50 kHz, 100 kHz, 250 kHz, 400 kHz or 750 kHz. The outputs B, D, E and G provide direct coupled outputs. Each of the DC amplifiers is a stabilized operational amplifier which has a bandwidth of 1 kHz.

4.3 SINGLE ELEMENT L-BAND RECEIVING SYSTEM

Figure 4-14 presents a functional block diagram of a single element L-band receiving system, a C-band receiving system and an L-band transmitting system. The operation of the single element L-band receiving system is discussed below.

The received signal is preamplified at the antenna and then shipped via coaxial cable into the receiver located in the equipment van for frequency conversion and detection. After the signal is converted to 136 MHz it is fed into a telemetry receiver (Defense Electronics Industries (DEI) Model TMR 74). The telemetry receiver proceeds to down convert the 136 MHz signal to 55 MHz and then to 10 MHz. A portion of the 10 MHz signal is then sent to a vector voltmeter for detection. The 10 MHz signal is simultaneously fed to a set of switchable bandwidth filters and then to the receiver's square-law detector. The predetection filter bandwidths that may be selected are 10, 30, 100, 300 and 2000 kHz. The output of the square-law detector is direct coupled to an external low

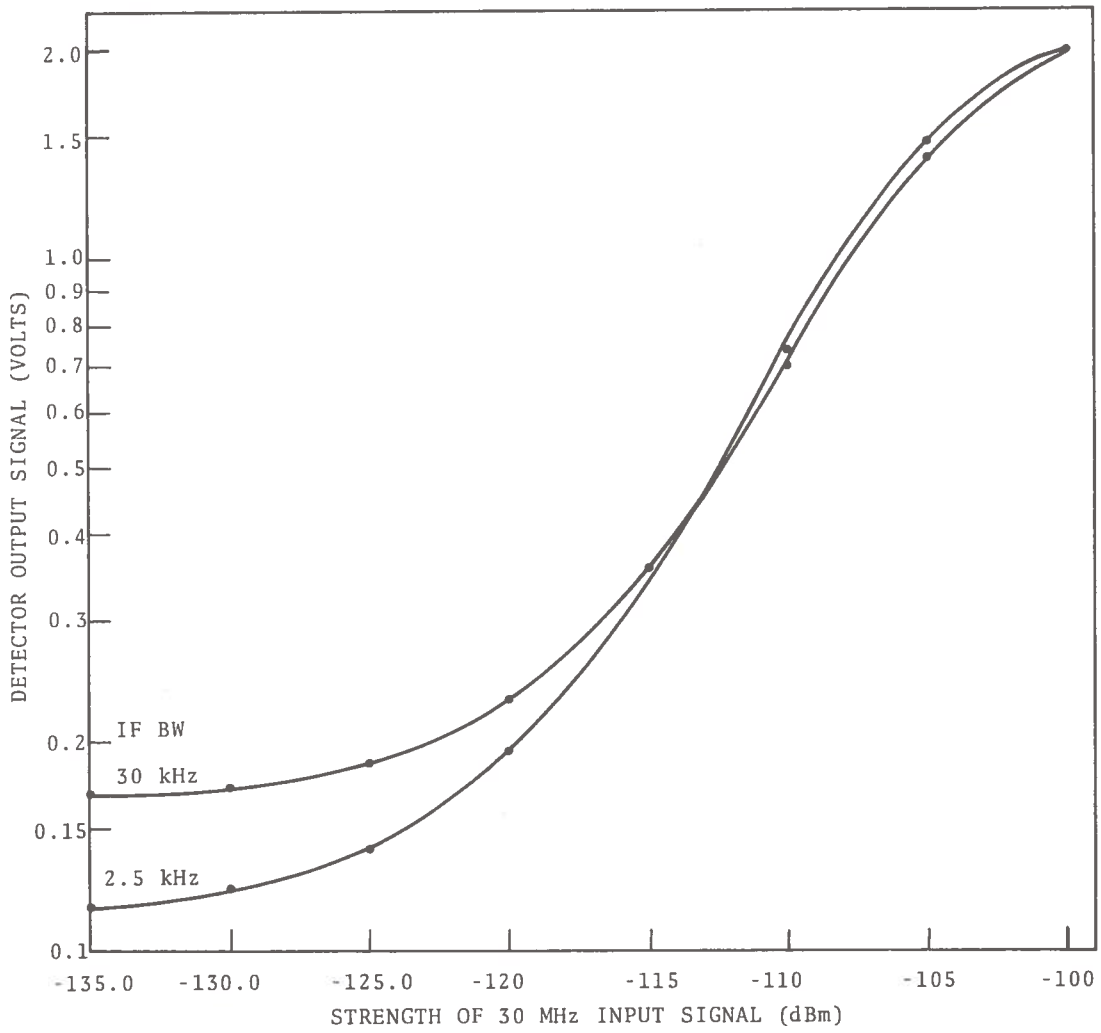

Figure 4-10 L-Band Receiver (Resdel/East) Detector Calibration

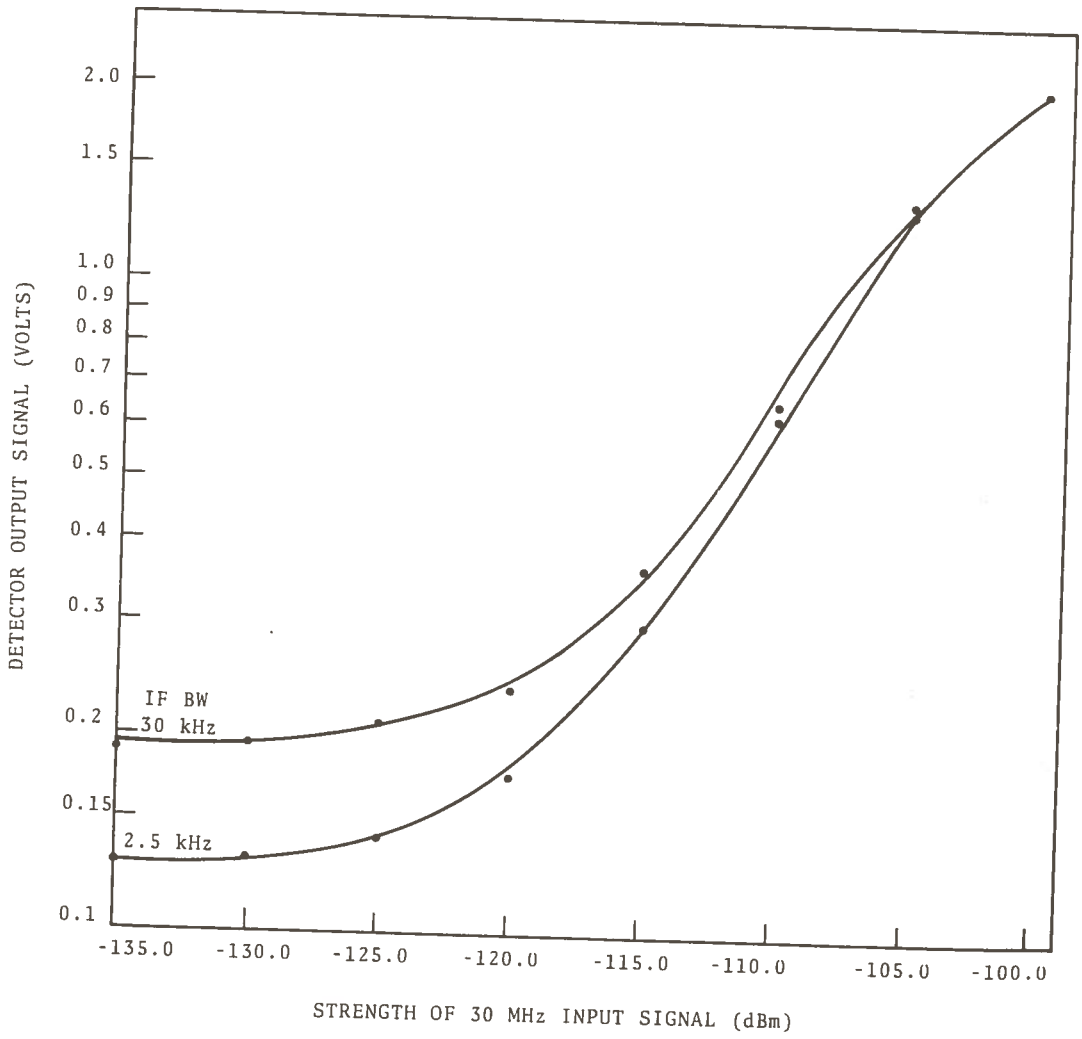

Figure 4-11. L-Band Receiver (Resdel/West) Detector Calibration

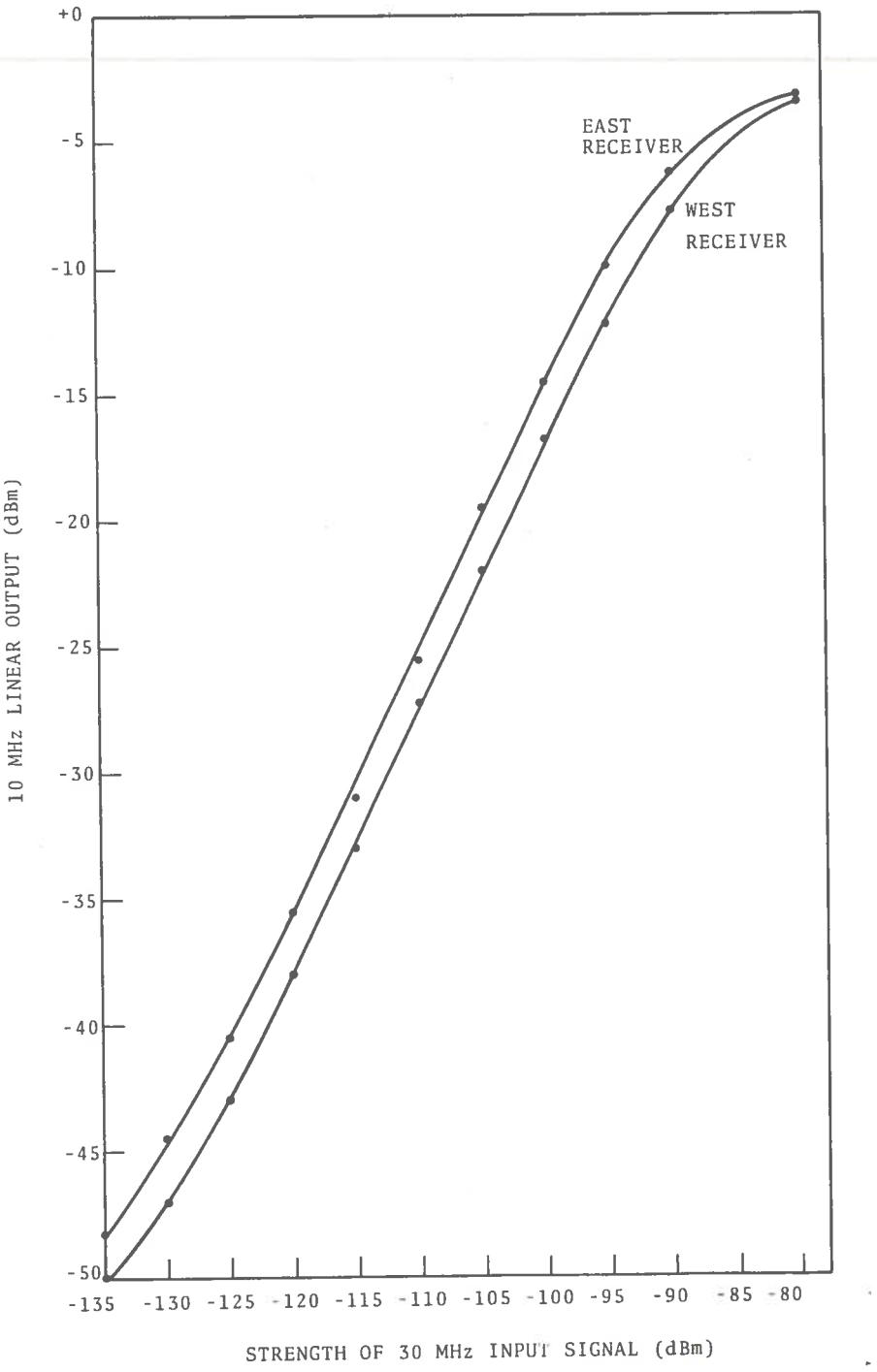

Figure 4-12 Frequency Conversion Response of L-Band Receivers (Resdel/East and West) From 30 MHz to 10 MHz

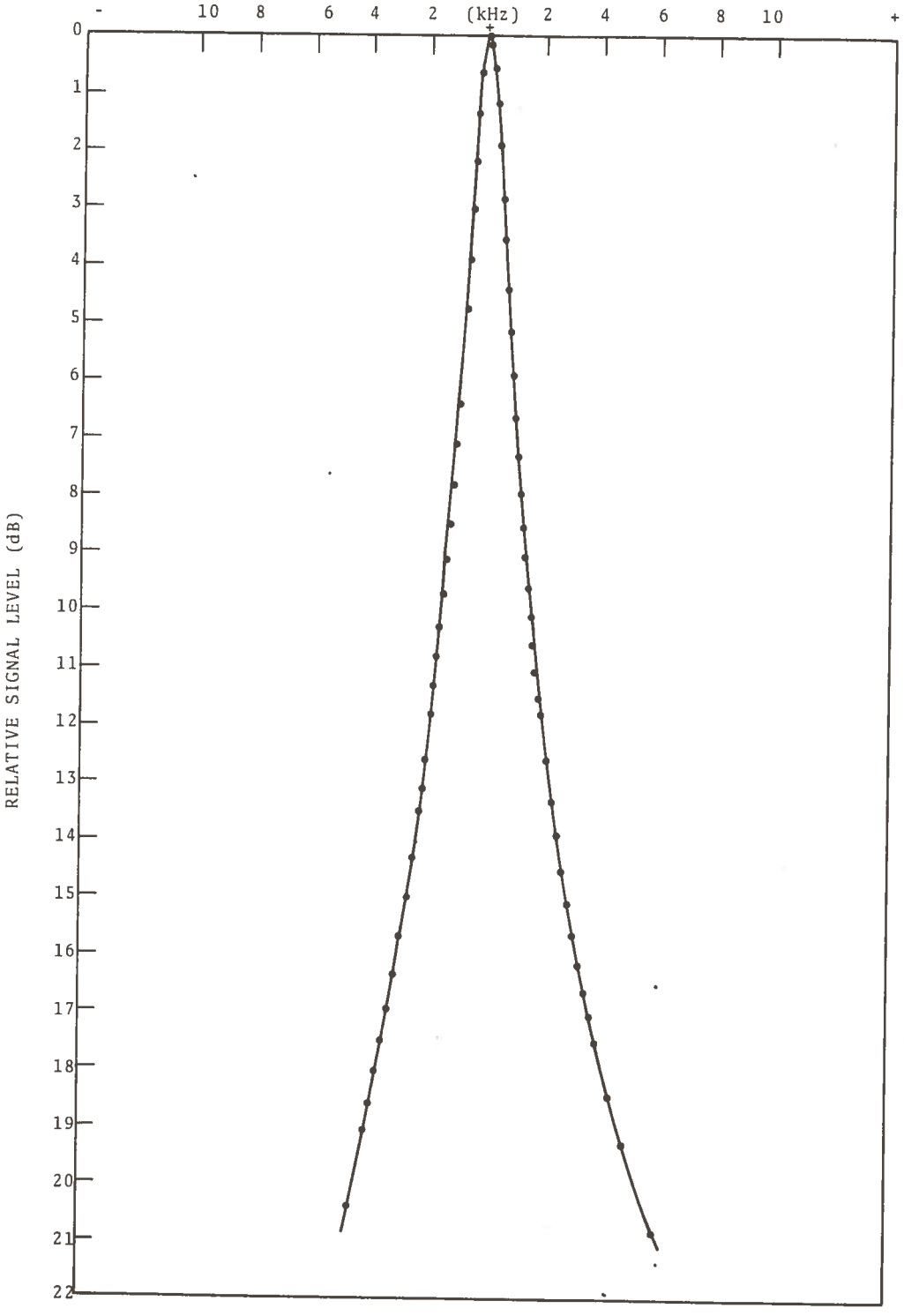

Figure 4-13 Vector Voltmeter (HP 8405A) Bandpass Characteristics

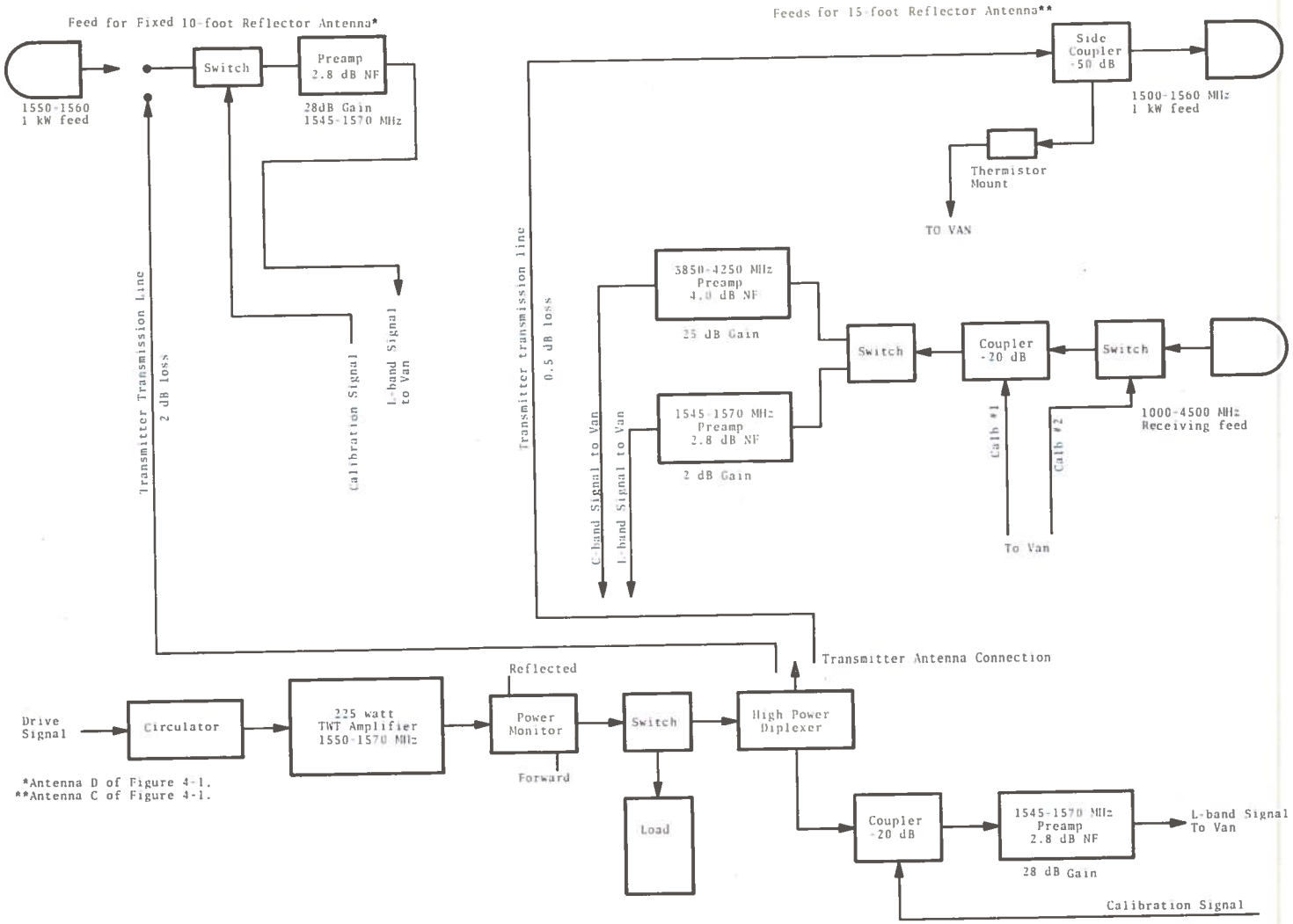

Figure 4-14 Functional Block Diagram of L-Band Receiving and Transmitting System and C-Band Receiving System

pass filter which has a two section RC filter with an adjustable bandwidth from 0.02 to 200 Hz. A portion of the 10 MHz intermediate frequency signal is also fed into the phase lock loop section of the receiver for coherent demodulation.

4.4 L-BAND TRANSMITTING SYSTEM

The L-band transmitter shown in Figure 4-14 can be connected to either the fixed 10-foot diameter antenna's feed (Antenna D of Figure 4-1) or the high power feed located in the steerable 15-foot diameter antenna's reflector (Antenna C of Figure 4-1).

4.5 C-BAND RECEIVING

The 15-foot diameter antenna is also equipped to receive signals at C-band as indicated in Figure 4-14.

4.6 VHF RECEIVING SYSTEM

A simplified block diagram of the 136 MHz receiving system is shown in Figure 4-15. The demodulated video signal from the VHF receiver goes to the computer interface unit for the operation of the Automatic Data Collection Facility reported in Brown, et al. (1973, 1974).

The sample of the intermediate frequency output at 29.17 MHz (corresponding to a received signal at 136.47 MHz is the VHF telemetry signal from the Applications Technology Satellite series of spacecraft described in detail in Brown et al. (1974). The detected signal is used to monitor the strength of the telemetry signal from the ATS-5 spacecraft.

4.7 AUTOMATIC DATA PROCESSING SYSTEM

Automatic data acquisition and processing is done on-site in real time using an Hewlett-Packard 2114B computer with a magnetic tape operating system. The data acquisition program used with the ATS-5 signal continuously digitizes the detected signal and incorporates the absolute calibration into the measurements. Since the pulsed signals are sampled many times, a faithful replica of the

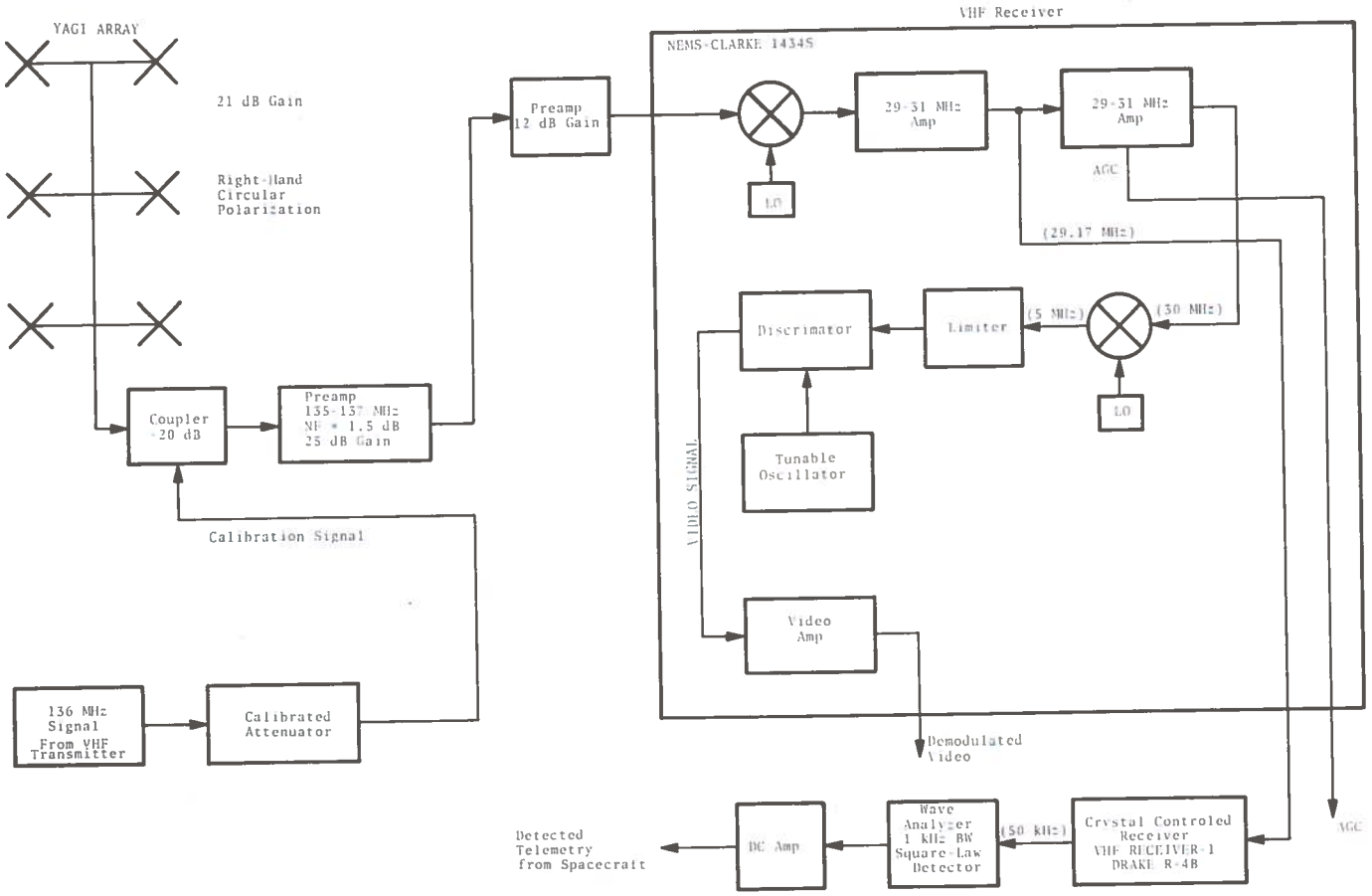

Figure 4-15 Functional Schematic Diagram of the VHF Receiving System

pulsed signal is stored in the computer. The individual samples of the pulse have an absolute accuracy of 0.1 dB.

The replica of each pulse is analyzed to find its maximum values. The procedure for finding the maximum of the pulse is such that several values leading up to the maximum and several values following the maximum are checked in order to ensure the value selected is in fact the maximum. This procedure prevents the noise peaks on the leading edge of a pulse from being picked as the maximum value of the pulse.

The peak values are then stored in a table with two hundred entries corresponding to the possible signal strength. The table covers a 20 dB dynamic range with 0.1 dB steps. Data may be added to the table for a period of time as short as 10 seconds or as long as 45 minutes.

At the end of the time interval that has been selected by the observer the values in the table are used to calculate the probability density function of the data for that particular time interval. The probability density may be typed out on a teleprinter, or plotted to illustrate the signal's behavior during the observing period. The table of signal strengths is also stored. At a later time the tables are combined and a probability density function for a much longer segment of time is calculated. Each time a density function is calculated a cumulative probabability distribution functions is calculated.

The use of two independent receiving systems allows equipment problems to be quickly identified in the data since the two receivers are operated with the same calibration. The procedure of taking data in short runs of 10 to 20 minutes makes it possible to examine runs before they are combined to form a long continuous data run.

5. L-BAND PERFORMANCE CHARACTERISTICS OF THE ATS-5 SPACECRAFT

Originally the ATS-5 satellite, shown in Figure 5-1, was designed to operate in a equatorial orbit of synchronous altitude. It was to be gravity gradient stabilized and utilize a high gain phased array antenna for L-band communications (Kissel, 1970). Difficulties were encountered during the orbit injection making it impossible to de-spin the spacecraft. Therefore, for all practical purposes the ATS-5 is spin stabilized. The current period of rotation is approximately 783.06 ms with the axis of spin approximately parallel with the Earth's spin axis. The spacecraft antenna thus illuminates the earth for a brief time during each spacecraft revolution. The -3 dB points illuminate the Earth station approximately 52.5 ms each revolution. The orbital geometry is shown in Figure 5-2. Figure 5-3 depicts the variations in intensity that may be expected over the Earth due to the orbit of the ATS-5 satellite.

The ATS-5 spacecraft has three major modes of operation. They are the multiple access, the frequency translation and wide-band modes. The multiple access and frequency translation modes may be cross-strapped between the C-band and L-band transponder.

The frequency translation mode employs two bandwidths: wide-band at 25 MHz and narrow-band at 2.5 MHz (in the C- to L-band cross-strap mode the wide-band bandwidth is 6 MHz). The narrow-band mode is identical to the wide-band except an improved signal-to-noise ratio is achieved for narrow-band signals by employing a narrow-band intermediate frequency amplifier prior to the limiter-amplifier and saturated traveling wave tube amplifier. The narrow-band intermediate frequency amplifier has 10 dB more gain than the wide-band intermediate frequency amplifier so that the intermediate frequency noise power will be the same for both bandwidths. Figure 5-4 is a block diagram of the ATS-5 L-band transponder and will be used to give a brief description of the transponder operation.

In the frequency translation mode the received signal at 1651 MHz is down converted to the transponder intermediate mode

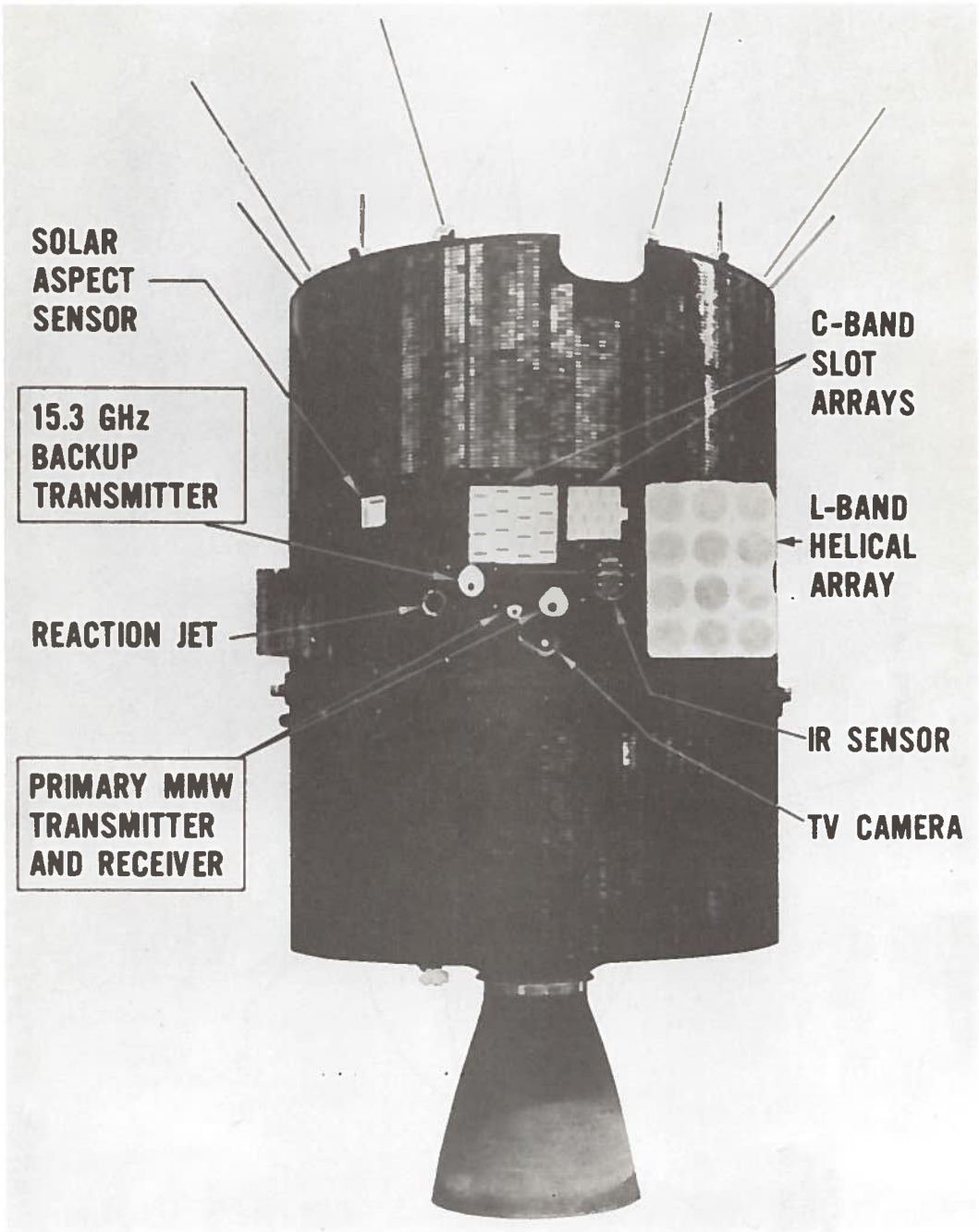

Figure 5-1. The ATS-5 Spacecraft

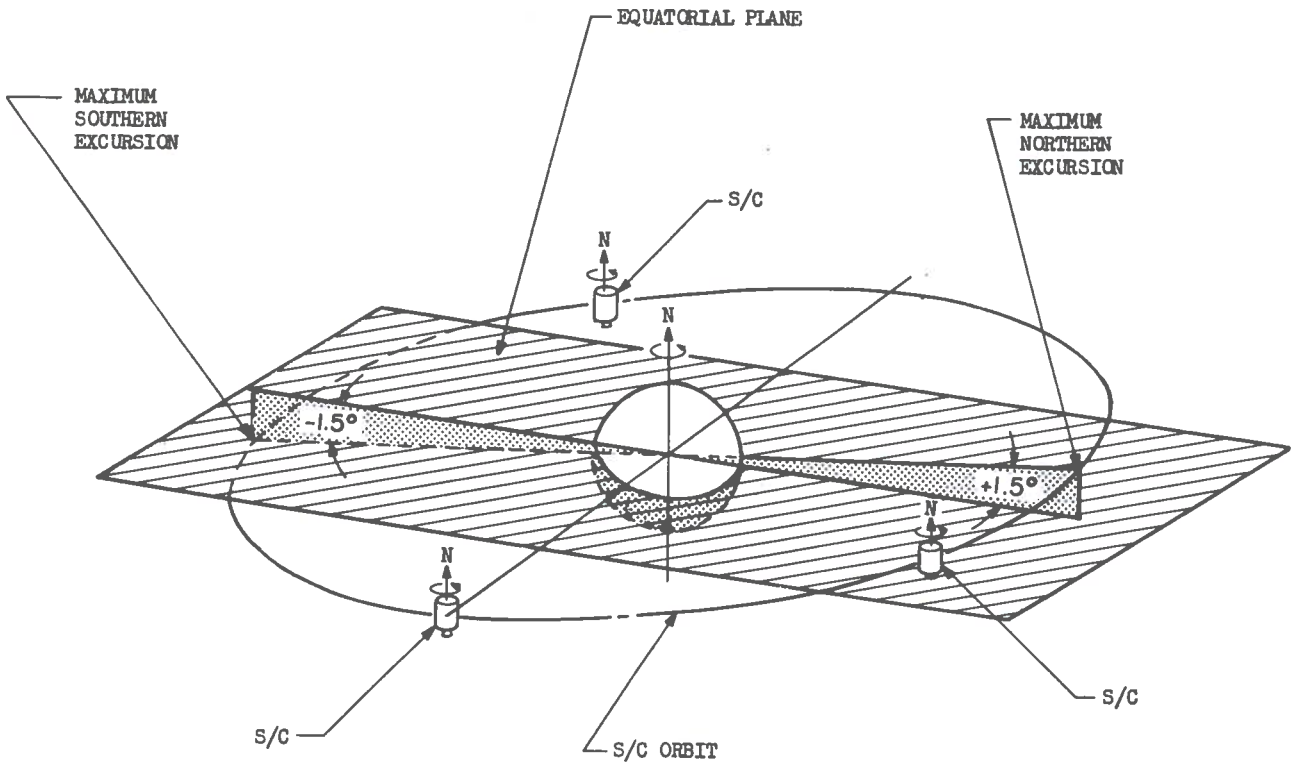

Figure 5-2. ATS-5 Orbit Geometry (July 1972). (After Kissel, 1970)

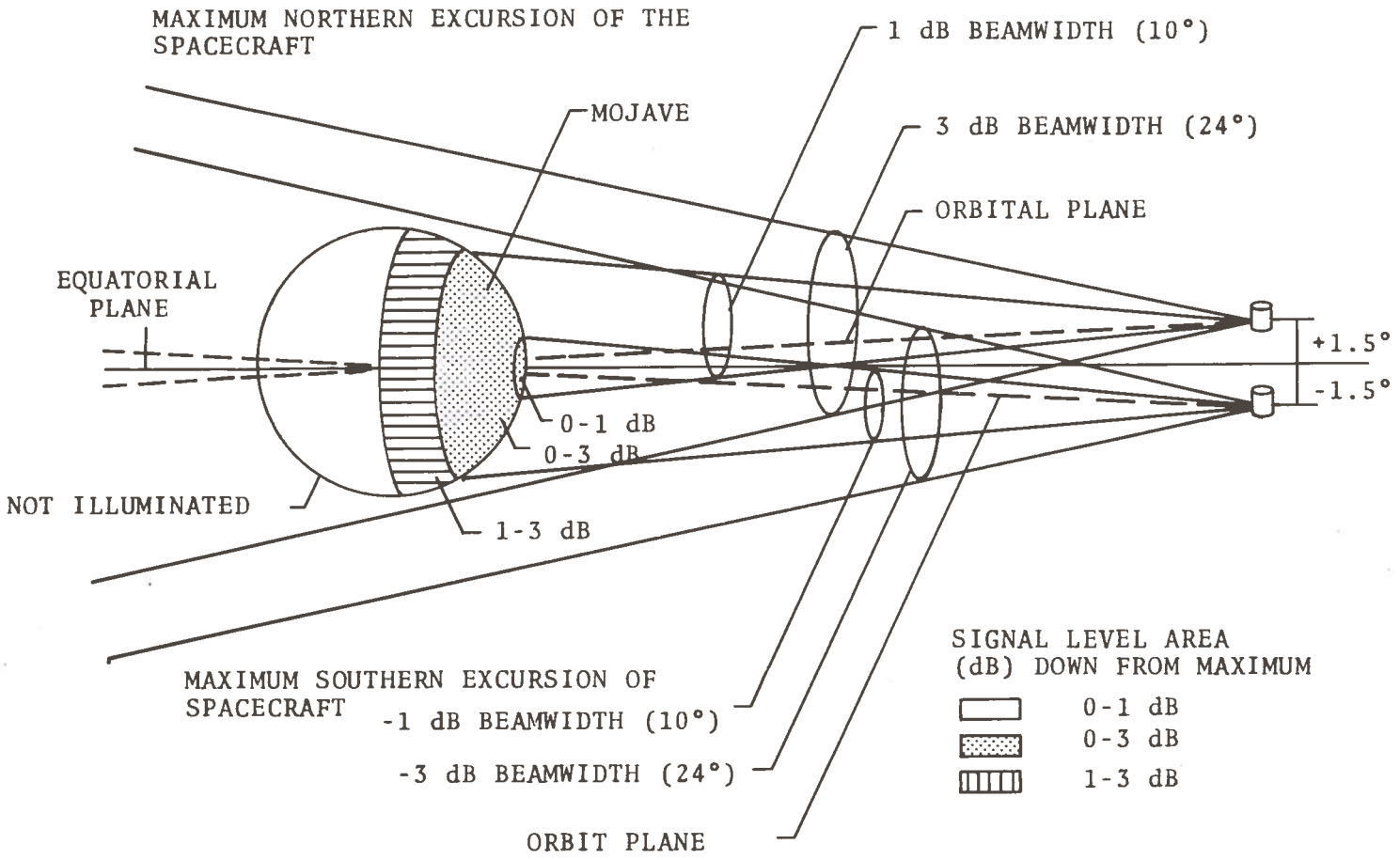

Figure 5-3. ATS-5 Earth Illumination Intensity (July 1972). (After Kissel 1970)

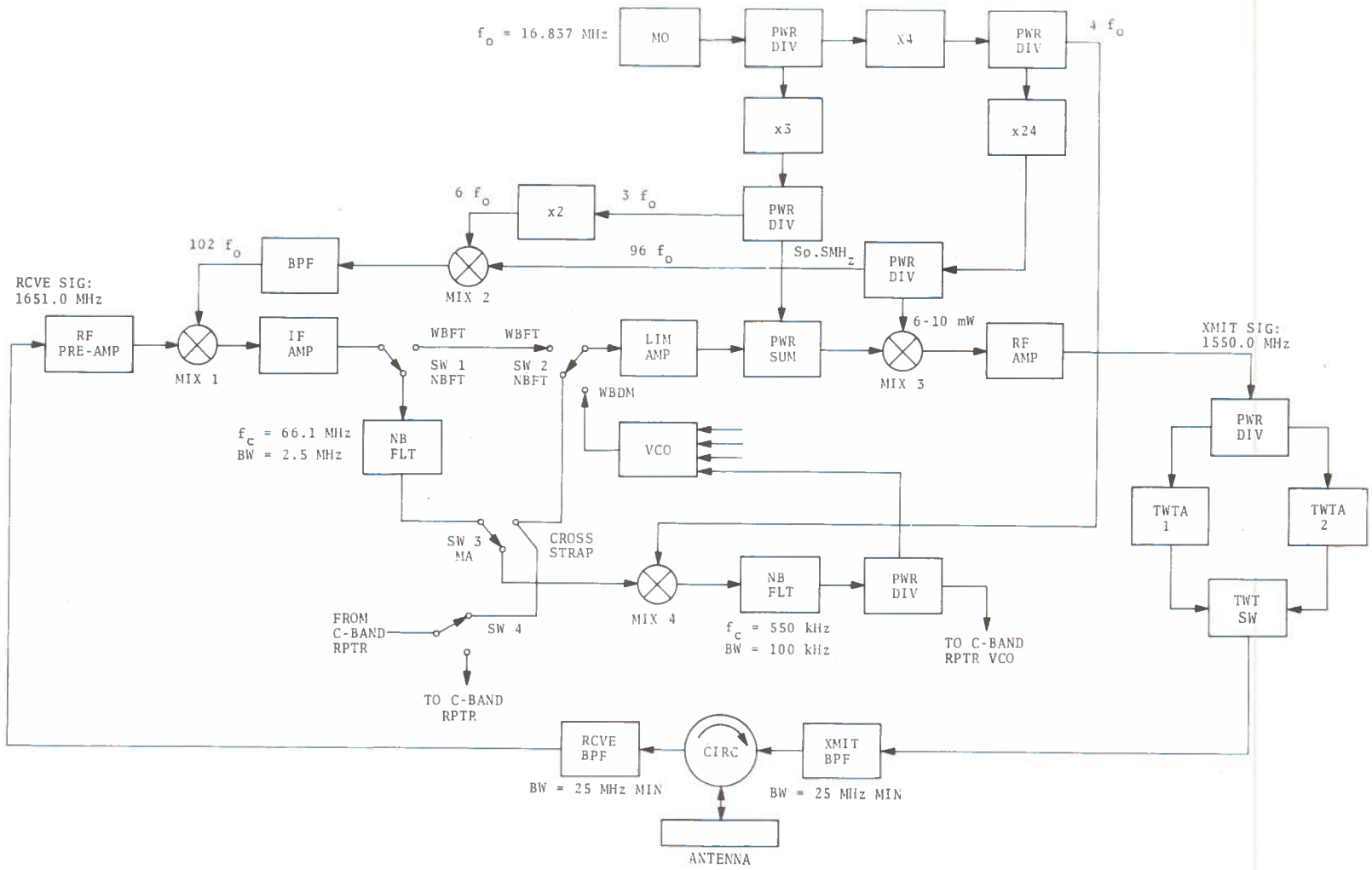

Figure 5-4. L-Band Transponder Block Diagram of the ATS-5 Spacecraft (After Kissel, 1970)

of 66.1 MHz in Mixer 1. The intermediate frequency signal is amplified and filtered if desired and limited. A beacon signal from the master oscillator at 50.511 MHz is then added to the intermediate frequency signal. The composite signal is then up converted in Mixer 3, amplified and retransmitted. The output power is shared between the transmitted signal and the beacon.

When the transponder is operated in the narrow-band frequency translation mode and the received signal at 1651 MHz is strong enough to saturate the intermediate frequency limiters, then the retransmitted signal will be at full strength and the beacon signal will be about 19 dB weaker than the retransmitted signal.*

If the received signal at 1651 is not strong enough to saturate the limiters the full retransmitted power will not be realized and the power at the beacon frequency will be stronger.

If no up-link signal is received and only receiver noise is retransmitted, then the beacon will be approximately 7 dB stronger than the case of the beacon when the retransmitted signal saturates the transponder's limiters. When the transponder is operated in the wide-band frequency translation mode and no signal is received, the beacon is the full 19 dB stronger or as strong as a carrier saturating the limiters would be.

When the transponder is operated in the C- to L-band cross-strap frequency translation mode the 66.1 MHz intermediate frequency signal from the C-band transponder is routed over to the L-band transponder for retransmission.

In the multiple access mode the received L-band signals are converted to video (500 to 600 kHz). The video signal is then used to modulate the transponder's voltage controlled oscillator. The nominal operating frequency of the transponder's voltage controlled oscillator is 65.89 MHz.

---

*The transponder's receiver now appears to have 6 dB less intermediate frequency gain than at launch, consequently it now takes a signal 6 dB stronger at 1651 MHz to saturate the limiter.

The wide-band data mode (WBDM) of operation is intended for transmitting spacecraft video data. In the wide-band data mode, no signal is received by the transponder. The 66 MHz voltage controlled oscillator that is used in the multiple access mode is also used to obtain an intermediate frequency signal for transmission at L-band. The intermediate frequency from the voltage controlled oscillator is strong enough to saturate the limiters. Under this condition there is no baseband video input to the voltage controlled oscillator which is left in a free running state. As a consequence, the L-band output in the wide-band data mode is an FM signal (the amplified voltage controlled oscillator signal) in which the FM modulation is comprised of the baseband video noise. Also the beacon in this mode is 19 dB below the wide-band signal.

The ATS-5 L-band transmit antenna pattern is shown in Figure 5-5 as measured at the Mojave STADAN ground station. Figure 5-6 illustrates the voltage controlled oscillator drift and master oscillator drift.

The final amplifier of the L-band transponder employs two 12 watt traveling wave tube amplifiers. The units may be run individually or in parallel. The circuit loss from the amplifier to the antenna is 2 dB and the antenna gain is 14 dB giving an equivalent iostropic radiated power of 52.8 dBm for one traveling wave tube (Kissel, 1970).

The transmitted signal is right-circular in polarization with an axial ratio less than 2 dB. For ground antennas with similar such ellipticities, the polarization loss is of the order of 0.2 dB. Table 5-1 lists the above factors in a power budget of the ATS-5 L-band signal.

The nominal signal strength received on the ground with an isotropic antenna is -136.7 dBm in the wide-band data mode or in the narrow-band frequency translation mode or the wide-band frequency translation mode if the uplink signal saturates the transponder's limiters. At the same time the beacon signal (approxi-

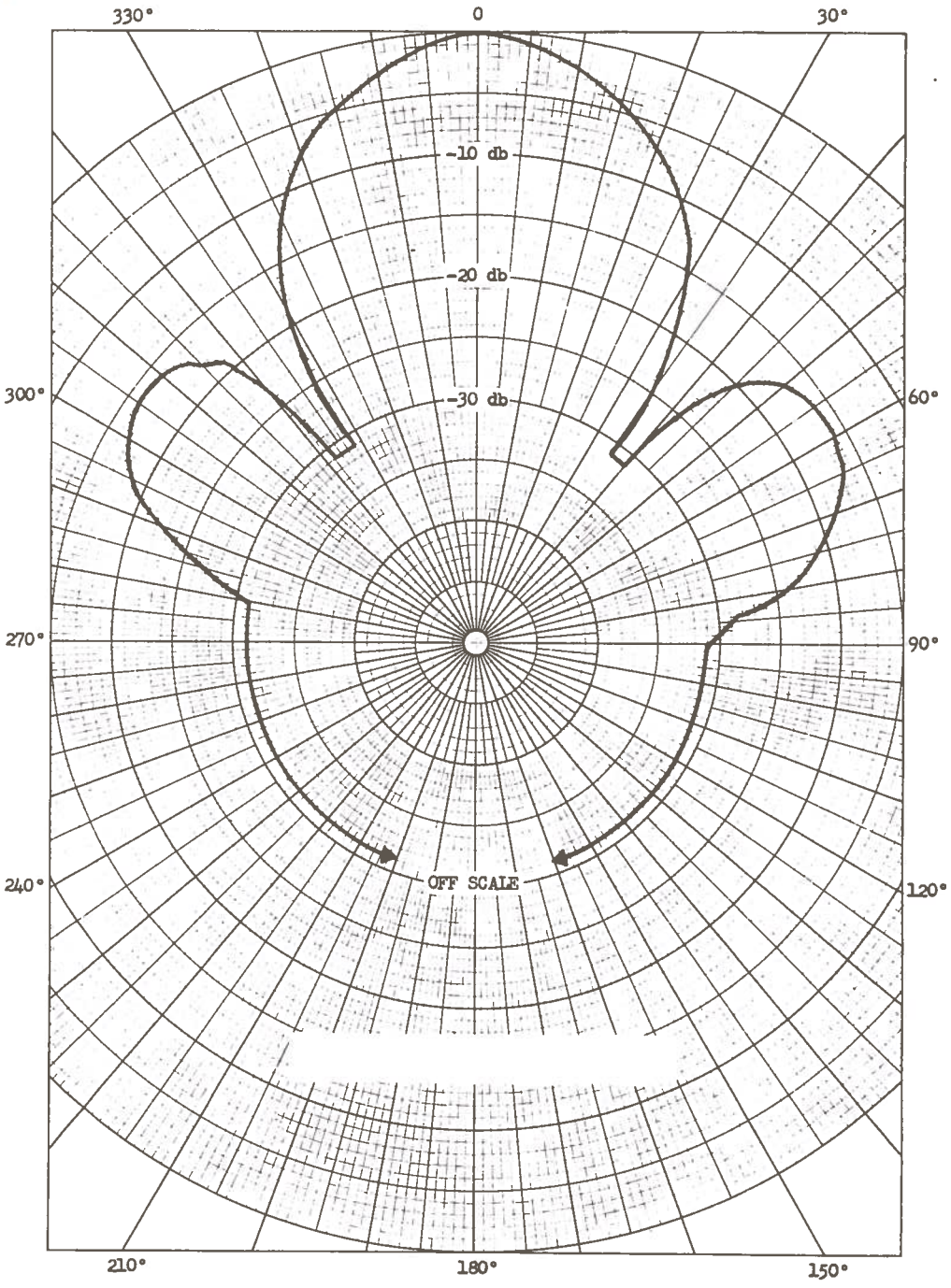

Figure 5-5. ATS-5 L-Band Transmit Antenna Pattern

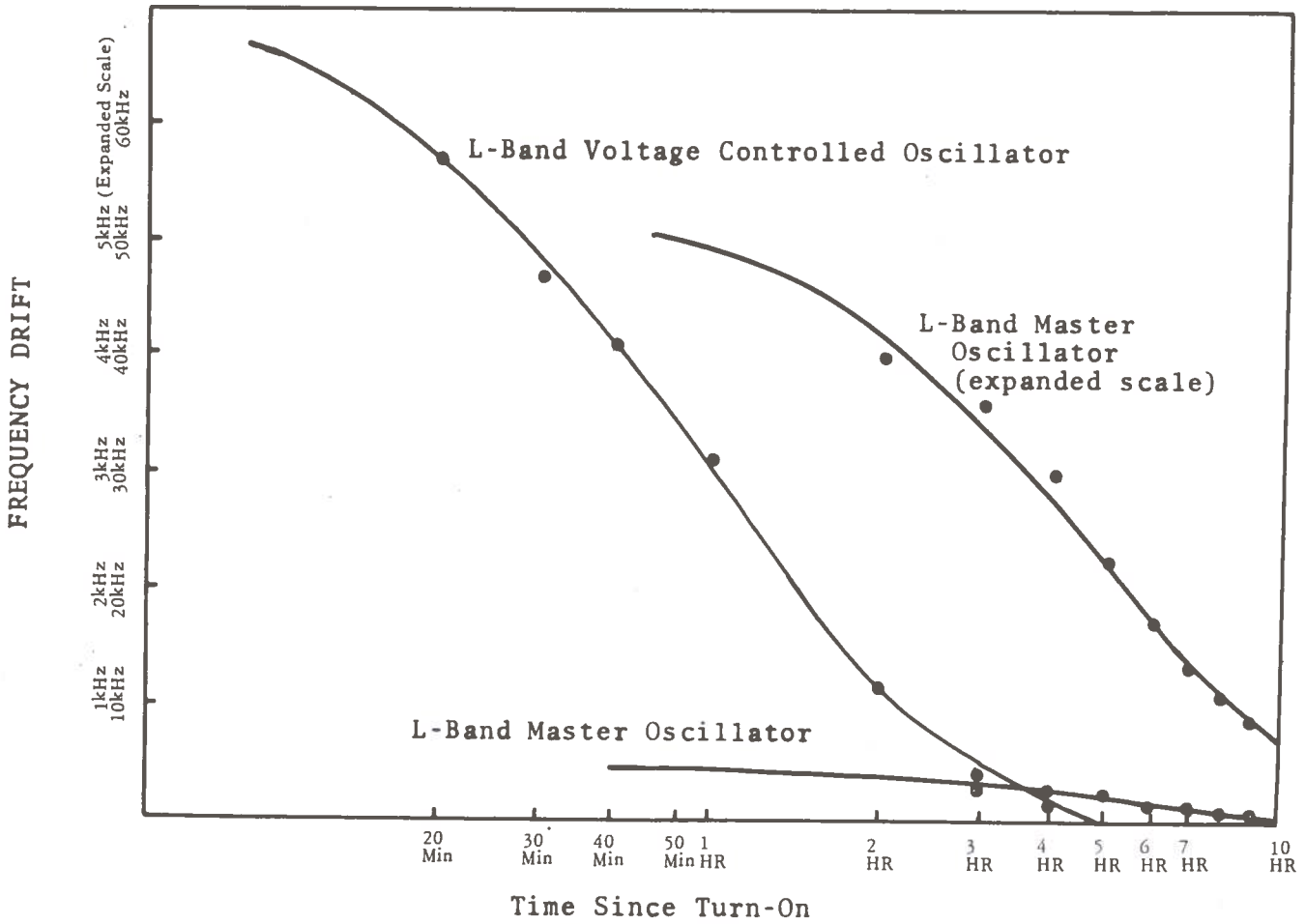

Figure 5-6. Plot of Voltage Controlled Oscillator and Master Oscillator Drift of the ATS-5 Satellite as a Function of Time since Turn-On

mately 16 MHz higher in frequency) would have a nominal strength of -156 dBm. The actual signal presented to the ground receiver will be stronger by the amount of the net antenna gain which in the case of a 10-foot diameter reflector is 30 dB.

Figure 5-7 illustrates the predicted variation in signal strength and elevation angle for the TSC/Westford Propagation Facility in Westford, Massachusetts. This figure was prepared from the NASA predictions for the ATS-5 spacecraft as would be seen from Westford. The predictions are calculated from the measured orbital elements of the ATS-5 spacecraft.

Figure 5-8 is the best estimate of the wide-band data mode spectrum. This was prepared from many measured spectra. The spectra were measured using an HP 8552/8553 spectrum analyzer. Figures 5-9a and 5-9b are typical of the wide-band data mode spectra. Figures 5-9c is typical of the spectrum of the beacon signal.

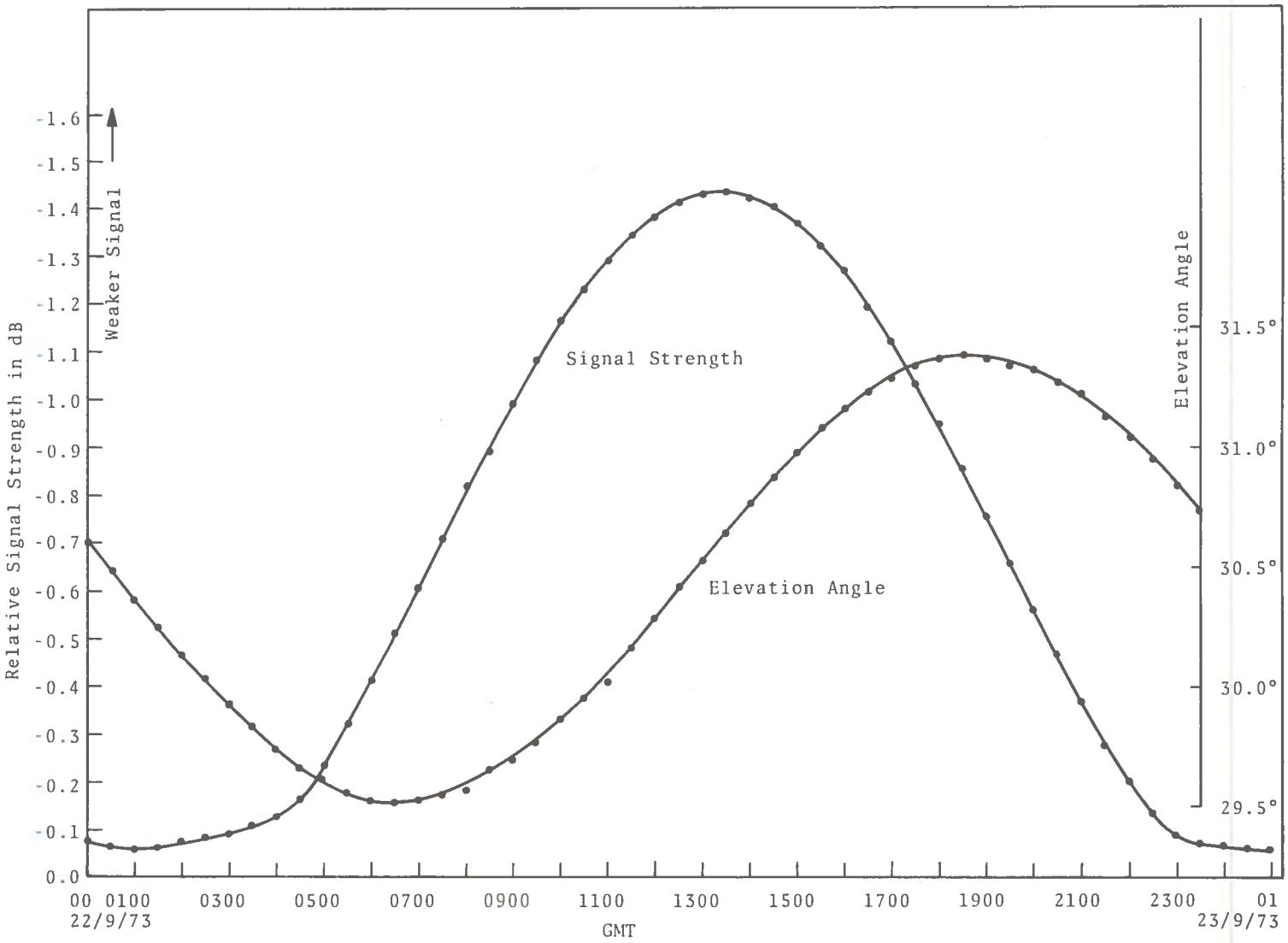

Figure 5-7. NASA Predictions of ATS-5 Signal Strength for the DOT/TSC/Westford Propagation Facility (22 Sept. 1973)

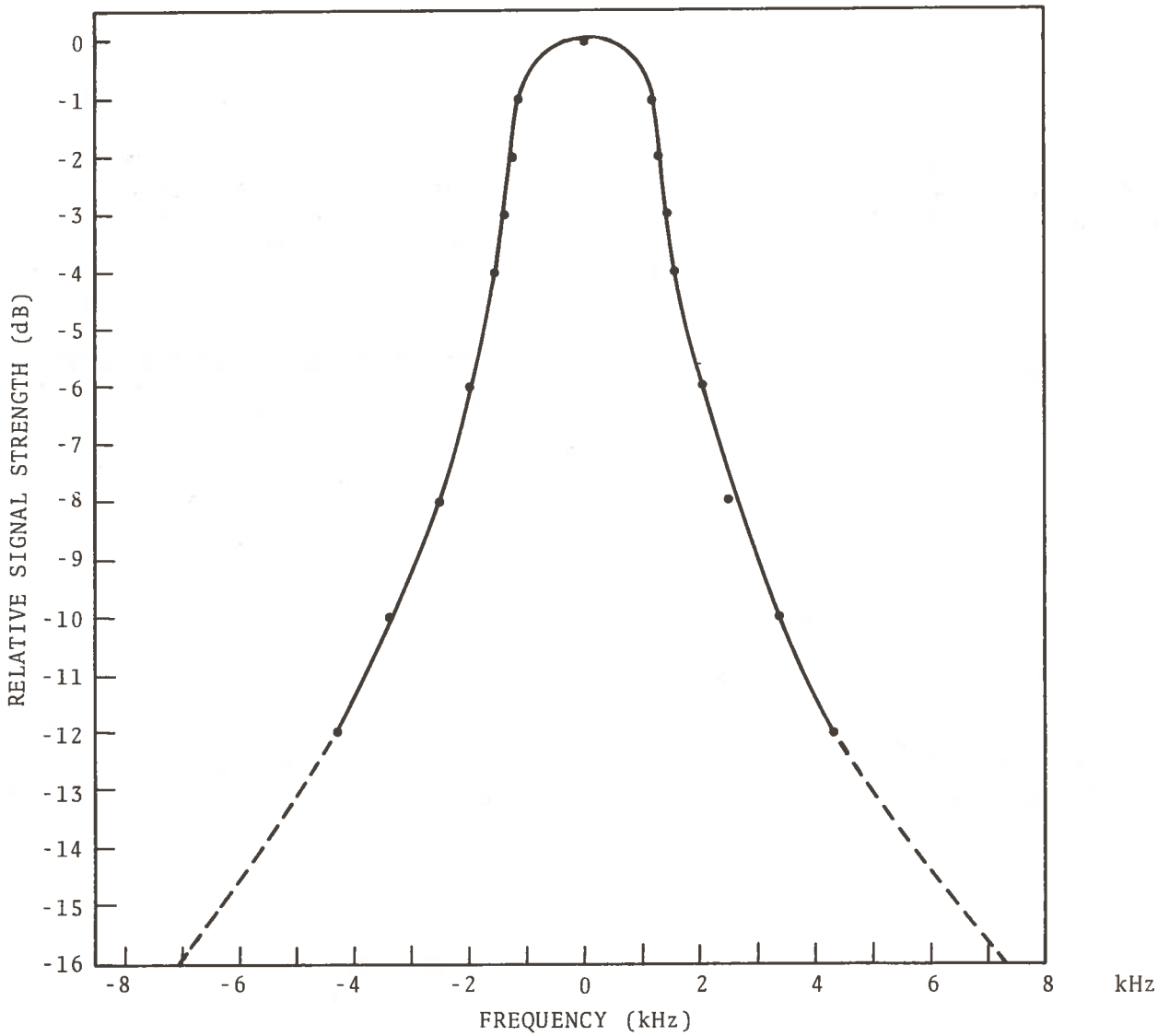

Figure 5-8. Spectrum of the Wide-Band Data Mode Signal

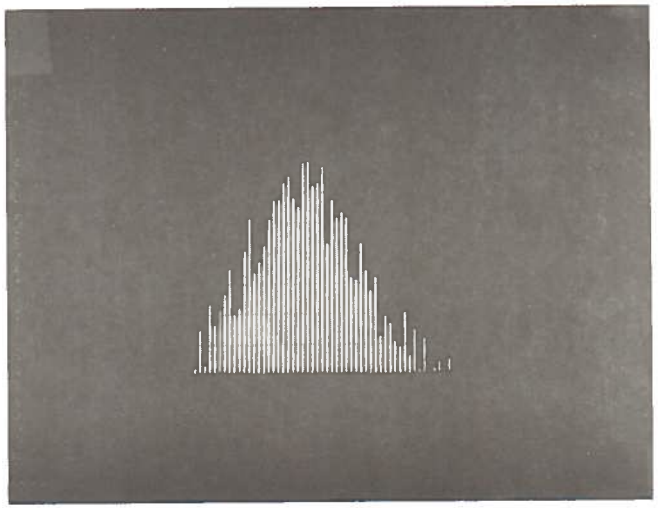

Figure 5-9a. Spectra of Wide-Band Data Mode (WBDM) Signal from ATS-5 Spacecraft (Vertical: 2 dB/div., Horizontal: 1 KHZ/div.)

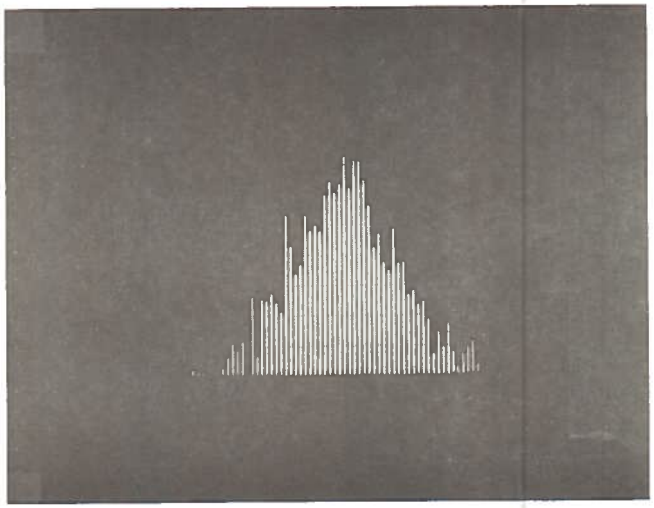

Figure 5-9b. Spectra of Wide-Band Data Mode (WBDM) Signal from ATS-5 Spacecraft (Vertical: 2 dB/div., Horizontal: 1 KHZ/div.)

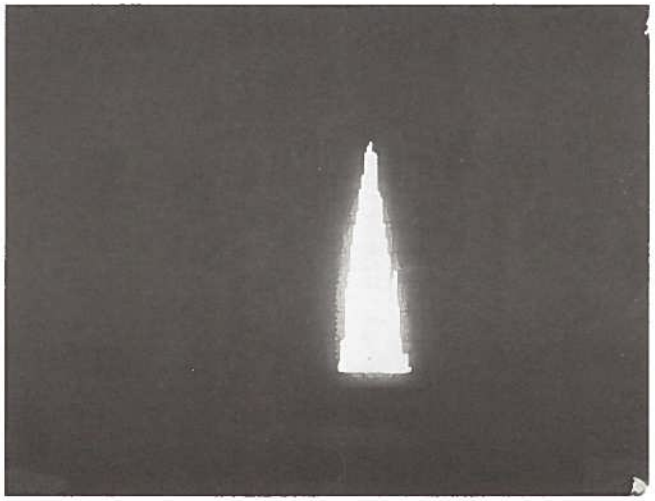

Figure 5-9c. Spectrum of the ATS-5 L-Band Beacon Signal
(Vertical: 2 dB/div., Horizontal: 50 Hz/div.)

6. THEORY OF THE AMPLITUDE MEASUREMENT

6.1 DISCUSSION OF VARIOUS MEASUREMENT TECHNIQUES

The two conventional techniques used for measuring the amplitude of a continuous wave signal are coherent and incoherent detection. In the case of coherent detection, the ground receiver's local oscillator is phase locked to the signal. In order to determine the signal strength the input signal is product-detected by the phase locked local oscillator which has been shifted in phase by 90°. The results of mixing are low-passed and the resulting DC voltage is proportional to the signal amplitude. Though the signal is continually "tuned-in", this detection technique has several limitations which are important. The first limitation is that the signal must be phased locked; in general this necessitates that at least a 6 dB signal-to-noise ratio in the lock loop exist, which in turn is determined by many factors. In the case of weak signal reception the phase lock tracking error may be too large to permit useable coherent detection techniques. Because of the method of signal detection, the linear dynamic range above lock is 10 to 12 dB, after which it is necessary to employ automatic gain control in order to assure that the phase detector in the lock loop is not overloaded.

The more conventional method of detection is to use a square-law detector after the final intermediate frequency amplifier. The signal in the output of the final intermediate frequency filter and amplifier is square-law detected. The linear dynamic range of this type of detector is greater than 20 dB. When the signal strength is greater than 20 dB it is necessary to employ automatic gain control in order to insure that the detector is operating in its linear range.

The automatic gain control voltage is developed by detecting the noise power across the whole bandpass of the receiver. Consider for example, a receiver employing a first intermediate frequency of 30 MHz with a 5 MHz bandwidth while the second intermediate frequency is 10 MHz, with a bandwidth of a few kilohertz.

A portion of the 5 MHz wide 30 MHz intermediate frequency is coupled into radio frequency amplifier automatic gain control detector. This detected voltage is appropriately filtered and applied to the first and second intermediate frequency stages to insure that the receiver does not become overloaded. In some more advanced receivers, a sample of the detected signal at the second intermediate frequency is proportionally added to the automatic gain control voltage detected at the first intermediate frequency. This combination is then used to perform the automatic gain control action of the receiver. In general, the automatic gain control voltage is indicative of the signal strength, but usually not as simply related to the signal strength as is the voltage developed in the phase detector or the square-law detector voltage. In the case of weak signals, the automatic gain control action is very small and consequently the automatic gain control voltage is usually directly related to the signal and noise power in the receiver's intermediate frequency amplifiers.

When the phase detector or the filtered intermediate frequency square-law detector are used for measuring signal strength, it is necessary that the detectors be operating in their linear range. When this is the case, only the constant relating signal strength to volts of output needs to be known for relative measurements. For absolute signal strengths, the absolute calibration of one point in the operating range also needs to be known. Care must be taken to insure that in fact, the detector is always operating in its linear operating range.

The use of the developed automatic gain control voltage, in general requires complete calibration throughout the operating range when used for accurate signal strength measurements.

6.2 CALIBRATION TECHNIQUES

The last section referenced the calibration required of the receiver used in the measurement. However, indicating and display devices using the detector voltages must also have their calibrations determined. This is true whether the device be a simple

voltmeter, a strip-chart recorder or an elaborate digital computer interface.

System calibration should first be performed by injection of a continuous wave signal of known level and purity into the receiver's radio frequency input port through a set of precision attenuators. This calibration signal may be used to insure that the overall receiving system is operating in a linear fashion. The actual detector response should be calibrated using precision intermediate frequency attenuators and not attenuators at radio frequency, since the intermediate frequency attenuators are usually much more accurate.

When it is desired to make an absolute signal strength measurement, the absolute strength of the injected signal must be known. Moreover, the long term stability of this calibration must be more than adequate to measure the long term absolute calibration of the receiving system. Also the losses and the stability of the losses not included in the system calibration (i.e. antenna transmission lines) must be known as well as the antenna gain.

6.3 DISCUSSION OF THE EQUIPMENT CALIBRATION USED IN THIS MEASUREMENT PROGRAM

In order to insure that the receiving system as well as the data acquisition, analysis and display systems are working properly, extensive calibration of the individual components as well as the overall system should be performed using techniques previously discussed. Since the measurement program involves using only incoherent detection, only the incoherent detection calibration will be discussed in the next section.

A signal generator is used for the overall system calibration. The generator was phase locked to a synthesizer to provide accurate phase stability and purity of the signal. The generator is internally amplitude leveled by using a PIN diode attenuator. Since the frequency controlling synthesizer is locked to the station standard, the generator's stability is that of the station standard (2 parts 10^{11} per day). The short term amplitude stability was found to be 0.05 dB peak to peak in a ten minute period and 0.1 dB peak to peak

in an hour. This provides an adequate means of measuring the overall system stability. This signal is also used to insure that the various intermediate frequency sections are also operating in their linear region of operation. The square-law response of the various detectors was established and calibrated using a precision intermediate frequency attenuator.

The calibration of the overall digital processing equipment should be established by using signals of known characteristics. These characteristics can be determined from careful analog measurements.

In the case of measurements of the ATS-5 spacecraft proper consideration must be given to modulation induced upon the signals by the spinning of the spacecraft. To accurately measure the receiver's response to the pulsating ATS-5 signal, a simulator was constructed that could be used to amplitude modulate the PIN attenuator of the calibration signal generator. Consequently the pulsed signal generator has the same rise and fall shape as well as the same pulse duration and period of the signal received from the ATS-5 spacecraft.[1]

Moreover, the spectral purity of the wide-band data signal is not the same as the beacon signal, consequently calibration must also be performed with a signal whose spectrum is similiar to that of the wide-band data mode signal of the satellite.

6.4 ERROR ANALYSIS OF THE MEASUREMENT

There are several possible sources of error in the measurement of a signal strength. Some errors may be measured, others calculated from measurements and others determined from system and operating parameters. Those errors associated with the receiver

---

1. Many communication receivers are not able to faithfully detect a pulsed signal. When such a receiver is calibrated with a continuous wave signal and then used to measure a pulsed signal the continuous wave calibration may be invalid measure of the response of the receiver to a pulsed signal.

involve the receiver noise, receiver bandwidth and operating signal-to-noise ratio.

In a properly designed and operating receiver, the overall system noise should be determined by the first radio frequency stage, be it an amplifier or a mixer. The ratio of the root-mean-square noise fluctuations to the signal level fluctuations of interest determines the limit of the precision that will be attainable in measuring the signal level.

The final intermediate frequency bandwidth just prior to detection should ideally be matched to the spectrum of the signal to be measured. Practical limitations such as tuning and frequency stability usually necessitate the use of wider bandwidth. Likewise, a noisy spectrum due to an unstable transmitter may dictate a wider receiving bandwidth. Consequently, if the receiving bandwidth is narrower than the signal's spectrum, then only a portion of radiated power will be received and the indicated signal strength will be less than expected without allowances for bandwidth.

The signal-to-noise ratio, or more precisely, the signal plus noise-to-noise ratio, places an upper bound on the precision with which a measurement of the signal is possible. The receiver's statistical noise fluctuations are related to the total noise power, predetection bandwidth and post detection filtering. As an example of the effect of signal-to-noise on measurement precision, a series of examples are worked out to illustrate these points.

The ATS-5 signal is used as an example with a signal strength of -137 dBm at the Earth (See Table 5-1, column 1). The -137 dBm, it will be recalled, is the signal strength as received by an isotrophic antenna. Also the transponder would be in the wide-band data mode or the frequency translation mode with the limiters saturated. As before, the beacon in these modes would be -156 dBm. If the mode is wide-band frequency translation and with no input signal then the beacon would again be -137 dBm.

Figure 6-1 may be used to determine the operating signal-to-noise ratio for various receiving combinations. The signal curve

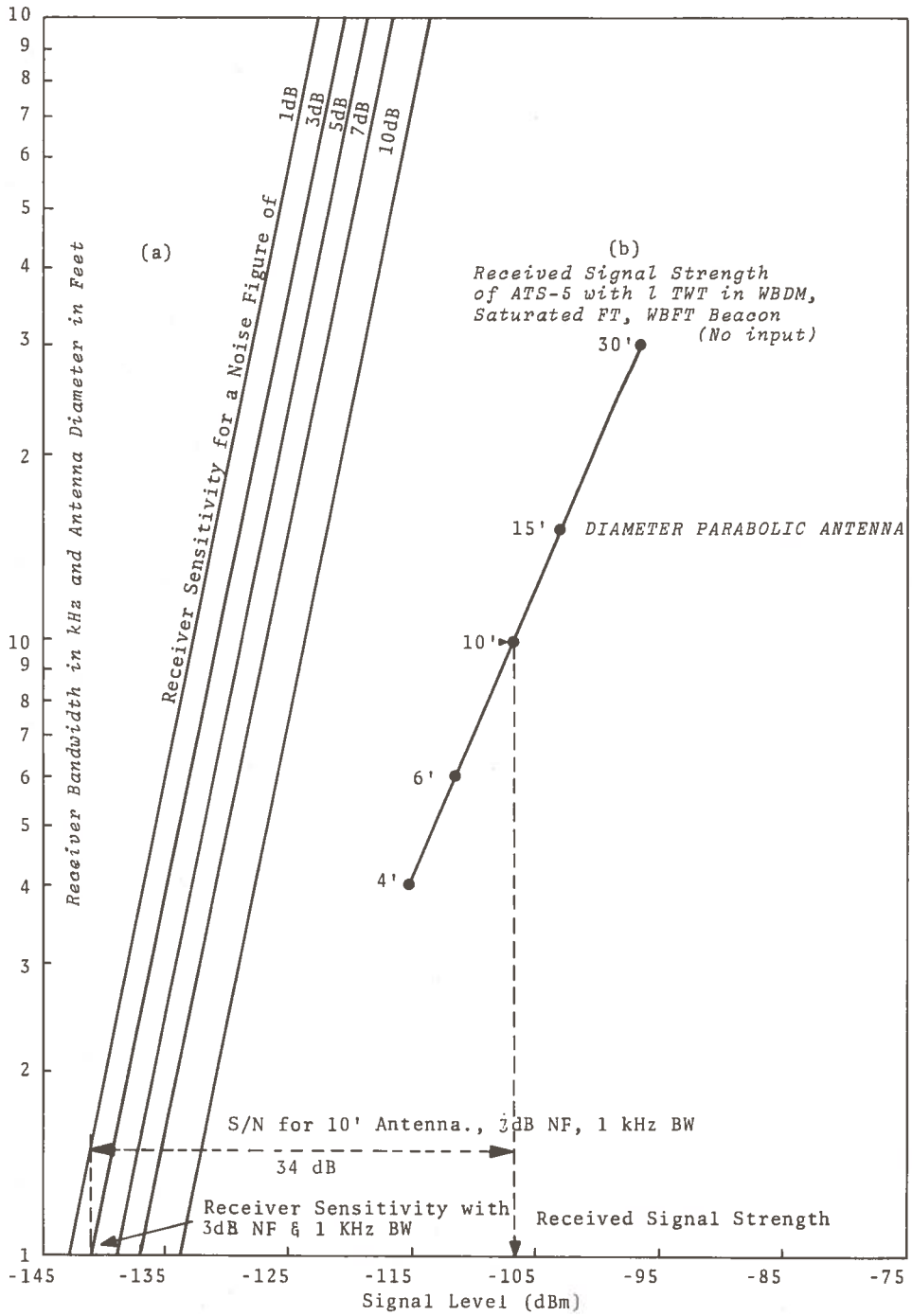

Figure 6-1 (a) Receiver Sensitivity Versus Various Noise Figures

(b) Signal Strength of ATS-5 L-Band Transmissions for Various Parabolic Antenna Diameters

on the right is used to determine the received signal strength for various antenna diameters. The example shown in Figure 6-1 illustrates the receiving equipment used for the measurements taken at Westford, Mass. The 10 foot mark on the ordinate corresponds to the -107 dBm mark on the abscissa when using the signal strength curve.

The set of 5 curves on the left of Figure 6-1 are used to determine the receiving system sensitivity for five different noise figures. To continue, for example, in using the 3 dB noise figure curve, a bandwidth of 1 kHz on the ordinate corresponds to a -141 dBm sensitivity on the abscissa.

The differences between the received signal strength (-107 dBm) and the receiving sensitivity (-141 dBm) is the operating signal-to-noise ratio for the example.

The receiver noise fluctuations present the upper limit of the precision with which the mean signal level may be measured. Figure 6-2 presents the root-mean-square noise fluctuations for various bandwidths and video time constants. For example, with a 20 kHz bandwidth and a 3 ms time constant, the root-mean-square fluctuation level is about 0.16 dB with the peak-to-peak fluctuations 5 to 6 times this value.

In addition to induced receiver noise errors, there is an error created as the signal strength is measured and processed. In the case of digital processing, an error occurs when the receiver's signal is digitized and addition errors occur as the digital number is processed. For the measurements taken at Westford the total digitizing error is composed of 0.055 dB root-mean-square encoding error and 0.05 dB quantizing error. The information from the measurements is outputed from the digital processing equipment with a resolution of 0.1 dB.

In an effort to measure the errors due to the overall system, a calibrated signal generator was used, as mentioned in the previous section. The particular equipment configuration used in the calibration data to be presented here is discussed in Section 4.2.3. Figure 4-9 is the appropriate block diagram. The detected

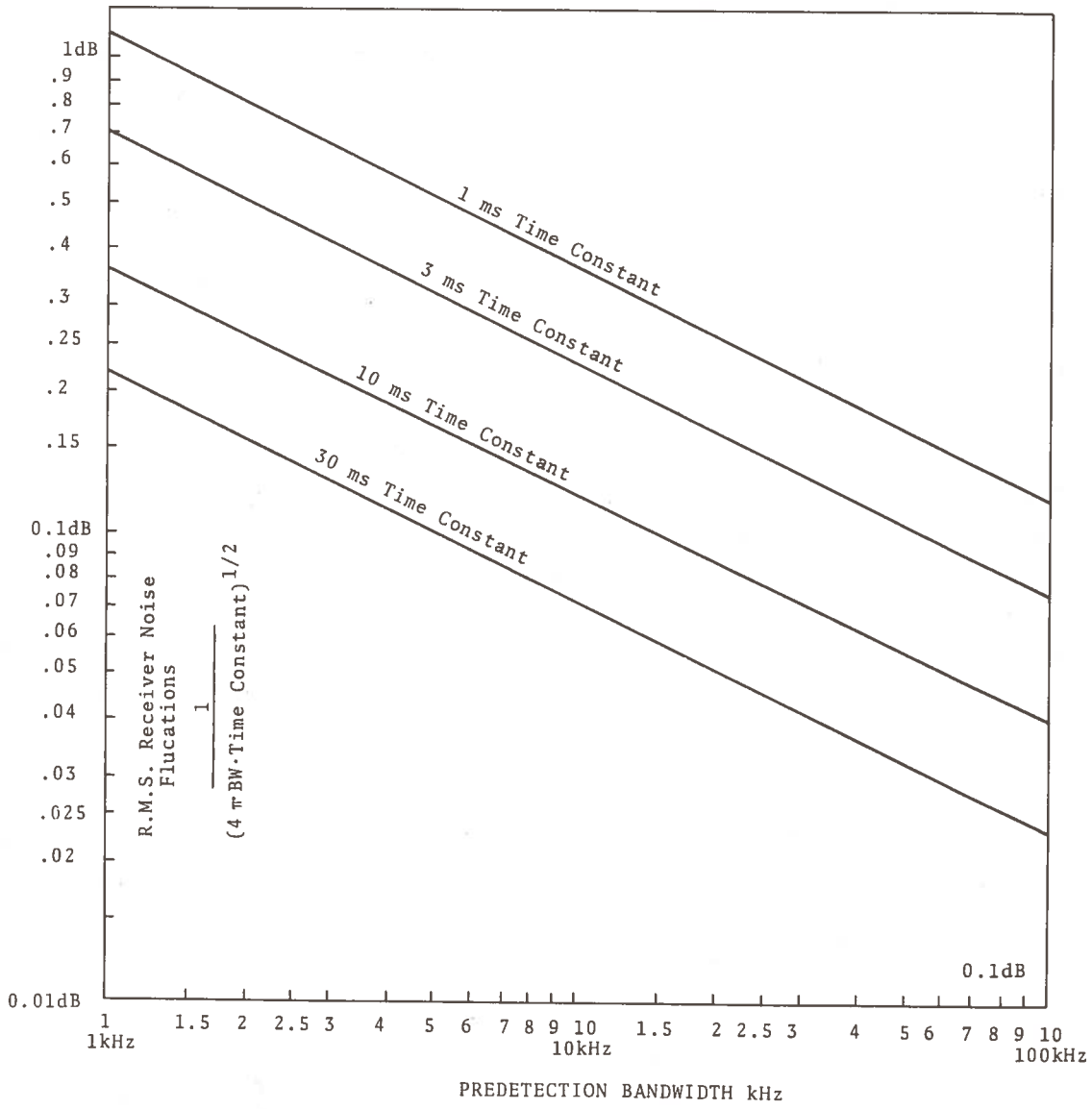

Figure 6-2. Root-Mean-Square Receiver Noise Fluctuations Versus Predetection Bandwidth for Various Video Time Constants

output "E" for the East receiving system and the output "E" for the West receiving system were used. They were fed into the computer multiplex unit as shown in Figure 4-6. They were also recorded on analog strip chart recorders.

Calibration for a pure continuous wave signal were obtained. Calibrations were also obtained using on FM noise modulated signal generator whose spectrum matched that of the spacecraft as nearly as possible.

Figure 6-3 is the measured probability density plot of the continuous wave signal generator for two fifteen minute periods. Each fifteen minute run is composed of three five minute runs. Figure 6-4 is the two fifteen minute runs averaged. Tables 6-1, 6-2 and 6-3 are the respective computer printouts for the first and second fifteen minute runs and the average of the two runs. The probability distribution plots for these respective densities are plotted in Figures 6-5 and 6-6. Tables 6-4, 6-5 and 6-6 are the respective computer printouts for the first and second fifteen minute runs and the average of the two runs. (Note that a gaussian distribution would appear as a straight line on Figures 6-5 and 6-6.)

Figure 6-7a is a photograph of the spectrum that was used to calibrate the system in order to simulate the wide-band data mode signal of the ATS-5 spacecraft. Figure 6-7b is a photograph of the wide-band data mode signal from the ATS-5 spacecraft.

Figure 6-8 is a plot of the measured probability density of the FM noise modulated signal generated for two fifteen minute periods. Each 15 minute period is composed of three five minute periods. Figure 6-9 is a plot of the two fifteen minute runs averaged. Tables 6-7, 6-8 and 6-9 are the respective computer printouts for the first and second fifteen minute runs and the average of the two. The probability distribution plots for these respective densities are plotted in Figures 6-10 and 6-11. Tables 6-10, 6-11, and 6-12 are the respective computer printours for the first and second fifteen minute runs and the average of the two.

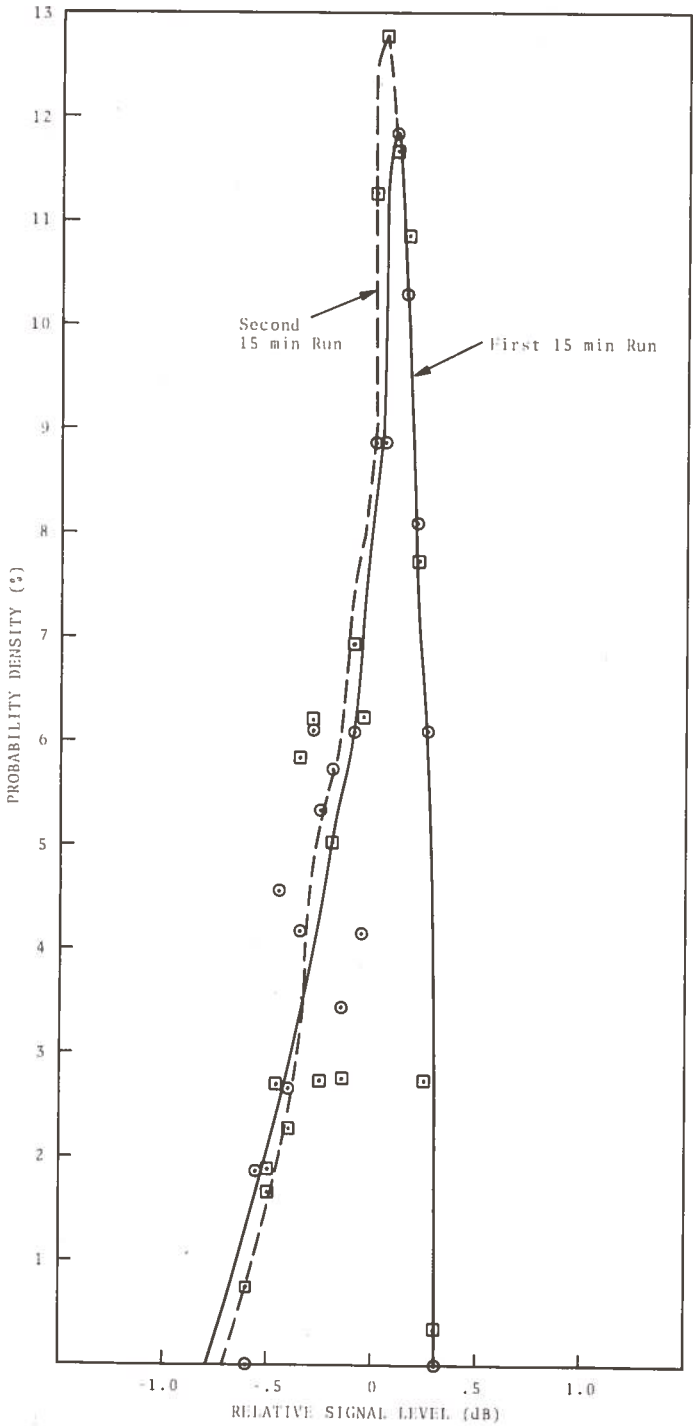

Figure 6-3 Probability Density Plot of the First and Second 15-Minute Runs of a Continuous Wave Signal Generator

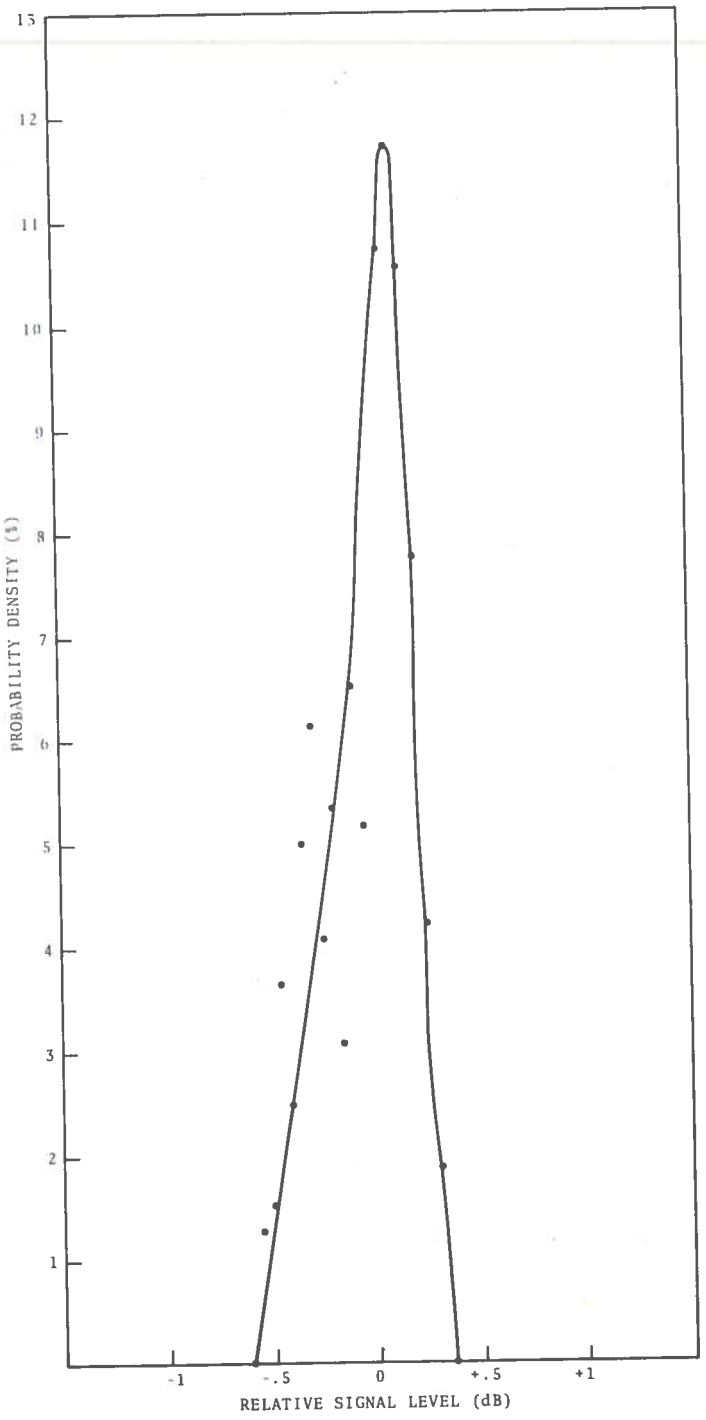

Figure 6-4 Probability Density Plot of the Average of the Two 15-Minute Runs of a Continuous Wave Signal Generator

TABLE 6-1 PROBABILITY DENSITY FOR THE FIRST 15-MINUTE RUN OF A CONTINUOUS WAVE SIGNAL GENERATOR

PROBABILITY DENSITY TABLE FOR ATS-5 DATA
VALUES GIVEN ARE IN PERCENT TIMES 100

	Ø.Ø	Ø.1	Ø.2	Ø.3	Ø.4	Ø.5	Ø.6	Ø.7	Ø.8	Ø.9
-105DBM	Ø	Ø	Ø	Ø	Ø	Ø	Ø	Ø	Ø	Ø
-106DBM	Ø	Ø	Ø	Ø	Ø	Ø	Ø	Ø	Ø	Ø
-107DBM	Ø	Ø	Ø	Ø	Ø	Ø	Ø	Ø	Ø	Ø
-108DBM	Ø	Ø	Ø	Ø	Ø	Ø	Ø	Ø	Ø	Ø
-109DBM	Ø	Ø	Ø	Ø	Ø	Ø	Ø	Ø	Ø	Ø
-110DBM	Ø	Ø	Ø	Ø	Ø	Ø	Ø	Ø	Ø	Ø
-111DBM	Ø	Ø	Ø	Ø	Ø	Ø	Ø	Ø	Ø	Ø
-112DBM	Ø	Ø	Ø	Ø	Ø	Ø	Ø	Ø	Ø	Ø
-113DBM	Ø	Ø	Ø	Ø	Ø	Ø	Ø	Ø	Ø	Ø
-114DBM	Ø	Ø	Ø	Ø	Ø	610	801	1030	1183	877
-115DBM	877	419	610	343	572	534	610	419	267	458
-116DBM	190	190	Ø	Ø	Ø	Ø	Ø	Ø	Ø	Ø
-117DBM	Ø	Ø	Ø	Ø	Ø	Ø	Ø	Ø	Ø	Ø
-118DBM	Ø	Ø	Ø	Ø	Ø	Ø	Ø	Ø	Ø	Ø
-119DBM	Ø	Ø	Ø	Ø	Ø	Ø	Ø	Ø	Ø	Ø
-120DBM	Ø	Ø	Ø	Ø	Ø	Ø	Ø	Ø	Ø	Ø
-121DBM	Ø	Ø	Ø	Ø	Ø	Ø	Ø	Ø	Ø	Ø
-122DBM	Ø	Ø	Ø	Ø	Ø	Ø	Ø	Ø	Ø	Ø
-123DBM	Ø	Ø	Ø	Ø	Ø	Ø	Ø	Ø	Ø	Ø
-124DBM	Ø	Ø	Ø	Ø	Ø	Ø	Ø	Ø	Ø	Ø

TABLE 6-2 PROBABILITY DENSITY FOR THE SECOND 15-MINUTE RUN OF A CONTINUOUS WAVE SIGNAL GENERATOR

PROBABILITY DENSITY TABLE FOR ATS-5 DATA
VALUES GIVEN ARE IN PERCENT TIMES 100

	Ø.Ø	Ø.1	Ø.2	Ø.3	Ø.4	Ø.5	Ø.6	Ø.7	Ø.8	Ø.9
-105DBM	Ø	Ø	Ø	Ø	Ø	Ø	Ø	Ø	Ø	Ø
-106DBM	Ø	Ø	Ø	Ø	Ø	Ø	Ø	Ø	Ø	Ø
-107DBM	Ø	Ø	Ø	Ø	Ø	Ø	Ø	Ø	Ø	Ø
-108DBM	Ø	Ø	Ø	Ø	Ø	Ø	Ø	Ø	Ø	Ø
-109DBM	Ø	Ø	Ø	Ø	Ø	Ø	Ø	Ø	Ø	Ø
-110DBM	Ø	Ø	Ø	Ø	Ø	Ø	Ø	Ø	Ø	Ø
-111DBM	Ø	Ø	Ø	Ø	Ø	Ø	Ø	Ø	Ø	Ø
-112DBM	Ø	Ø	Ø	Ø	Ø	Ø	Ø	Ø	Ø	Ø
-113DBM	Ø	Ø	Ø	Ø	Ø	Ø	Ø	Ø	Ø	Ø
-114DBM	Ø	Ø	Ø	Ø	38	271	775	1085	1162	1279
-115DBM	1124	620	697	271	503	271	620	581	232	271
-116DBM	116	77	Ø	Ø	Ø	Ø	Ø	Ø	Ø	Ø
-117DBM	Ø	Ø	Ø	Ø	Ø	Ø	Ø	Ø	Ø	Ø
-118DBM	Ø	Ø	Ø	Ø	Ø	Ø	Ø	Ø	Ø	Ø
-119DBM	Ø	Ø	Ø	Ø	Ø	Ø	Ø	Ø	Ø	Ø
-120DBM	Ø	Ø	Ø	Ø	Ø	Ø	Ø	Ø	Ø	Ø
-121DBM	Ø	Ø	Ø	Ø	Ø	Ø	Ø	Ø	Ø	Ø
-122DBM	Ø	Ø	Ø	Ø	Ø	Ø	Ø	Ø	Ø	Ø
-123DBM	Ø	Ø	Ø	Ø	Ø	Ø	Ø	Ø	Ø	Ø
-124DBM	Ø	Ø	Ø	Ø	Ø	Ø	Ø	Ø	Ø	Ø

TABLE 6-3 PROBABILITY DENSITY FOR THE AVERAGE OF THE FIRST AND SECOND 15-MINUTE RUNS OF A CONTINUOUS WAVE SIGNAL GENERATOR

PROBABILITY DENSITY TABLE FOR ATS-5 DATA
VALUES GIVEN ARE IN PERCENT TIMES 100

	Ø.Ø	Ø.1	Ø.2	Ø.3	Ø.4	Ø.5	Ø.6	Ø.7	Ø.8	Ø.9
-105DBM	Ø	Ø	Ø	Ø	Ø	Ø	Ø	Ø	Ø	Ø
-106DBM	Ø	Ø	Ø	Ø	Ø	Ø	Ø	Ø	Ø	Ø
-107DBM	Ø	Ø	Ø	Ø	Ø	Ø	Ø	Ø	Ø	Ø
-108DBM	Ø	Ø	Ø	Ø	Ø	Ø	Ø	Ø	Ø	Ø
-109DBM	Ø	Ø	Ø	Ø	Ø	Ø	Ø	Ø	Ø	Ø
-110DBM	Ø	Ø	Ø	Ø	Ø	Ø	Ø	Ø	Ø	Ø
-111DBM	Ø	Ø	Ø	Ø	Ø	Ø	Ø	Ø	Ø	Ø
-112DBM	Ø	Ø	Ø	Ø	Ø	Ø	Ø	Ø	Ø	Ø
-113DBM	Ø	Ø	Ø	Ø	Ø	Ø	Ø	Ø	Ø	Ø
-114DBM	Ø	Ø	Ø	Ø	19	442	788	1057	1173	1076
-115DBM	1000	519	653	307	538	403	615	500	250	365
-116DBM	153	134	Ø	Ø	Ø	Ø	Ø	Ø	Ø	Ø
-117DBM	Ø	Ø	Ø	Ø	Ø	Ø	Ø	Ø	Ø	Ø
-118DBM	Ø	Ø	Ø	Ø	Ø	Ø	Ø	Ø	Ø	Ø
-119DBM	Ø	Ø	Ø	Ø	Ø	Ø	Ø	Ø	Ø	Ø
-120DBM	Ø	Ø	Ø	Ø	Ø	Ø	Ø	Ø	Ø	Ø
-121DBM	Ø	Ø	Ø	Ø	Ø	Ø	Ø	Ø	Ø	Ø
-122DBM	Ø	Ø	Ø	Ø	Ø	Ø	Ø	Ø	Ø	Ø
-123DBM	Ø	Ø	Ø	Ø	Ø	Ø	Ø	Ø	Ø	Ø
-124DBM	Ø	Ø	Ø	Ø	Ø	Ø	Ø	Ø	Ø	Ø

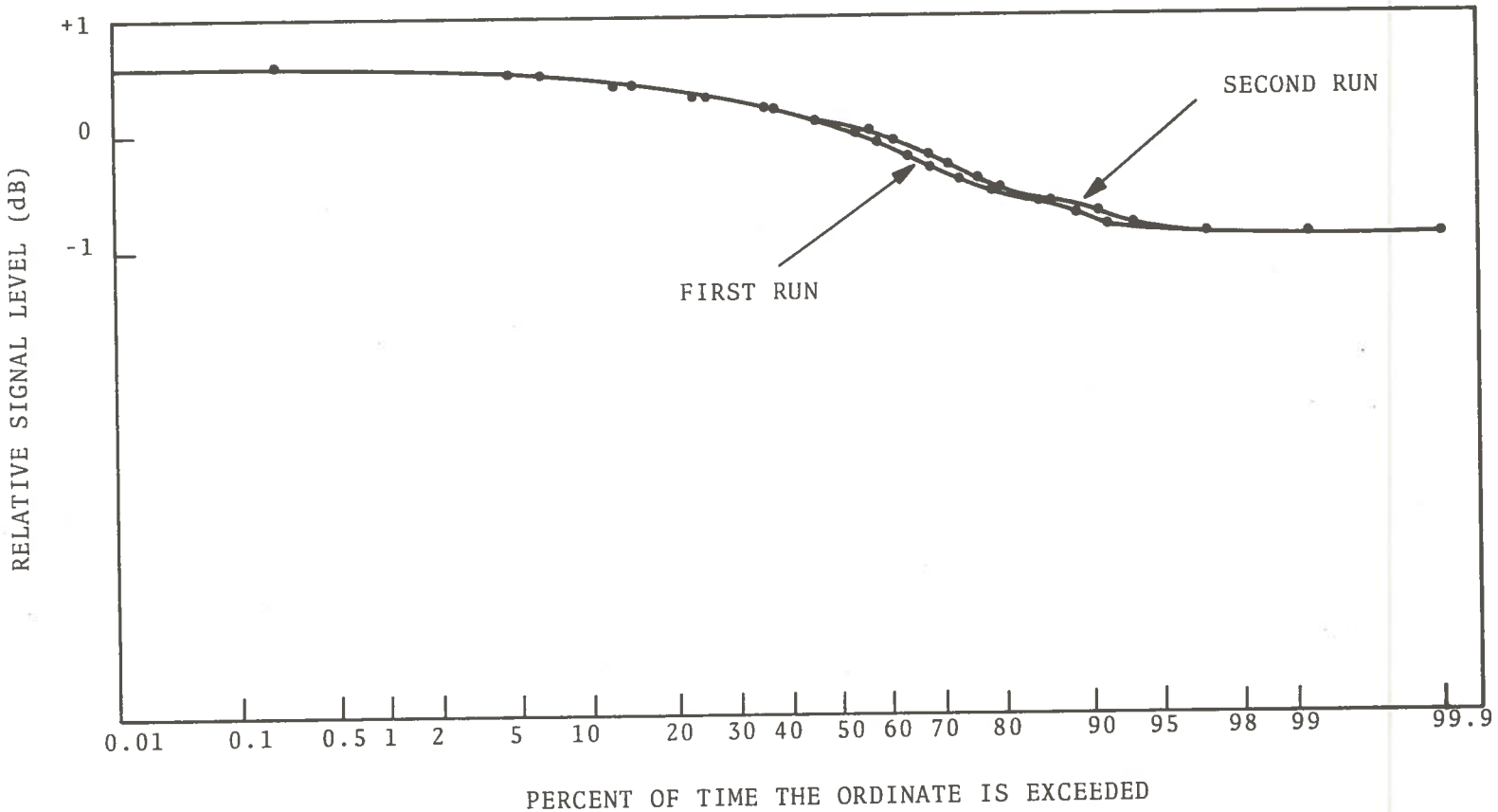

Figure 6-5 Probability Distribution Plot of the First and Second Runs of a Continuous Wave Signal Generator

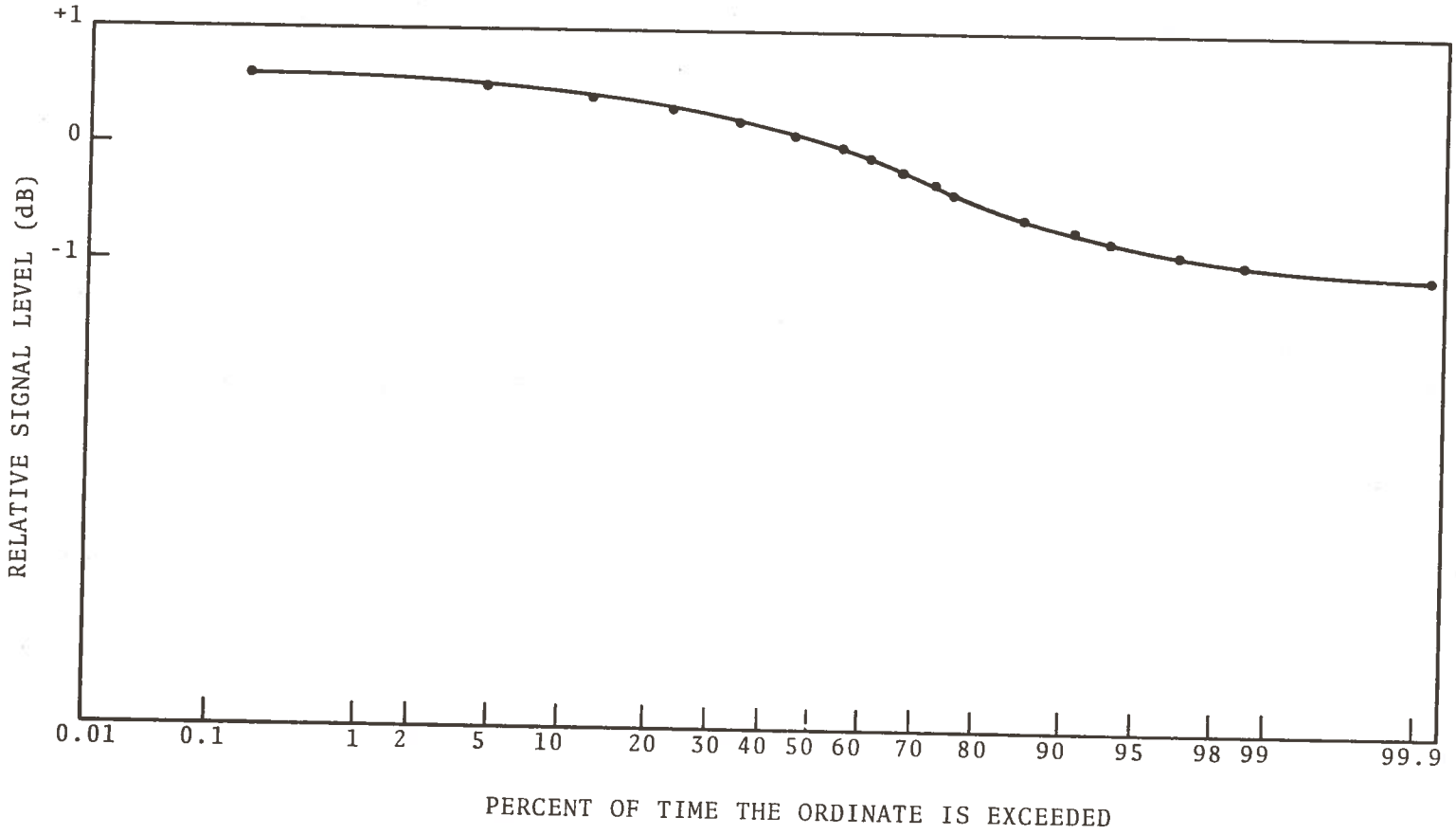

Figure 6-6 Probability Distribution Plot of the Average of the Two 15-Minute Runs of a Continuous Wave Signal Generator

TABLE 6-4 PROBABILITY DISTRIBUTION OF THE FIRST 15-MINUTE RUN OF A CONTINUOUS WAVE SIGNAL GENERATOR

PROBABILITY DISTRIBUTION FOR ATS-5 DATA
VALUES GIVEN ARE IN PERCENT TIMES 100

	Ø.Ø	Ø.1	Ø.2	Ø.3	Ø.4	Ø.5	Ø.6	Ø.7	Ø.8	Ø.9
-105DBM	Ø	Ø	Ø	Ø	Ø	Ø	Ø	Ø	Ø	Ø
-106DBM	Ø	Ø	Ø	Ø	Ø	Ø	Ø	Ø	Ø	Ø
-107DBM	Ø	Ø	Ø	Ø	Ø	Ø	Ø	Ø	Ø	Ø
-108DBM	Ø	Ø	Ø	Ø	Ø	Ø	Ø	Ø	Ø	Ø
-109DBM	Ø	Ø	Ø	Ø	Ø	Ø	Ø	Ø	Ø	Ø
-110DBM	Ø	Ø	Ø	Ø	Ø	Ø	Ø	Ø	Ø	Ø
-111DBM	Ø	Ø	Ø	Ø	Ø	Ø	Ø	Ø	Ø	Ø
-112DBM	Ø	Ø	Ø	Ø	Ø	Ø	Ø	Ø	Ø	Ø
-113DBM	Ø	Ø	Ø	Ø	Ø	Ø	Ø	Ø	Ø	Ø
-114DBM	Ø	Ø	Ø	Ø	Ø	61Ø	1411	2441	3624	4501
-115DBM	5378	5797	6407	6750	7322	7856	8466	8885	9152	961Ø
-116DBM	98ØØ	9990	9990	9990	9990	9990	9990	9990	9990	9990
-117DBM	9990	9990	9990	9990	9990	9990	9990	9990	9990	9990
-118DBM	9990	9990	9990	9990	9990	9990	9990	9990	9990	9990
-119DBM	9990	9990	9990	9990	9990	9990	9990	9990	9990	9990
-120DBM	9990	9990	9990	9990	9990	9990	9990	9990	9990	9990
-121DBM	9990	9990	9990	9990	9990	9990	9990	9990	9990	9990
-122DBM	9990	9990	9990	9990	9990	9990	9990	9990	9990	9990
-123DBM	9990	9990	9990	9990	9990	9990	9990	9990	9990	9990
-124DBM	9990	9990	9990	9990	9990	9990	9990	9990	9990	9990

TABLE 6-5 PROBABILITY DISTRIBUTION OF THE SECOND 15-MINUTE RUN OF A CONTINUOUS WAVE GENERATOR

PROBABILITY DISTRIBUTION FOR ATS-5 DATA
VALUES GIVEN ARE IN PERCENT TIMES 100

	0.0	0.1	0.2	0.3	0.4	0.5	0.6	0.7	0.8	0.9
-105DBM	0	0	0	0	0	0	0	0	0	0
-106DBM	0	0	0	0	0	0	0	0	0	0
-107DBM	0	0	0	0	0	0	0	0	0	0
-108DBM	0	0	0	0	0	0	0	0	0	0
-109DBM	0	0	0	0	0	0	0	0	0	0
-110DBM	0	0	0	0	0	0	0	0	0	0
-111DBM	0	0	0	0	0	0	0	0	0	0
-112DBM	0	0	0	0	0	0	0	0	0	0
-113DBM	0	0	0	0	0	0	0	0	0	0
-114DBM	0	0	0	0	38	309	1084	2169	3331	4610
-115DBM	5734	6354	7051	7322	7625	8096	8716	9297	9529	9800
-116DBM	9916	9993	9993	9993	9993	9993	9993	9993	9993	9993
-117DBM	9993	9993	9993	9993	9993	9993	9993	9993	9993	9993
-118DBM	9993	9993	9993	9993	9993	9993	9993	9993	9993	9993
-119DBM	9993	9993	9993	9993	9993	9993	9993	9993	9993	9993
-120DBM	9993	9993	9993	9993	9993	9993	9993	9993	9993	9993
-121DBM	9993	9993	9993	9993	9993	9993	9993	9993	9993	9993
-122DBM	9993	9993	9993	9993	9993	9993	9993	9993	9993	9993
-123DBM	9993	9993	9993	9993	9993	9993	9993	9993	9993	9993
-124DBM	9993	9993	9993	9993	9993	9993	9993	9993	9993	9993

TABLE 6-6 PROBABILITY DISTRIBUTION OF THE AVERAGE OF THE FIRST AND SECOND 15-MINUTE RUN OF A CONTINUOUS WAVE SIGNAL GENERATOR

PROBABILITY DISTRIBUTION FOR ATS-5 DATA
VALUES GIVEN ARE IN PERCENT TIMES 100

	0.0	0.1	0.2	0.3	0.4	0.5	0.6	0.7	0.8	0.9
-105DBM	0	0	0	0	0	0	0	0	0	0
-106DBM	0	0	0	0	0	0	0	0	0	0
-107DBM	0	0	0	0	0	0	0	0	0	0
-108DBM	0	0	0	0	0	0	0	0	0	0
-109DBM	0	0	0	0	0	0	0	0	0	0
-110DBM	0	0	0	0	0	0	0	0	0	0
-111DBM	0	0	0	0	0	0	0	0	0	0
-112DBM	0	0	0	0	0	0	0	0	0	0
-113DBM	0	0	0	0	0	0	0	0	0	0
-114DBM	0	0	0	0	19	461	1249	2306	3479	4555
-115DBM	5555	6074	6727	7034	7572	7975	8590	9090	9340	9705
-116DBM	9858	9992	9992	9992	9992	9992	9992	9992	9992	9992
-117DBM	9992	9992	9992	9992	9992	9992	9992	9992	9992	9992
-118DBM	9992	9992	9992	9992	9992	9992	9992	9992	9992	9992
-119DBM	9992	9992	9992	9992	9992	9992	9992	9992	9992	9992
-120DBM	9992	9992	9992	9992	9992	9992	9992	9992	9992	9992
-121DBM	9992	9992	9992	9992	9992	9992	9992	9992	9992	9992
-122DBM	9992	9992	9992	9992	9992	9992	9992	9992	9992	9992
-123DBM	9992	9992	9992	9992	9992	9992	9992	9992	9992	9992
-124DBM	9992	9992	9992	9992	9992	9992	9992	9992	9992	9992

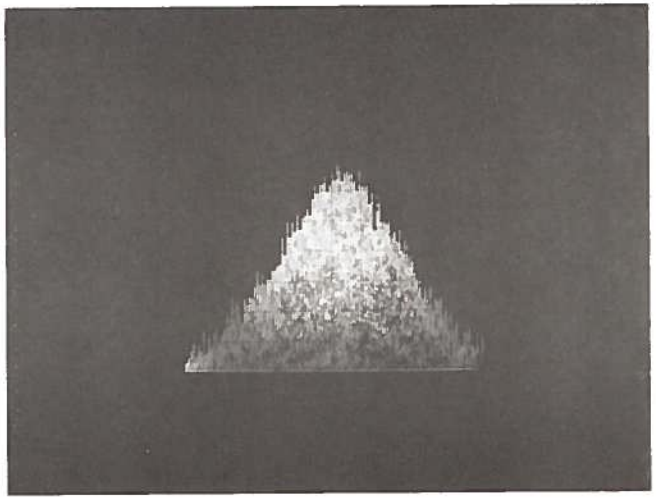

(a)

FM Modulated Signal Generator
Scale: Horizontal: 1 KHZ/Div
Vertical: 2 dB/Div

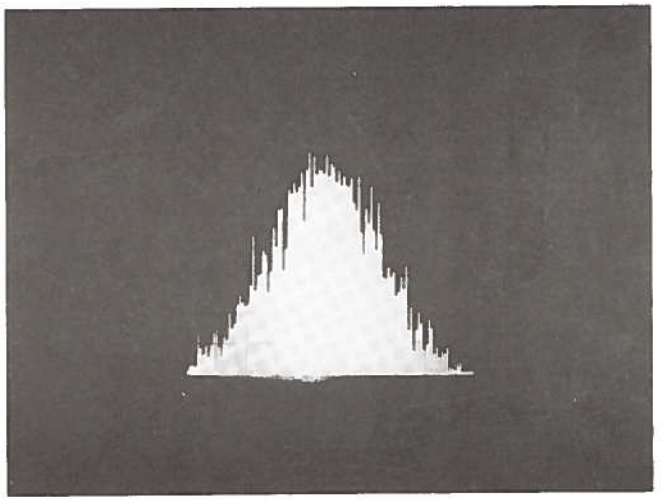

(b)

WBDM Signal of ATS-5
Scale: Horizontal: 1 KHZ/Div
Vertical: 2 dB/Div

Figure 6-7 Spectrum Photographs of FM Signal Generator and Wide-Band Data Mode Signal of the ATS-5 Spacecraft

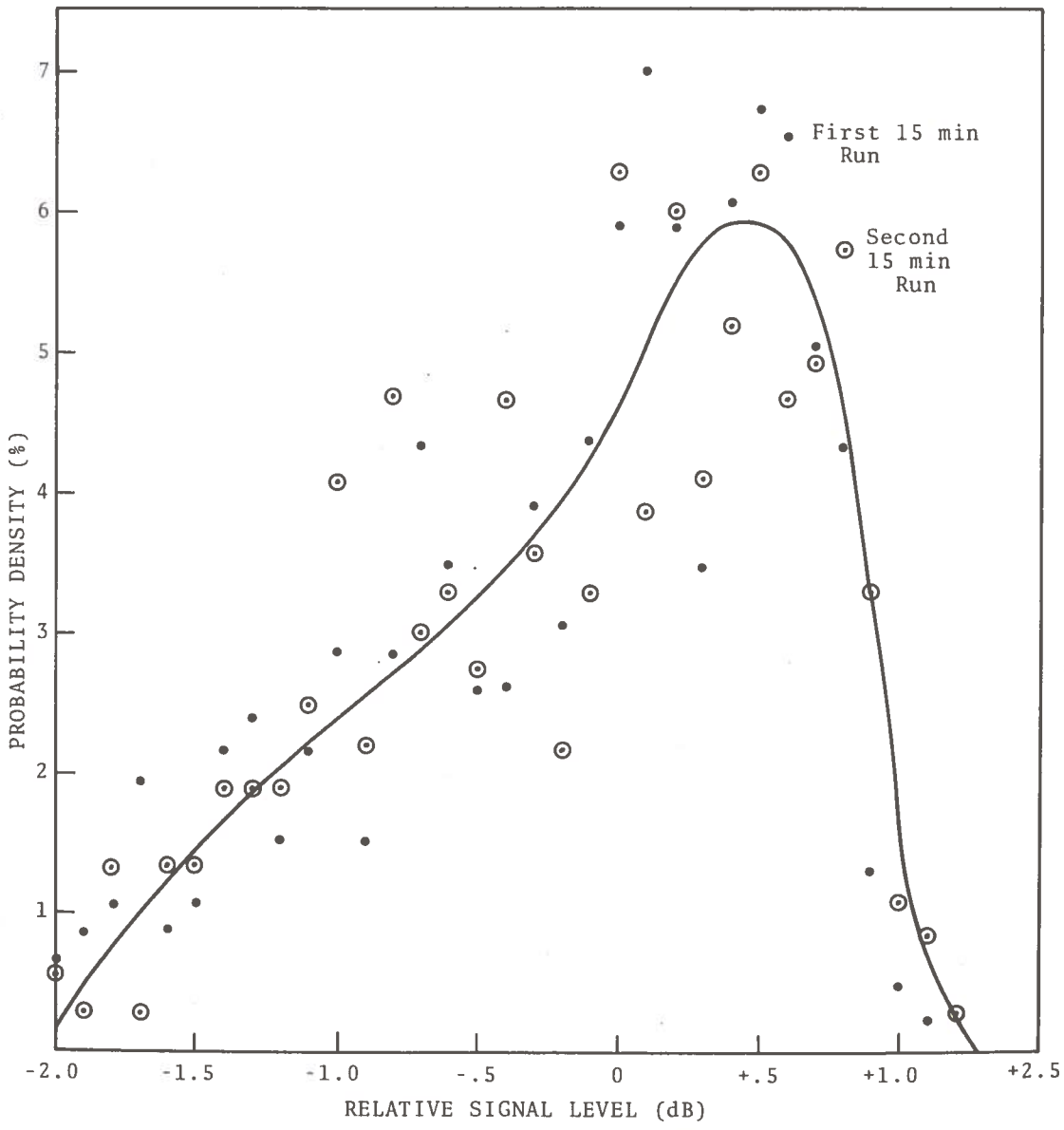

Figure 6-8 Probability Density Plot of the First and Second 15-Minute Runs of a FM Noise Modulated Signal Generator

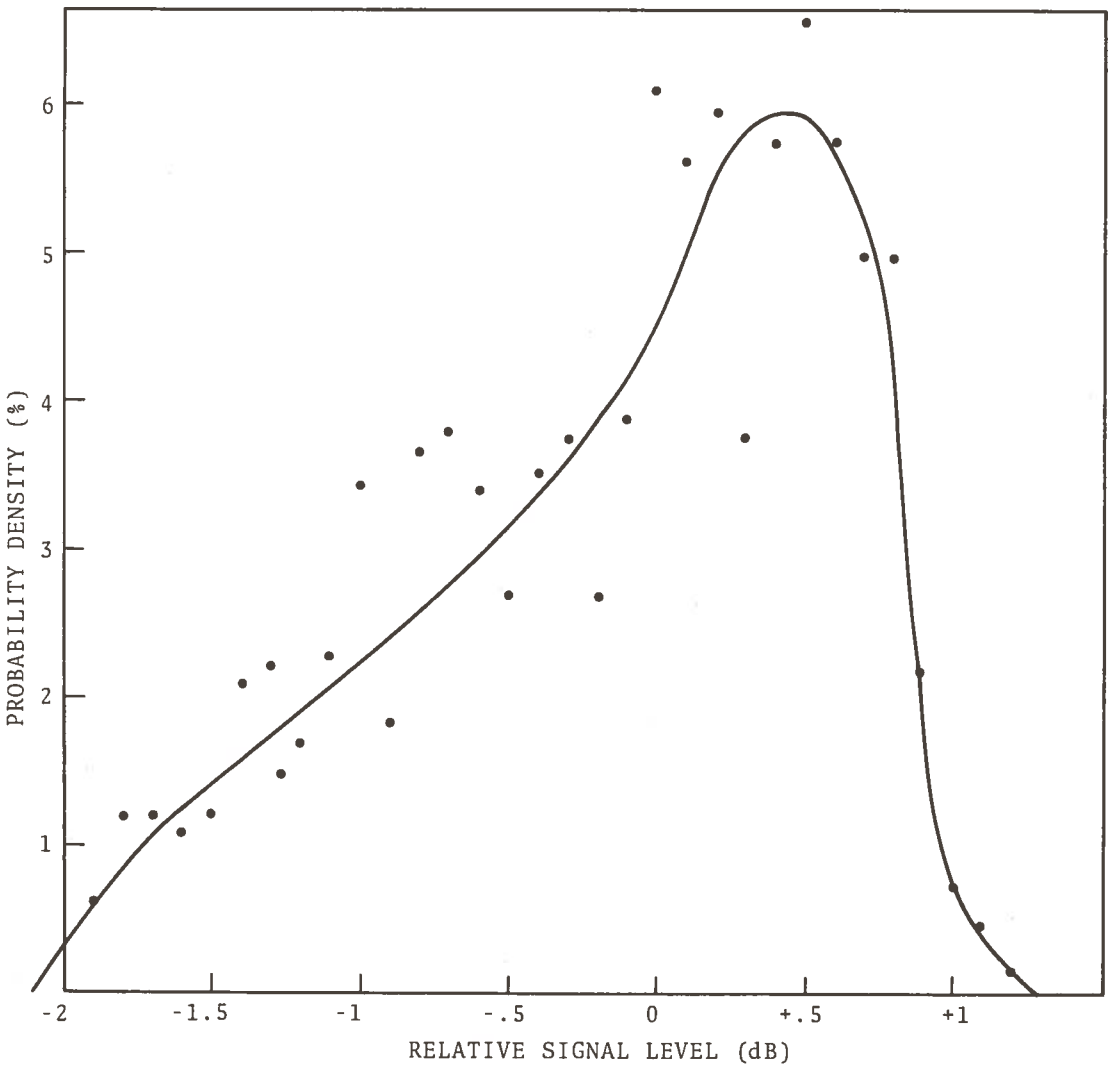

Figure 6-9 Probability Density Plot of the Average of the First and Second 15-Minute Run of FM Noise Modulated Signal Generator

TABLE 6-7 PROBABILITY DENSITY FOR THE FIRST 15-MINUTE RUN OF A "NOISE MODULATED" SIGNAL GENERATOR

PROBABILITY DENSITY TABLE FOR ATS-5 DATA
VALUES GIVEN ARE IN PERCENT TIMES 100

	0.0	0.1	0.2	0.3	0.4	0.5	0.6	0.7	0.8	0.9
-105DBM	0	0	0	0	0	0	0	0	0	0
-106DBM	0	0	0	0	0	0	0	0	0	0
-107DBM	0	0	0	0	0	0	0	0	0	0
-108DBM	0	0	0	0	0	0	0	0	0	0
-109DBM	0	0	0	0	0	0	0	0	0	0
-110DBM	0	0	0	0	0	0	0	0	0	0
-111DBM	0	0	0	0	0	0	0	0	0	0
-112DBM	0	0	0	0	0	0	0	0	0	0
-113DBM	0	0	0	0	0	0	0	0	0	21
-114DBM	43	131	437	503	656	678	612	350	590	700
-115DBM	590	437	306	393	262	262	350	437	284	153
-116DBM	284	218	153	240	218	109	87	196	109	87
-117DBM	65	21	0	0	0	0	0	0	0	0
-118DBM	0	0	0	0	0	0	0	0	0	0
-119DBM	0	0	0	0	0	0	0	0	0	0
-120DBM	0	0	0	0	0	0	0	0	0	0
-121DBM	0	0	0	0	0	0	0	0	0	0
-122DBM	0	0	0	0	0	0	0	0	0	0
-123DBM	0	0	0	0	0	0	0	0	0	0
-124DBM	0	0	0	0	0	0	0	0	0	0

TABLE 6-8 PROBABILITY DENSITY FOR THE SECOND 15-MINUTE RUN OF A "NOISE MODULATED" SIGNAL GENERATOR

PROBABILITY DENSITY TABLE FOR ATS-5 DATA
VALUES GIVEN ARE IN PERCENT TIMES 100

	0.0	0.1	0.2	0.3	0.4	0.5	0.6	0.7	0.8	0.9
-105DBM	0	0	0	0	0	0	0	0	0	0
-106DBM	0	0	0	0	0	0	0	0	0	0
-107DBM	0	0	0	0	0	0	0	0	0	0
-108DBM	0	0	0	0	0	0	0	0	0	0
-109DBM	0	0	0	0	0	0	0	0	0	0
-110DBM	0	0	0	0	0	0	0	0	0	0
-111DBM	0	0	0	0	0	0	0	0	0	0
-112DBM	0	0	0	0	0	0	0	0	0	0
-113DBM	0	0	0	0	0	0	0	0	27	82
-114DBM	109	329	576	494	467	631	521	412	604	384
-115DBM	631	329	219	357	467	274	329	302	467	219
-116DBM	412	247	192	192	192	137	137	27	137	27
-117DBM	54	0	0	0	0	0	0	0	0	0
-118DBM	0	0	0	0	0	0	0	0	0	0
-119DBM	0	0	0	0	0	0	0	0	0	0
-120DBM	0	0	0	0	0	0	0	0	0	0
-121DBM	0	0	0	0	0	0	0	0	0	0
-122DBM	0	0	0	0	0	0	0	0	0	0
-123DBM	0	0	0	0	0	0	0	0	0	0
-124DBM	0	0	0	0	0	0	0	0	0	0

TABLE 6-9 PROBABILITY DENSITY FOR THE AVERAGE OF THE FIRST AND SECOND 15-MINUTE RUNS OF A "NOISE MODULATED" SIGNAL GENERATOR

PROBABILITY DENSITY TABLE FOR ATS-5 DATA
VALUES GIVEN ARE IN PERCENT TIMES 100

	0.0	0.1	0.2	0.3	0.4	0.5	0.6	0.7	0.8	0.9
-105DBM	0	0	0	0	0	0	0	0	0	0
-106DBM	0	0	0	0	0	0	0	0	0	0
-107DBM	0	0	0	0	0	0	0	0	0	0
-108DBM	0	0	0	0	0	0	0	0	0	0
-109DBM	0	0	0	0	0	0	0	0	0	0
-110DBM	0	0	0	0	0	0	0	0	0	0
-111DBM	0	0	0	0	0	0	0	0	0	0
-112DBM	0	0	0	0	0	0	0	0	0	0
-113DBM	0	0	0	0	0	0	0	0	12	48
-114DBM	73	219	499	499	572	657	572	377	596	560
-115DBM	609	389	267	377	353	267	341	377	365	182
-116DBM	341	231	170	219	207	121	109	121	121	60
-117DBM	60	12	0	0	0	0	0	0	0	0
-118DBM	0	0	0	0	0	0	0	0	0	0
-119DBM	0	0	0	0	0	0	0	0	0	0
-120DBM	0	0	0	0	0	0	0	0	0	0
-121DBM	0	0	0	0	0	0	0	0	0	0
-122DBM	0	0	0	0	0	0	0	0	0	0
-123DBM	0	0	0	0	0	0	0	0	0	0
-124DBM	0	0	0	0	0	0	0	0	0	0

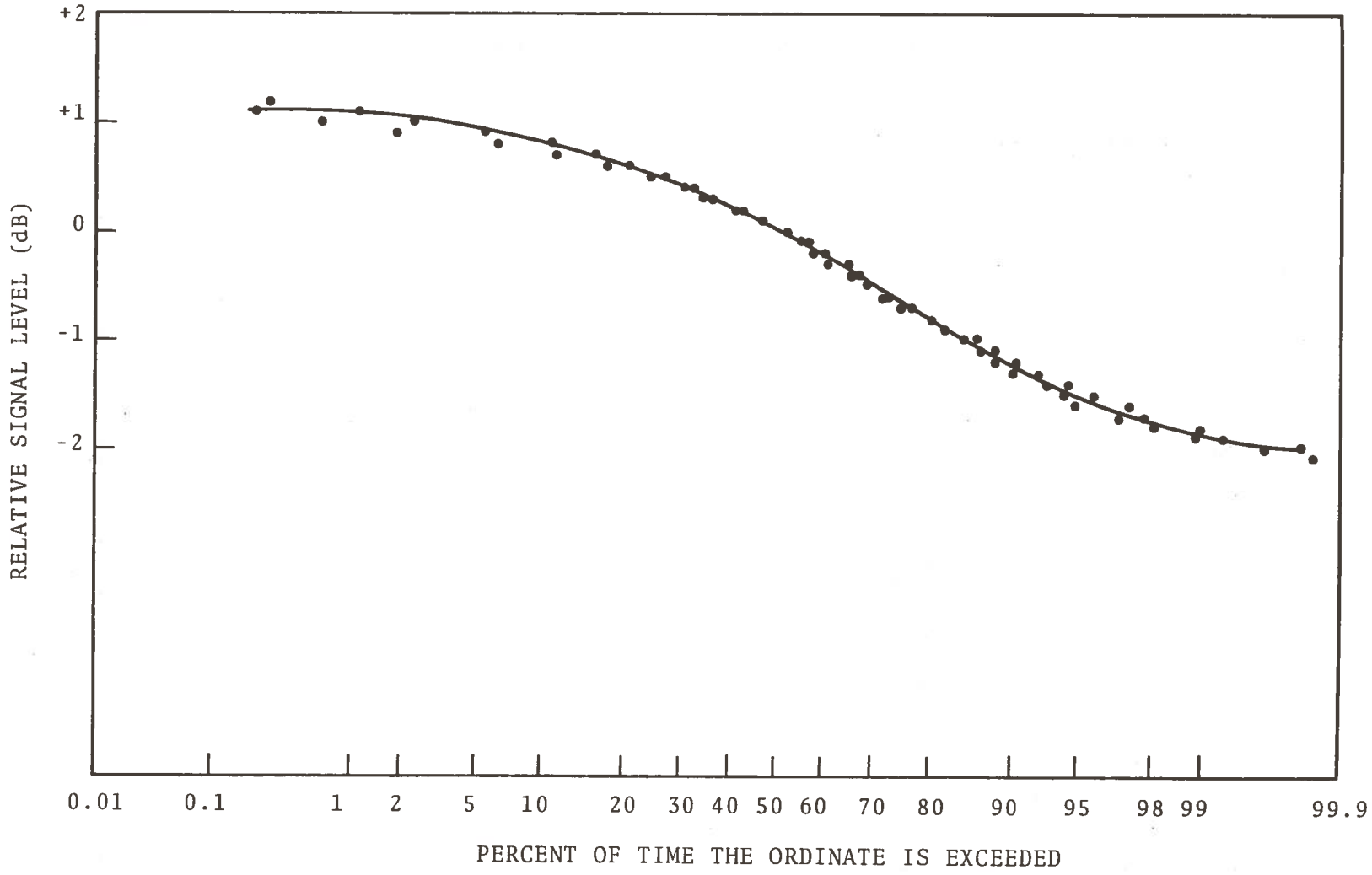

Figure 6-10 Probability Distribution Plot of the First and Second 15-Minute Runs of a FM "Noise Modulated" Signal Generator

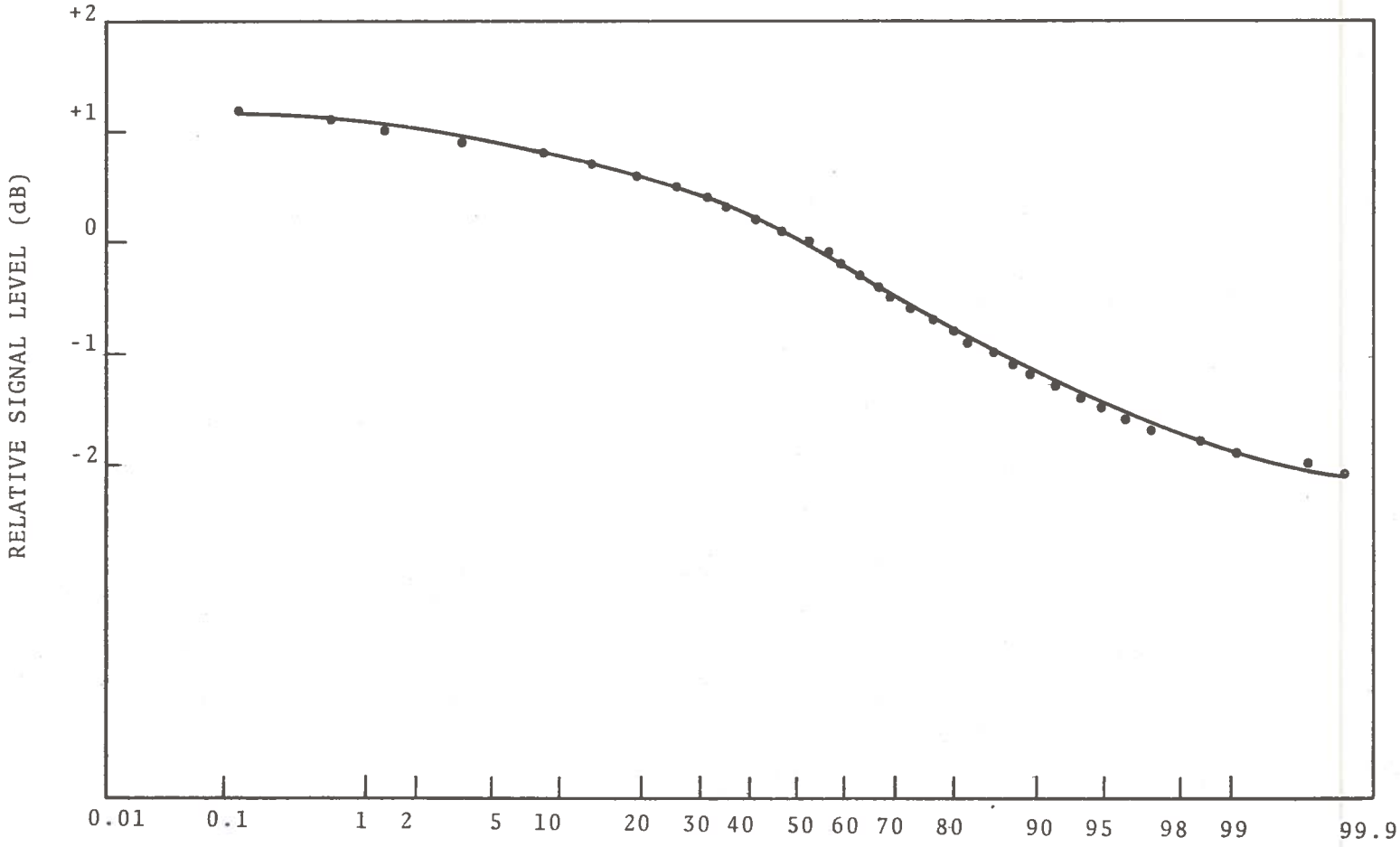

Figure 6-11 Probability Distribution Plot of the Average of the First and Second 15-Minute Runs of a FM "Noise Modulated" Signal Generator

TABLE 6-10 PROBABILITY DISTRIBUTION OF THE FIRST 15-MINUTE RUN OF A FM "NOISE MODULATED" SIGNAL GENERATOR

PROBABILITY DISTRIBUTION FOR ATS-5 DATA
VALUES GIVEN ARE IN PERCENT TIMES 100

	0.0	0.1	0.2	0.3	0.4	0.5	0.6	0.7	0.8	0.9
-105DBM	0	0	0	0	0	0	0	0	0	0
-106DBM	0	0	0	0	0	0	0	0	0	0
-107DBM	0	0	0	0	0	0	0	0	0	0
-108DBM	0	0	0	0	0	0	0	0	0	0
-109DBM	0	0	0	0	0	0	0	0	0	0
-110DBM	0	0	0	0	0	0	0	0	0	0
-111DBM	0	0	0	0	0	0	0	0	0	0
-112DBM	0	0	0	0	0	0	0	0	0	0
-113DBM	0	0	0	0	0	0	0	0	0	21
-114DBM	64	195	632	1135	1791	2469	3081	3431	4021	4721
-115DBM	5311	5748	6054	6447	6709	6971	7321	7758	8042	8195
-116DBM	8479	8697	8850	9090	9308	9417	9504	9700	9809	9896
-117DBM	9961	9982	9982	9982	9982	9982	9982	9982	9982	9982
-118DBM	9982	9982	9982	9982	9982	9982	9982	9982	9982	9982
-119DBM	9982	9982	9982	9982	9982	9982	9982	9982	9982	9982
-120DBM	9982	9982	9982	9982	9982	9982	9982	9982	9982	9982
-121DBM	9982	9982	9982	9982	9982	9982	9982	9982	9982	9982
-122DBM	9982	9982	9982	9982	9982	9982	9982	9982	9982	9982
-123DBM	9982	9982	9982	9982	9982	9982	9982	9982	9982	9982
-124DBM	9982	9982	9982	9982	9982	9982	9982	9982	9982	9982

TABLE 6-11 PROBABILITY DISTRIBUTION OF THE SECOND 15-MINUTE RUN OF A FM "NOISE MODULATED" SIGNAL GENERATOR

PROBABILITY DISTRIBUTION FOR ATS-5 DATA
VALUES GIVEN ARE IN PERCENT TIMES 100

	0.0	0.1	0.2	0.3	0.4	0.5	0.6	0.7	0.8	0.9
-105DBM	0	0	0	0	0	0	0	0	0	0
-106DBM	0	0	0	0	0	0	0	0	0	0
-107DBM	0	0	0	0	0	0	0	0	0	0
-108DBM	0	0	0	0	0	0	0	0	0	0
-109DBM	0	0	0	0	0	0	0	0	0	0
-110DBM	0	0	0	0	0	0	0	0	0	0
-111DBM	0	0	0	0	0	0	0	0	0	0
-112DBM	0	0	0	0	0	0	0	0	0	0
-113DBM	0	0	0	0	0	0	0	0	27	109
-114DBM	218	547	1123	1617	2084	2715	3236	3648	4252	4636
-115DBM	5267	5596	5815	6172	6639	6913	7242	7544	8011	8239
-116DBM	8642	8889	9081	9273	9465	9602	9739	9766	9903	9930
-117DBM	9984	9984	9984	9984	9984	9984	9984	9984	9984	9984
-118DBM	9984	9984	9984	9984	9984	9984	9984	9984	9984	9984
-119DBM	9984	9984	9984	9984	9984	9984	9984	9984	9984	9984
-120DBM	9984	9984	9984	9984	9984	9984	9984	9984	9984	9984
-121DBM	9984	9984	9984	9984	9984	9984	9984	9984	9984	9984
-122DBM	9984	9984	9984	9984	9984	9984	9984	9984	9984	9984
-123DBM	9984	9984	9984	9984	9984	9984	9984	9984	9984	9984
-124DBM	9984	9984	9984	9984	9984	9984	9984	9984	9984	9984

TABLE 6-12 PROBABILITY DISTRIBUTION OF THE AVERAGE OF THE FIRST AND SECOND 15-MINUTE RUNS OF A FM "NOISE MODULATED" SIGNAL GENERATOR

PROBABILITY DISTRIBUTION FOR ATS-5 DATA
VALUES GIVEN ARE IN PERCENT TIMES 100

	Ø.Ø	Ø.1	Ø.2	Ø.3	Ø.4	Ø.5	Ø.6	Ø.7	Ø.8	Ø.9
-105DBM	Ø	Ø	Ø	Ø	Ø	Ø	Ø	Ø	Ø	Ø
-106DBM	Ø	Ø	Ø	Ø	Ø	Ø	Ø	Ø	Ø	Ø
-107DBM	Ø	Ø	Ø	Ø	Ø	Ø	Ø	Ø	Ø	Ø
-108DBM	Ø	Ø	Ø	Ø	Ø	Ø	Ø	Ø	Ø	Ø
-109DBM	Ø	Ø	Ø	Ø	Ø	Ø	Ø	Ø	Ø	Ø
-110DBM	Ø	Ø	Ø	Ø	Ø	Ø	Ø	Ø	Ø	Ø
-111DBM	Ø	Ø	Ø	Ø	Ø	Ø	Ø	Ø	Ø	Ø
-112DBM	Ø	Ø	Ø	Ø	Ø	Ø	Ø	Ø	Ø	Ø
-113DBM	Ø	Ø	Ø	Ø	Ø	Ø	Ø	Ø	12	60
-114DBM	133	352	851	1350	1922	2579	3151	3528	4124	4684
-115DBM	5293	5682	5949	6326	6679	6946	7287	7664	8029	8211
-116DBM	8552	8783	8953	9172	9379	9500	9639	9730	9851	9911
-117DBM	9971	9983	9983	9983	9983	9983	9983	9983	9983	9983
-118DBM	9983	9983	9983	9983	9983	9983	9983	9983	9983	9983
-119DBM	9983	9983	9983	9983	9983	9983	9983	9983	9983	9983
-120DBM	9983	9983	9983	9983	9983	9983	9983	9983	9983	9983
-121DBM	9983	9983	9983	9983	9983	9983	9983	9983	9983	9983
-122DBM	9983	9983	9983	9983	9983	9983	9983	9983	9983	9983
-123DBM	9983	9983	9983	9983	9983	9983	9983	9983	9983	9983
-124DBM	9983	9983	9983	9983	9983	9983	9983	9983	9983	9983

Figure 6-12 is the analog chart recording of the calibration run. Figure 6-12a is the continuous wave signal as detected by the East and West vector voltmeter's receivers. The size of the calibration step every 5 minutes is 1 dB. Figure 6-12b is the FM noise modulated signal generator as received by the East and West vector voltmeter receivers. The size of the calibration step every 5 minutes is 1 dB.

There are statistical uncertainities due to the number of measurements taken (i.e. the sample size). In addition to the errors introduced by the experimental equipment when conducting an individual measurement. Each measurement made by the equipment is an estimate of the actual value. When taking a number of estimates, the actual value of these measurements can then be stated with a certain degree of confidence.

Figure 6-13 may be used to find the number of measurements necessary to obtain a certain confidence in the variance of a quantity. This figure is explained in Bendat and Piersol (1971) and Jenkins and Watts (1968). Consider the following example. Suppose we have 500 samples of the signal strength (typically a 15 minute observing period of the ATS-5) and our calculations indicate that the root-mean-square or standard deviation is 0.19 dB (5%). For a 99% confidence we find the upper confidence 1.1 times the standard deviation and the lower confidence 0.9 times the standard deviation. Consequently, the standard deviation is 0.185 dB $\leq$ 0.19 dB < 0.21 dB. If for example instead of 500 measurements, we had 5 measurements, the standard deviation would be approximatel $(100)^{1/2}$ times bigger (i.e. 1.76 dB) and its 99% confidence limit would be approximately 3.5 and 0.55 for the upper and lower confidences, respectively. The spread of the standard deviation would now be 1 dB $\leq$ 1.76 dB < 4 dB.

A second example is as follows; the value of the 99th percentile of the probability distribution with a 99% confidence of 0.1 dB is desired. A ratio of 0.1 dB corresponds to 2%. Thus the coefficients for the standard deviation, σm are 0.98 and 1.02 in the 99% confidence interval. This requires approximately 2500 measurements at the 99th percentile level or approximately 250,000

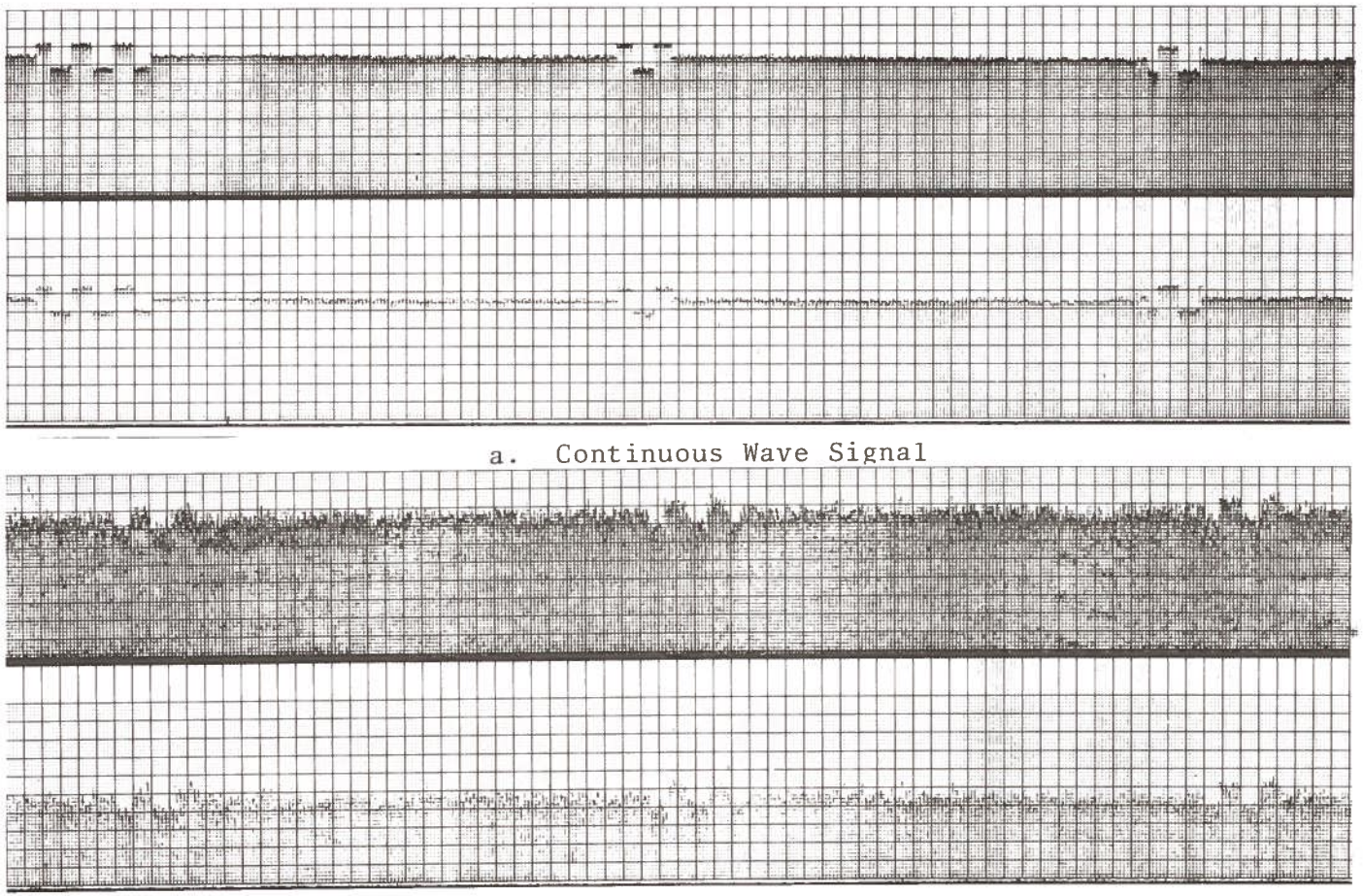

a. Continuous Wave Signal

b. FM Noise Modulated Signal Generator

Figure 6-12. Analog Strip Chart Recording of the East and West Elements of the L-Band Interferometer During A Calibration Run

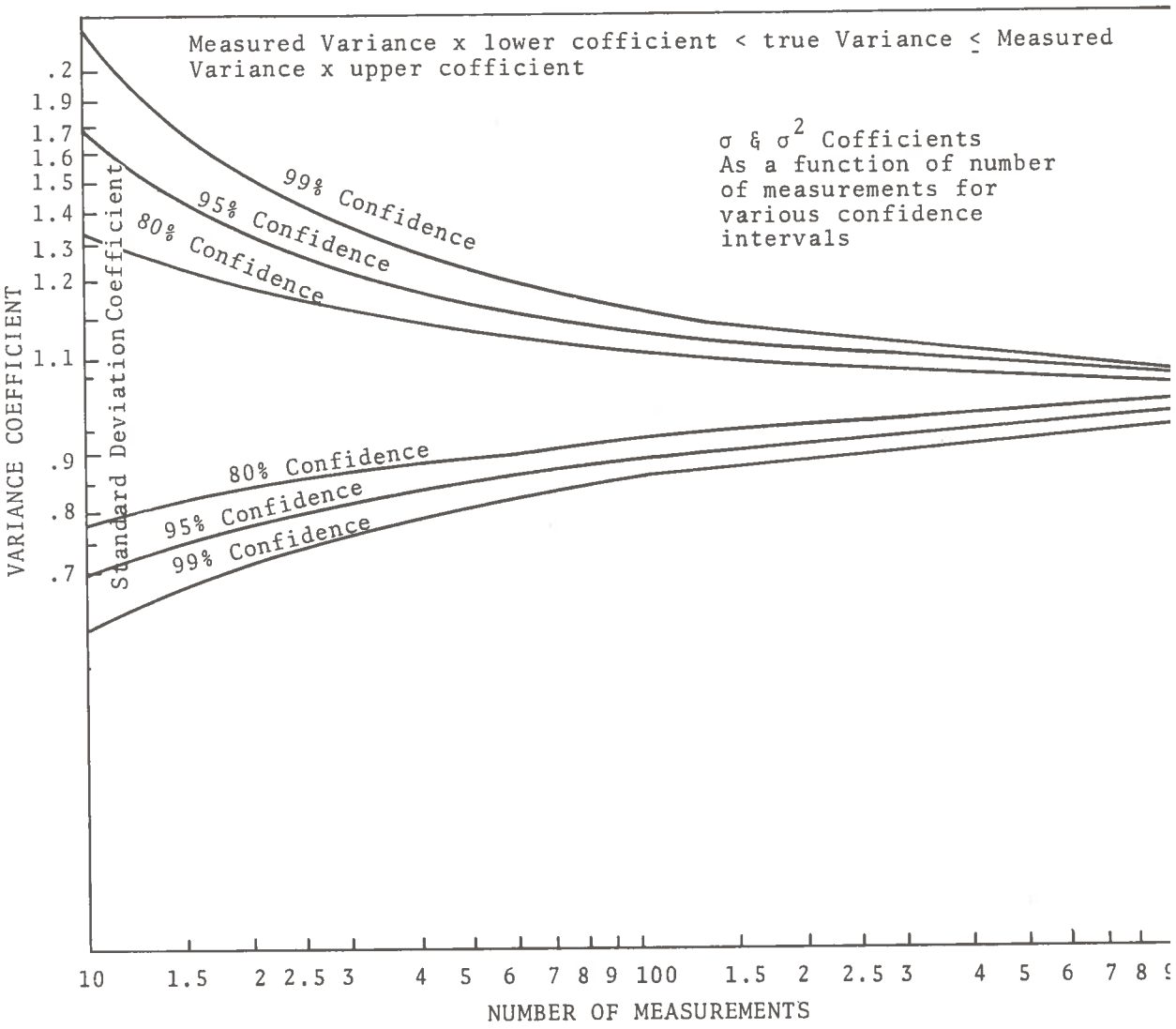

Courtesy: The Institute of Electrical and Electronics Engineers, Inc., 345 East 47th Street, New York NY 10017

Figure 6-13 Variance Coefficient Versus Number of Measurements for Various Standard Deviations (After Jenkin and Watts, 1968)

total measurements if any signal level were equally probable during the observing interval. Though 250,000 measurements are made in approximately 100 hours of observing, unfortunately the periods of fading do not occur continuously for 100 hours. This means in order to get 2500 samples of fades more than 100 hours of observing are necessary.

Though the receiving system is calibrated before and after a short observing interval, there is always the problem of the gain stability during the observing interval. Typically, a receiver has 90 dB of radio frequency gain and 30 to 40 dB of DC video gain. The overall gain being of the order of 120 dB. A stability of 0.1 dB (2.3%) is achievable. A stability of 0.2 dB to 0.3 dB in one half of an hour are typical of good receivers.

7. BIBLIOGRAPHY

Aarons, J., Editor, (1963), Radio Astronomical and Satellite Studies of the Atmosphere, North-Holland Publishing Co., Amsterdam.

Aarons, J. (1969), Special problems in scintillations, pp. 55-88 in A Survey of Scintillation Data and its Relationship to Satellite Communication, NATO Advisory Group for Aerospace Research and Development, Paris, France, N70-32239#.

Aarons, J. (1970A), Ionospheric limitations on performance on VHF navigation and communication satellite systems, in AGARD Application of Propagation Data to VHF Satellite Communication and Navigation Systems, NATO Advisory Group for Aerospace Research and Development, Paris, France, N71-16228#.

Aarons, J. (1970B), A survey of scintillation data and its relationship to satellite communications, Report No. AFCRL-70-0053, Air Force Cambridge Research Laboratories, Bedford, MA, AD-715891; N71-18534#.

Aarons, J., Editor, (1973), Total electron content and scintillation studies of the ionosphere, Report No. AGARDograph-166, NATO/Advisory Group for Aerospace Research & Development, Paris, France, N73-22350#.

Aarons, J. and R. S. Allen, (1966), Scintillation of a radio star at a sub-auroral latitude, Radio Science, 1, 1180-1186.

Aarons, J., R. S. Allen, and T. J. Elkins, (1967), Frequency dependence of radio star scintillation, J. Geophysical Research, 72, 2891-2902.

Aarons, J. and J. P. Mullen, (1965), A synoptic study of scintillations of ionospheric origin in satellite signals, Environmental Research Paper No. 94, Air Force Cambridge Research Laboratories, Bedford, MA.

Aarons, J., J. P. Mullen, and S. Basu, (1963), Goemagnetic control of satellite scintillations, J. Geophysical Research, 68, 3159-3168.

Aarons, J., J. P. Mullen and H. E. Whitney, (1969), The scintillation boundary, J. Geophysical Research, 74, 884.

Aarons, J., J. P. Mullen, H. E. Whitney and F. Steenstr...(1972), Seasonal, diurnal and magnetic dependence of ionospheric scintillation at 64 degrees invariant latitude, Planetary & Space Science, 20, 957-.

Aarons, J. and H. E. Whitney, (1967), Ionospheric scintillation at 136 MHz from a synchronous satellite, J. Atmospheric & Terrestrial Physics, 16, 21-28.

Aarons, J. and H. E. Whitney, (1972), Observations of scintillations of 2 satellite beacons near boundary F irregularity region, Planetary & Space Science, 20, 965-.

Aarons, J., H. E. Whitney, and R. S. Allen, (1969), Scintillation observations of synchronous satellites, Report No. AFCRL-69-0011, Air Force Cambridge Research Laboratories, Bedford, MA, AD-683241, N69-26422#.

Aarons, J., H. E. Whitney, and R. S. Allen, (1970), World wide morphology of scintillations, in AGARD Application of Propagation Data to VHF Satellite Communication and Navigation Systems, NATO Advisory Group for Aerospace Research and Development, Paris, France, N71-16232#.

Aarons, J., H. E. Whitney and R. S. Allen, (1971), Global morphology of ionospheric scintillations, Proc. IEEE, 59, 159-172.

Aarons, J., H. E. Whitney, R. S. Allen, D. Seeman, (1973), High latitude models, observations and analysis of ionospheric scintillations, Report No. AFCRL-TR-73-0048, Air Force Cambridge Research Laboratories, Bedford, MA, AD-762282; N73-28483#.

AFCRL, (1969), Summaries of Papers at the Symposium on the Application of Atmospheric Studies to Satellite Transmissions, Boston, Mass., Sept. 3-5, 1969, Sponsored by the Air Force Cambridge Research Laboratories, Bedford, MA, A70-12564#.

AGARD, (1970), Application of Propagation Data to VHF Satellite Communication and Navigation Systems, Report No. AGARD-LS-41, NATO Advisory Group for Aerospace Research & Development, Paris, France, AD-717264, N71-16226#.

AGARD, (1972), AGARD Conf. Proceeding on Effects of Atmospheric Acoustic Gravity Waves on Electromagnetic Wave Propagation, AGARD CP-115, NATO/Advisory Group for Aerospace Research & Development, Paris, France.

Albrecht, H. J. (1971), Prediction of ionospheric scintillations for satellite signals in communications and navigation, Report-7-71, Paper at IIC Conf., Genoa, Oct., Forschungsinstitut fuer Hochfrequenzphysik, Werthoven, W. Germany, N72-27189#.

Allen, R. S. (1968), Morphology of fading of radio waves traversing the auroral ionosphere, pp. 294-315 in Ionospheric Radio Communications, K. Folkstadt, Editor, Plenum, New York.

Allen, R. S. (1969), Application of the statistics of ionospheric scintillation to VHF and UHF systems, pp. 39-53 in AGARD (1970), N70-32238#.

Allen, R. S. and J. Aarons,(1970), On the temporal variations of scintillation, in Future Applications of Satellite Beacon Experiments, Report of Air Force Cambridge Research Laboratories, Bedford, MA, N71-37885#.

Allen, R. S., J. Aarons and H. E. Whitney, (1964A), Measurements of radio star and satellite scintillations at a sub-auroral latitude, IEEE Trans. Military Electronics, MIL-8, 146-156, AD-612818.

Allen, R. S., J. Aarons and H. E. Whitney, (1964B), Measurements of radio star and satellite scintillations at a sub-auroral latitude, IEEE Trans. Antennas & Propagation, AP-12, 812-822.

Al'pert, Ja. L., V. M. Sinelnikov, L. N. Vitshas and V. I. Krajushkina, (1971), On investigations of the inhomogeneous structure of the outer ionosphere by means of coherent radio waves emitted from artificial earth satellites - II J. Atmospheric & Terrestrial Physics, 33, 1779-1787.

Anderson, R. E. (1972), A technique for synoptic measurement of ionospheric propagation delays by ranging from geostationary satellites to a network of unmanned transponders, Paper presented at the International Johannes-Kepler-Symposium on the Future Application of Satellite Beacon Measurements, 29 May - 2 June, Univ. of Graz, Austria.

Anonymous, (1969), Proc. 3rd. International Symposium on Equatorial Aeronomy, Ahmedabad, India, Feb. 3-10, Radio Science, 4, Sept., A69-42422.

Armstrong, J. W. and W. A. Coles, (1972), Analysis of three-station interplanetary scintillation, J. Geophysical Research, 77, 4602-4610.

ASTRA, (1971A), Report of the fourth meeting of the ASTRA panel, Report No. ASTRA IV-WP/45, Application of Space Techniques Relating to Aviation Panel, ICAO, Montreal, Canada.

ASTRA, (1971B), Technical considerations of factors affecting the satellite-aircraft-satellite link, Section 3 in ASTRA (1971A).

Awe, O. (1964A), Effects of errors in correlation on the analysis of the fading of radio waves, J. Atmospheric & Terrestrial Physics, 26, 1257-1271.

Bandyopadhyay, P. (1970), Measurements of total electron content at Huancayo, Peru, Planetary & Space Science, 18, 129-136.

Bandyopadhyay, P. and J. Aarons, (1970), The equatorial F layer irregularitity extent as observed from Huancayo, Peru, Radio Science, 5, (6), 931-938.

Barabanenkov, Yu. N., Yu A. Kravtvsov, S. M. Rytov and V. I. Tamarskii, (1971), Status of the theory of propagation of waves in a randomly inhomogeneous medium, Soviet Physics Uspekhi, 13, 551-680, Usp. Fiz. Nauk, 102, 3-42, (1970).

Barnla, J. D., D. H. Westwood, and O. J. Hanas, (1971), System 621B/ATS-5 signal demonstration test, Final Technical Report No. SAMSO TR 71-35 on Contract No. F04701-70-C-0281 Applied Information Industries, Moorestown, N.J.

Barton, T. H. (1965), Measurements of the strength and polarization of VHF signals from a synchronous satellite, Proc. IEEE Conf. on Aerospace and Navigational Electronics, Institute of Electrical and Electronics Engineers, Inc., New York.

Basu, S., R. L. Vesprini and E. Martin,(1973), HF and VHF oblique backscatter and scintillation, Report No. AFCRL-TR-73-0207, Contract No. F19628-71-C-0250, Emmanuel College, Boston, MA, N73-27349#.

Bates, H. F. (1971), The aspect sensitivity of spread-F irregularities, J. Atmospheric & Terrestrial Physics, 33, 111-115.

Bell Aerospace Cp. (1971), PLACE ground equipment critical design review report, Revision 1, Report No. 6225-933003, Bell Aerospace Co., Buffalo, NY.

Bello, P. A. (1970), Multipath measurement with the spinning ATS-5 satellite, unpublished report by Signatron Inc., Lexington, MA.

Bendat, J. S. and A. G. Piersol, (1971), Random Data: Analysis and Measurement Procedures, Wiley, New York.

Bent, R. B., S. K. Llewellyn and P. E. Schmid, (1971), Ionospheric refraction corrections in satellite tracking, Paper at 14th Plenary Mtg. COSPAR, Seattle, WA, June 18 - July 2, Contract No. NAS5-11730, DBA Systems, Inc., Melbourne, FL, A71-33734#.

Besprozvannaya, A. S. and L. A. Yudovich, (1971), Local foci of the anomalous midday ionization of the F2 layer in the temperate latitudes, pp. 309-323 in Zevakina and Lyakhova (1971), in Report No. NASA-TT-F-746, National Aeronautics & Space Administration, Washington, DC, N73-22331.

Beynon, W. J. G. (1969), The physics of the ionosphere, Science Progress, 57, 415-433, A70-12071#.

Bisaga, J. J., E. J. Holliman and A. Schneider, (1970), Radio frequency utilization in the bands of principal interest for aeronautical satellites, Report No. X-490-70-447, NASA Goddard Space Flight Center, Greenbelt, MD, N71-25920#.

Bischoff, K. and B. Chytil, (1969), A note on scintillation indices, Planetary & Space Sciences, 17, 1066-1069.

Blackband, W. T., Editor, (1967), Propagation Factors in Space Communications, AGARD Conf. Proc. No. 3, NATO Advisory Group for Aerospace Research and Development, Technivision, Maidenhead, England, A68-23069.

Blank, H. A. and T. S. Golden, (1972), Very High Frequency (VHF) ionospheric scintillation fading measurements at Lima, Peru, Report No. X-810-72-177, NASA/Goddard Space Flight Center, Greenbelt, MD.

Boeing, Co. (1969A), Aircraft communication/surveillance via satellite at L-band - Revised Experimental Program, Report No. D6-60119, The Boeing Co., Commercial Airplane Group, Seattle, WA.

Boeing Co. (1969B), Experimental Program - Aircraft Communications/ surveillance by a Satellite at L-band, Report No. D6-24392, The Boeing Co., Commercial Airplane Group, Seattle, WA.

Boeing Co. (1970A), Material on FAA Contract No. DOT-FA69WA-2109 on Experimental Program Aircraft Communication/Surveillance via Satellite at L-band, The Boeing Co., Commercial Airplane Group, Seattle, WA.

Boeing Co. (1970B), Multipath/ranging L-band experimental program using ATS-5, Report No. D6-60125 on Contract No. DOT FA69WA-2109, The Boeing Co., Commercial Airplane Group, Seattle, WA.

Booker, H. G. (1958), The use of radio stars to study irregular refraction of radio waves in the ionosphere, Proc. IRE, 46, 298-314.

Booker, H. G., C. M. Crain and E. C. Fields, (1970A), A panoramic view of ionospheric reflection and transmission under ambient and disturbed conditions, Report No. R-559-PR on Contract No. F44620-67-C-0045, The RAND Corp., Santa Monica, CA, AD-716679, N71-19748#.

Booker, H. G., C. M. Crain, and E. C. Field, (1970B), Transmission of electromagnetic waves through normal and disturbed ionospheres, Report No. R-558-PR on Contract No. F44620-67-C-0045, The RAND Corp., Santa Monica, CA, AD-716678, N71-19753#.

Booker, H. G. and W. E. Gordon, (1950), A theory of radio scattering in the troposphere, Proc. IRE, 38, 401-412.

Booker, H. G., J. A. Ratcliffe and D. H. Shinn, (1950), Diffraction from an irregular screen with applications to ionospheric problems, Phil. Trans. Royal Soc., (London), A242, 579-609.

Bourgois, G. (1972), Study of solar-wind using power spectrum interplanetary scintillation of radio sources, Astronomy & Astrophysics, 19, 200-ff.

Bowhill, S. A. (1961A), The scattering of radio waves by an extended randomly refracting medium, J. Atmospheric & Terrestrial Physics, 20, 9-18.

Bowhill, S. A. (1961B), Statistics of a radio wave diffracted by a random ionosphere, J. Research National Bureau of Standards, 65D, 275-292.

Bowhill, S. A. (1967), Ionosphere, pp. 498-501 in The Encyclopedia of Atmospheric Sciences and Astrogeology, R. W. Fairbridge, Editor, Reinhold, New York.

Bramley, E. N. (1951), Diversity effects in spaced aerial reception of ionospheric waves, Proc. IEEE, 98, Pt. III, 19-25.

Bramley, E. N. (1954), The diffraction of waves by an irregular refracting medium, Proc. Royal Society, A225, 515-518.

Bramley, E. N. (1967), Diffraction of an angular spectrum of waves by a phase changing screen, J. Atmospheric & Terrestrial Physics, 29, 1-28.

Bramley, E. N. and R. Ruster, (1971), The effects of electric fields and ion drag in the middle-latitude F-region, J. Atmospheric & Terrestrial Physics, 33, 269-274.

Briggs, B. H. (1958), A study of the ionospheric irregularities which cause spread-F echoes and scintillations of radio stars, J. Atmospheric & Terrestrial Physics, 12, 34-45.

Briggs, B. H. (1964), Observations of radio star scintillations and spread F echoes over a solar cycle, J. Atmospheric & Terrestrial Physics, 26, 1-23.

Briggs, B. H. and I. A. Parkin, (1963), On the variation of radio star and satellite scintillations with zenith angle, J. Atmospheric & Terrestrial Physics, 25, 339-365.

Briggs, B. H., G. J. Phillips and D. H. Shinn, (1950), Analysis of fading at spaced receivers, Proc. Royal Society, B63, 106-ff.

Britt, C. L. and P. G. Smith, (1967), Signal acquisition techniques for receiving arrays of large-aperture antennas, IEEE Trans. Aerospace Electronics. AES-3, 447-459.

Brown, D. L. (1971), Air traffic control satellite simulation experiment, pp. 144-154 in Proc. International Conf. Space and Communication: Acquisition and Transmission of Data in Space Applications Systems, Vol. 1, A71-36510.

Brown, W. E., III, G. G. Haroules and W. I. Thompson, III (1973), Experimental plan for conducting ionospheric scintillation measurements using ATS geostationary satellites at 136 and 1550 MHz, Report No. DOT-TSC-OST-72-33, DOT/Transportation Systems Center, Cambridge, MA.

Brown, W. E., III, G. G. Haroules and W. I. Thompson, III (1974), Description of a remote ionospheric scintillation data collection facility, Report No. DOT-TSC-OST-73-17, DOT/Transportation Systems Center, Cambridge, MA.

Budden, K. G. (1965), The amplitude fluctuations of the radio wave scattered from a thick ionospheric layer with weak irregularities, J. Atmospheric & Terrestrial Physics, 27, 155-172.

Budden, K. G. and B. J. Uscinski, (1972), Scintillation of extended radio-sources when receiver has a finite bandwidth, 3 Further methods, Proc. Royal Society, 330A, 65-77.

Burns, A. A. (1971), Preliminary analysis of a proposed high stability frequency standard distribution system, IEEE Trans. Aerospace & Electronic Systems, AES-7, 385-391.

Burns, A. A. and E. J. Fremouw, (1970), A real-time correction technique for transionospheric ranging error, IEEE Trans. Antennas & Propagation, AP-18, 785-790, A71-17714.

Chandra, S. and P. Stubbe, (1971), On explaining the F-region seasonal anomaly in terms of composition changes in the lower atmosphere, Planetary & Space Science, 19, 1014-1016.

Chen, A. A. and G. S. Kent, (1972), Determination of orientation of ionospheric irregularities causing scintillation of signals from earth satellites, J. Atmospheric & Terrestrial Physics, 34, 1411-ff.

Chernov, L. A. (1961), Wave Propagation in a Random Medium, Translated by R. A. Silverman, McGraw-Hill, New York.

Chernysheva, S. P., A. M. Mozhaev, V. M. Sheftel and I. K. Ryss, (1971), Sporadic formations in the F-region of the ionosphere, Geomagnetizm i Aeronomiia, 11, 338-339, A71-28555, English Translation in Geomagnetism and Aeronomy.

Chivers, H. J. A. (1960A), The simultaneous observation of radio star scintillations on different radio frequencies, J. Atmospheric & Terrestrial Physics, 17, 181-187.

Chivers, H. J. A. (1960B), Observed variations in the amplitude scintillations of the Cassiopeia, 23N5A, radio star, J. Atmospheric & Terrestrial Physics, 19, 54-64.

Chivers, H. J. A. (1963), Radio star scintillations and spread-F echoes, J. Atmospheric & Terrestrial Physics, 25, 268-273.

Chivers, H. J. A. (1971), Power spectrum of scintillations of a two-component radio source, J. Geophysical Research, 76, 2526-2530.

Chivers, H. J. A. and R. D. Davies, (1962), A comparison of radio star scintillations at 1390 MHz and 79 MHz at low elevation angles, J. Atmospheric & Terrestrial Physics, 24. 573-584.

Christiansen, R. M. (1971), Preliminary report of S-band propagation disturbance during ALSEP Mission Support, Nov. 19, 1969 - June 30, 1970, Report No. X-861-71-239, NASA Goddard Space Flight Center, Greenbelt, MD.

Chytil, B. (1967), The distribution of amplitude scintillations and the conversion of scintillation indicies, J. Atmospheric & Terrestrial Physics, 29, 1175-1177.

Clark, D. H. (1971), The latitude variation of sizes of the ionospheric irregularities producing radio-satellite scintillation, J. Atmospheric & Terrestrial Physics, 33, 1267-1272, A71-38043.

Clark, D. H., J. Mawdsley, and W. Ireland, (1970), Mid-latitude radio-satellite scintillation: The height of the irregularities, Planetary & Space Science, 18, 1785-1791.

Coates, R. J. and T. S. Golden, (1968A), Ionospheric effects on telemetry and tracking signals from orbiting spacecraft, Paper in National Telemetering Conference, pp. 43-48, A68-26984#.

Coates, R. J. and T. S. Golden, (1968B), Ionospheric effects on telemetry and tracking signals from orbiting spacecraft, Report No. NASA-TM-X-63152, NASA Goddard Space Flight Center, Greenbelt, MD, N68-20043#.

Cohen, M. H. and E. J. Gundermann, (1967), Angular diameter of 3C 279 from interplanetary scintillations, Astrophysical J., 148, L49-L51.

COSPAR, (1972), Proc. of the International Johannes-Kepler-Symp. on the Future Application of Satellite Beacon Measurements, 29 May - 2 June, Univ. Graz, Austria, Committee on Space Research of the International Council of Scientific Unions, A3004.

Craft, H. D., Jr. (1971A), Investigation of satellite link propagation anomalies at 4 and 6 GHz, Preliminary Report, Technical Memorandum CL-9-71, Comsat Laboratories, Clarksburg, MD.

Craft, H. D., Jr. (1971B), Some measurements of ionospheric scintillations at 4 and 6 GHz, Paper at Spring URSI USNC, International Union of Scientific Radio. Washington, DC, April 16-18.

Craft, H. D., Jr. (1971C), Scintillation on signals to earth stations at low elevation angles, Report No. CL-55-71, Comsat Laboratories, Clarksburg, MD.

Craft, H. D., Jr. and L. H. Westerlund, (1972), Scintillation at 4 and 6 GHz, Paper at AIAA 10th Meeting, Jan., Comsat Laboratories, Clarksburg, MD, American Institute of Astronautics and Aeronautics, New York.

Crampton, E. E., Jr. and W. B. Sessions, (1971), Experimental results of simultaneous measurement of ionospheric amplitude variations of 136 MHz and 1550 MHz signals at the geomagnetic equator, Report No. X-490-71-54, NASA Goddard Space Flight Center, Greenbelt, MD, N71-25025#.

Cummack, C. H. (1969), Perturbations in a non-linear F-region at night, J. Atmospheric & Terrestrial Physics, 31, 1107-1118, A69-38559.

Dagg, M. (1957), Diurnal variations of radio-star scintillations, Spread-F and geomagnetic activity, J. Atmospheric & Terrestrial Physics, 10, 204-214.

Danilou, A. D. (1970), Chemistry of the Ionosphere, Translated into English from the Russian, Plenum, New York.

DaRosa, A. V. (1969), Propagation errors in VHF satellite-to-aircraft ranging, IEEE Trans. Antennas & Propagation, AP-16, 628-634.

DaRosa, A. V. (1973), Recent results from satellite beacon measurements, Report No. NASA-CR-133475 on Contract No. NGR-05-020-001, Stanford Univ., Radioscience Laboratory, Stanford, CA, N73-28446#.

Davies, K. (1969), Ionospheric Radio Waves, Blaisdell, Waltham, MA.

Davies, K. (1970), Editor, Phase and Frequency Instabilities in Electromagnetic Wave Propagation, 13th NATO AGARD Symp., Ankara, Turkey, Oct. 9-12, 1967, Published by Technivision Services, Pelham, NY, A71-24185.

Deam, A. P. and B. M. Fannin, (1955), Phase difference variations in 9350 Megacycle radio signals arriving at spaced antennas, Proc. IRE, 43. 1402-1404.

DeBarber, J. P. (1961), An instrument to observe the phase and amplitude fluctuations of VHF radiations from artificial earth satellites, Ionospheric Research Scientific Report No. 151, Contract No. AF33(616)-6157, Pennsylvania State Univ., University Park, PA, AD-263442.

DeBarber, J. P. (1962), The diffraction of high frequency radio waves by irregularities in the ionosphere with emphasis on waves emanating from artificial earth satellites, Report No. 169 on Contract No. AF33(616)-6157:, Pennsylvania State Univ., University Park, PA.

DeBarber, J. P., G. E. Chisholm and W. J. Ross, (1963), The nature of the irregularities in electron density causing scintillations in satellite signals, Proc. International Conf. on the Ionosphere Imperial College, London, July 1962, A. C. Strickland, Editor, The Institute of Physics and the Physical Society, London, pp. 267-270.

de Wolf, D.A. (1965), Point-to-point wave propagation through an intermediate layer of random anisotropic irregularities, IEEE Trans. Antennas & Propagation, AP-13, 48-52.

Duncan, R. C. (1969), Satellite navigation aids, Chapter 12 in Avionics Navigation Systems, M. Kayton and W. R. Fried, Editors, Wiley, New York.

Dyson, P. L. (1969), Direct measurements of the size and amplitude of irregularities in the topside ionosphere, J. Geophysical Research, 74. 6291-6303.

Dyson, P. L. (1971A), On the significance of electrostatic probe observations of electron density irregularities, J. Geophysical Research, 76, 4689-4690.

Dyson, P. L. (1971B), Comparison of scintillation, Spread-F and electrostatic probe observations of electron density irregularities, J. Atmospheric & Terrestrial Physics, 33, 1185-1192, A71-38035.

Edenhofer, P. and D. Glesner, (1968), Description of a digital computing program evaluating the tropospheric and ionospheric angle and range errors, Report. No. DLR-MITT-68-17, Duetsche Versuchsanstalt für Luftund Raumfahrt, Oberpfaffenhofen, W. Germany, N69-14864#.

Edenhofer, P., D. Glesner and V. Stein, (1970), The influence of atmosphere on the accuracy of a satellite tracking system, pp. 29-1 to 29-11 in Symposium on Future Application of Satellite Beacon Experiments, Lindau über Northeim, W. Germany, A71-19028#.

Elkins, T. J. (1969), Summary of properties of F-region irregularities, pp. 13-37 in A Survey of Scintillation Data and its Relationship to Satellite Communication, See Aarons (1970B), N70-32237#.

Elkins, T. J. and M. D. Papagiannis, (1969), Measurement and interpretation of power spectrums of ionospheric scintillation at a sub-auroral location, J. Geophysical Research, 74, 4105-4115.

Elkins, T. J. and F. F. Slack, (1969), Observations of traveling ionospheric disturbances using stationary satellites, J. Atmospheric & Terrestrial Physics, 31, 421-439.

Evans, D. L., Compiler, (1971), Ionospheric and tropospheric limitations on radar accuracy, Report No. AFCRL-71-0169, Air Force Cambridge Research Laboratories, Bedford, MA, AD-722046, N71-28337#.

Evans, J. V. (1968), Propagation in the ionosphere, Chapter 2, Part II in Radar Astronomy, J. V. Evans and T. Hagfors, Editors, McGraw-Hill, New York.

Evans, J. V. (1970), Incoherent scatter measurements of F-region density, temperature and vertical velocity at Millstone Hill, Report No. ESD-TR-70-98, Report No. 477, MIT Lincoln Laboratory, Lexington, MA.

Evans, J. V. (1971A), Observations of F-region vertical velocities at Millstone Hill: 2. Evidence for fluxes into and out of the protonsphere, Radio Science, 6, 843-854.

Evans, J. V. (1971B), Observations of F-region vertical velocities at Millstone Hill: Evidence for drifts due to expansion, contraction, and winds, Radio Science, 6, 609-626.

Evans, J. V. (1971C), Observations of F-region vertical velocities at Millstone Hill: 3. Determination of altitude distribution of H^+, Radio Science, 6, 855-862.

Evans, J. V. (1972), Ionospheric movements by incoherent scatter: a review, J. Atmospheric & Terrestrial Physics, 34, 175-209.

Fejer, J. A. (1953), The diffraction of waves in passing through an irregular refracting medium, Proceeding of the Royal Society (London), A220, 455-471.

Fooks, G. L. (1965), Ionospheric drift measurements using correlation analysis: Methods of computation and interpretation of results, J. Atmospheric & Terrestrial Physics, 27, 979-989.

Forsyth, P. A. (1970), Amplitude, phase and angle-of-arrival fluctuations, in AGARD Application of Propagation Data to VHF Satellite Communication and Navigation Systems, NATO Advisory Group for Aerospace Research & Development, Paris, France, N71-16230#.

Forsyth, P. A. and K. V. Paulson, (1961), Radio star scintillations and the auroral zone, Canadian J. Physics, 39, 502-509.

Fremouw, E. J. (1966), Aberrations of VHF-UHF signals traversing the auroral ionosphere, Report No. UAG R-181, Univ. of Alaska, College, AK.

Fremouw, E. J. (1967), Effects of ionospheric irregularities on space data acquisition in the auroral zone, pp. 225-239 in Blackband (1967), A68-23082.

Fremouw, E. J. (1972), A planned polar-orbiting wideband beacon, pp 1-8 in Leitinger (1972), A73-13627#.

Fremouw, E. J. and H. F. Bates, (1971), Worldwide behavior of average VHF-UHF scintillation, Radio Science, 6, 863-869.

Fremouw, E. J. and C. L. Rino, (1971), Development of a worldwide model for F-layer produced scintillation, Final Report on Contract No. NAS5-21551, Stanford Research Institude, Menlo Park, CA.

Frihagen, J. (1963), Study of fine scale ionospheric structure by satellite techniques, in Radio Astronomical and Satellite Studies of the Atmosphere, J. Aarons, Editor, North-Holland Publishing Co., Amsterdam.

Frihagen, J. (1971), Occurrence of high latitude ionospheric irregularities giving rise to ionospheric scintillation, J. Atmospheric & Terrestrial Physics, 33, 21-30.

Frost, A. D. and R. R. Clark, (1969), A radio interferometer for ionospheric scintillation observations at 136 MHz, pp. 89-92 in AFCRL, (1969), Univ. of New Hampshire, Durham, NH.

Garriott, O. K., F. L. Smith, III and P. C. Yuen, (1965), Observations of ionospheric electron content using a geostationary satellite, Planetary & Space Research, 13, 829-838.

General Electric, (1969A), ATS ranging and position fixing experiment, 25 Nov. 1968 - 25 Aug. 1969, Quarterly Progress Report No. NASA-CR-100732 on Contract No. NAS5-11634, General Electric Co., Research & Development Center, Schenectady, NY, N69-24053#.

General Electric, (1969B), VHF ranging and position fixing experiment using ATS satellites, Interim Report 25 Nov. 1968 - 9 Oct. 1969, Contract No. NAS5-11634, General Electric Co., Research & Development Center, Schenectady, NY, N70-21688#.

General Electric, (1969C), Second Quarterly Report for ATS ranging and position fixing experiment, Report No. S-69-1101 on Contract No. NAS5-11634, General Electric Co., Research & Development Center, Schenectady, NY.

General Electric, (1971A), VHF ranging and position fixing experiment using ATS satellites, Executive Summary of Final Report on Phases 1 and 2 on Contract No. NAS5-11634, General Electric Co., Corporate Research & Development, Schenectady, NY.

General Electric, (1971B), ATS ranging and position fixing experiments, Progress Report No. NASA-CR-118648 on Contract No. NAS5-11634, General Electric Co., Corporate Research & Development, Schenectady, NY, N71-26713#.

General Electric, (1971C), Final Report on Phases 1 and 2 VHF ranging and position fixing experiment using ATS satellites, 25 Nov. 1968 - 1 May 1971, Contract No. NAS-11634, General Electric Co., Corporate Research & Development, Schenectady, NY.

General Electric Co. (1973A), Final Report on Phase 3 ATS ranging and position fixing experiment, Report No. SRD-73-062 on Contract No. NAS5-11634, General Electric Co., Corporate Research & Development, Schenectady, NY.

General Electric Co. (1973B), Operating Manual L-Band/VHF Transponder, Report No. GEI-45108 on Contract No. NAS5-11634, General Electric Co., Corporate Research & Development, Schenectady, NY.

Gentle, K. W. (1972), Plasma turbulence - theories and experiments, Radio Science, 7, 799-808.

Golden, T. S. (1968), Ionospheric distortion of minitrack signals in South America, Report No. NASA-TM-X-63136, NASA Goddard Space Flight Center, Greenbelt, MD, N68-19383#.

Golden, T. S. (1969), A note on correlation distance of the equatorial ionosphere, Paper at Symposium, See AFCRL (1969), NASA Goddard Space Flight Center, Greenbelt, MD, A71-11307#.

Golden, T. S. (1970A), A note on correlation distance of VHF fading from irregularities in the equatorial ionosphere, Radio Science, 5, 943-947, (See Golden, 1969).

Golden, T. S. (1970B), A note on equatorial ionospheric scintillation at 136 MHz and 1550 MHz, Report No. X-520-70-397, NASA Goddard Space Flight Center, Greenbelt, MD.

Golden, T. S. (1970C), Amplitude effects of the auroral ionosphere on satellite telemetry at 136 and 1700 MHz, Report No. X-520-70-109, NASA Goddard Space Flight Center, Greenbelt, MD.

Golden, T. S. (1971), A brief review of ionospheric scintillation fading effects as observed in NASA Satellite Tracking and Data Acquisition Networks, Report No. X-810-71-402, NASA Goddard Space Flight Center, Greenbelt, MD.

Golden, T. S. (1972), A brief review of ionospheric scintillation fading effects as observed in NASA satellite tracking and data acquisition networks, AIAA Paper No. 72-220 at AIAA 10th Aerospace Sciences Mtg., American Institute of Aeronautics & Astronautics, New York.

Golden, T. S. and E. A. Wolff; Editors, (1973), Scintillation Advisory Panel Workshop Report, June 15, 1973, NASA/Goddard Space Flight Center, Greenbelt, MD, Unpublished Report.

Goncharov, L. P. and A. I. Kudrevsky, (1972), The equatorial anomaly in the ionosphere layer F2 by the data of vertical sounding above the Pacific in the years of the low solar activity, Geomagnitism & Aeronomy, No. 2.

Gopal Rao, M. S. V. and R. Sambasiva Rao, (1969), The hysteresis variation in F-2 layer parameters, J. Atmospheric & Terrestrial Physics, 31, 1119-1125, A69-38560#.

Guier, W. H. and G. C. Weiffenbach, (1960), A satellite Doppler navigation system, Proc. IRE, 48, 506-ff.

Hajkowicz, L. A. (1972A), Wavelike structure of magnetic field-aligned irregularities detected by phase interferometry, Canadian J. Physics, 50, 2654-2661.

Hajkowicz, L. A. (1972B), Distribution of ionospheric irregularities causing scintillation in satellite beacon transmissions, Nature, Physical Sciences, 238, 132-134.

Hanas, O. J., M. E. Illikainen, D. L. Kratzer and E. A. Spaans, (1970), L-band ATS-5/Orion/S. S. Manhattan marine navigation and communication experiment, Final Report No. NASA-CR-109877 on Contract No. NAS12-2260, Applied Information Industries, Moorestown, NJ, N70-34300#, with an Appendix.

Hanson, W. B. and S. Sanatani, (1971), Relationship between Fe plus ions and equatorial spread F, J. Geophysical Research, 76, 7761-7768.

Hargreaves, J. K. (1970), ATS-F: observational opportunities, in Future Applications of Satellite Beacon Experiments, Dept. of Environmental Sciences, Lancaster Univ., England, N71-37898#.

Harmon, L. (1970), Worldwide VHF satellite scintillations/fading tests, Report. No. X-460-70-127, NASA Goddard Space Flight Center, Greenbelt, MD.

Hartmann, G. (1970), Low angle fluctuation, in AGARD (1970), N71-16231#.

Hartmann, G. K. (1972), Brief review of scintillation studies, pp. 1221-1228 in Space Research XII, Proc. 14th Plenary Mtg., Seattle, Washington, June 18-July 2, 1971, Vol. 2, Akademie-Verlag GmbH, Berlin, E. Germany, A73-12300#.

Herman, J. R. (1966), Spread-F and ionospheric irregularities, Reviews of Geophysics, 4, 255-299.

Hewish, A. (1951), The diffraction of radio waves in passing through a phase-changing ionosphere, Proc. Royal Society, A209, 81-96.

Hewish, A. (1952), The diffraction of galactic radio waves as a method of investigating the irregular structure of the ionosphere, Proc. Royal Society, 214, 494-514.

Hewish, A. and L. T. Little, (1967), Comments on interplanetary scintillations, 2, Observations, Astrophysical J., 150, L195-L197.

Hey, J. S., S. J. Parsons, and J. W. Phillips, (1946), Fluctuations in cosmic radiation at radio frequencies, Nature, 158, 234.

Hines, C. O. (1959), Motions in the ionosphere, Proc. IRE, 47, 176-186.

Hirschmann, E. (1967), Tropospheric and ionospheric effects upon radio frequency, VHF-SHF, Communications, Report No. X-731-67-89, NASA Goddard Space Flight Center, Greenbelt, MD, N67-19054#.

Hoffman, W. C., Editor, (1960), Statistical Methods in Radio Wave Propagation, Pergamon, New York

Huang, Y-N and C-Y Yeh, (1970), On the occurrence of Spread-F and the geomagnetic activity over Taipei, Taiwan, J. Atmospheric & Terrestrial Physics, 32, 1765-1772.

Hunter, A. N. (1969), Faraday rotation of the 136 MHz transmission from the geostationary satellite Canary Bird observed at Nairobi, in Anonymous, (1969), Radio Science, 4, 811-816, A69-42433.

Hutton, P. F. and D. K. Leichtman, (1971), A test program for defining scintillation fading characteristics at 400 MHz, Report No. MITRE WP-3722, The MITRE Corp., Bedford, MA.

Ichimaru, A. (1969), Fluctuations of a beam propagating through a locally homogeneous medium, Radio Science, 4, 295-306.

IEE, (1973), Satellite Systems for Mobile Communications and Surveillance, 13-15 March, IEE Conference Publication No. 95, Institute of Electrical Engineers, London.

James, P. W. (1962), The correlation analysis of the fading of radio signals received from satellites, J. Atmospheric & Terrestrial Physics, 24, 237-244.

Jenkins, G. M. and D. G. Watts, (1968), Spectral Analysis and its Applications, Holden-Day, San Francisco, CA.

Jespersen, J. L. (1967), Topside spread-F and satellite radio scintillations, AGARD Conf. Proc. No. 3, See Blackband, (1969), A68-23080.

Jespersen, J. L. and G. Kamas, (1963), Satellite scintillation observations at Boulder, Colorado. NBS Report 7915, DOC National Bureau of Standards, Boulder, CO, June.

Jaspersen, J. L. and G. Kamas, (1964), Satellite scintillation observations at Boulder, Colorado, J. Atmospheric & Terrestrial Physics, 26, 457-473.

Johnson, A. L. (1972), Equatorial ionospheric scintillation flight test, Report No. AFAL-TR-72-363, AFAL/Wright-Patterson Air Force Base, OH.

Johnson, A. L., R. C. Beach and T. A. Grizinski, (1973), UHF/SHF ionospheric scintillation test, Report No. AAI TM-73-6, USAF/AFSC/Wright-Patterson Air Force Base, OH.

Joint Satellite Studies Group, (1965), A synoptic study of scintillations of ionospheric origin in satellite signals, Planetary & Space Science, 13, 51-62.

Jones, I. L. (1960), Future observations of radio star scintillation, J. Atmospheric & Terrestrial Physics, 10, 26-36.

Kaminski, H. and W. Rueskamp, (1969), Studies of the ionosphere using transmissions from active synchronous satellites, Final Report No. ATCRB-70-0203 on Contract No. F61052-68-C-0054, Bochum Observatory, W. Germany, AD-703740; N70-31691#.

Kelleher, R. F. (1966), Some statistical properties of the ground diffraction patterns of vertically reflected radio waves, J. Atmospheric & Terrestrial Physics, 28, 213-223.

Kelleher, R. F. and N. J. Skinner, (1971), Studies of F region irregularities at Nairobi II - by direct backscatter at 27.8 MHz, Annales de Geophysique, 27, 195-200.

Kelley, M. C. (1972), Relationship between turbulence and spread-F, J. Geophysical Research, Letters, 77, 1327.

Kent, G. S. (1959), High frequency fading observed on the 40 MHz wave radiated from artificial satellite 1957a, J. Atmospheric & Terrestrial Physics, 16, 10-20.

Kent, G. S. (1961), High frequency fading of the 108 MHz wave radiated from an artificial earth satellite as observed at an equatorial station, J. Atmospheric & Terrestrial Physics, 22, 255-269.

Kent, G. S. and A. B. Gupta, (1971), Small fluctuations in the F-region critical frequency observed at Delhi, India, J. Atmospheric & Terrestrial Physics, 33, 281-284.

Kent, G. S. and J. R. Koster, (1966A), Some studies of nighttime F layer irregularities at the equator using very high frequency signals radiated from earth satellites, pp. 333-356 in Newman, 1966, A67-30290.

Kent, G. S. and J. R. Koster, (1966B), Some studies of nighttime F layer irregularities at the equator using very high frequency signals radiated from earth satellites, Annales de Geophysique, 22, Fasc. 3, 405-417, A67-12828.

Kent, G. S. and R. W. H. Wright, (1968), Movements of ionospheric irregularities and atmospheric winds, J. Atmospheric & Terrestrial Physics, 30, 657-691.

Kersley, L., D. B. Jenking and K. J. Edwards, (1972), Relative movements of mid-latitude trough and scintillation boundary, Nature, Physical Science, 239, 11-ff.

Kieburtz, R. B. (1967), A critique of angle-of-arrival measurements by the phase difference method, IEEE Trans. Antennas & Propagation, AP-15, 584-585.

King, G. A. M. (1970), Spread-F on ionograms, J. Atmospheric & Terrestrial Physics, 32, 209-222, See 33, p. 111 for comments.

King, G. A. M. (1971), The ionospheric F-region storms, J. Atmospheric & Terrestrial Physics, 33, 1223-1240.

Kissel, F. J. (1970), L-band performance characteristics of the ATS-5 spacecraft, Report No. X-731-70-51, NASA Goddard Space Flight Center, Greenbelt, MD, N70-30423#.

Klass, P. J. (1971), Aerosat specifications delineated, Aviation Week & Space Technology, Oct. 11, pp. 53, 54, 57.

Klein, P. I. (1969), Propagation factors in radio-interferometer navigation satellite systems, pp. 27-30 in AFCRL, (1969), Comsat Corp., Washington, DC, A70-12567#.

Klobuchar, J. A. (1970), World wide morphology of total electron content, in AGARD, (1970), N71-16235#.

Ko, H. C. (1959), Radio star scintillation at 915 MHz, Report No. 12, Final Report on Contract No. AF 19(604)-1591, Ohio State Univ., Columbus, OH.

Ko, H. C. (1960), Amplitude scintillation of radio star at ultra-high frequency, Proc. IRE, 48, 1871-1880.

Koster, J. R. (1963), Some measurements of the irregularity giving rise to radio star scintillation at the equator, J. Geophysical Research, 68, 2579-2590.

Koster, J. R. (1967), Studies of the equatorial ionosphere using transmissions from active satellites, Final Scientific Report No. AFCRL-68-0020 on Contract No. AF 61 (052)-800, Univ. Ghana, Dept. of Physics, Legon, AD-664902, N68-20088#.

Koster, J. R. (1968A), Equatorial scintillations at Legon - A Summary Report of the Joint Satellites Studies Group, JSSG Report No. 3, Contract No. F61052-67-C-0088, Report No. AFCRL-68-0260, Univ. Ghana, Dept. of Physics, Legon.

Koster, J. R. (1968B), Equatorial studies of the VHF signal radiated by Intelsat II, F-3, 1: Ionospheric scintillation, Report No. AFCRL-69-0006 on Contract No. F61052-67-C-0027, Univ. Ghana, Dept. of Physics, Legon, AD-681462, N69-21782#.

Koster, J. R. (1969), Equatorial scintillation, pp. 68-73 in AFCRL, (1969).

Koster, J. R., I. Katsriku and M. Tete, (1966), Studies of the equatorial ionosphere using transmissions from active satellites, Annual Summary Report, 1 Feb. 1964 - 31 Jan. 1966, Report No. AFCRL-66-814, Univ. of Ghana, Dept. of Physics, Legon, AD-650722, N67-28634.

Koster, J. R., W. L. Korfker and D. Yeboah-Amankwah, (1970), Studies of equatorial ionospheric phenomena using transmissions from active satellites, Final Scientific Report No. AFCRL-70-0603 on Contract No. F61052-67-C-0027, Univ. Ghana, Dept. of Physics, Legon, AD-719872, N71-25627#.

Koster, J. R. and R. W. Wright, (1960), Scintillation, spread F and transequatorial scatter, J. Geophysical Research, 65, 2303-2306.

Kuegler, G. K. (1969), Equatorial scintillations experienced during Apollo 11 support July 12 to July 24, 1969, Report No. X-460-69-534, NASA Goddard Space Flight Center, Greenbelt, MD, N70-30830#.

Kuegler, G. K. (1970), Equatorial scintillations experienced during Apollo 13 support Mar. 30 to April 18, 1970, Report No. X-460-70-240, Contract No. NAS 5-21129, NASA Goddard Space Flight Center, Greenbelt, ND, N70-36584#.

Lansinger, J. M. (1966), High latitude radio star scintillation measurements at 68 MHz made with a phase sweep interferometer system, Radio Science, 1, (New Series), 1176-ff.

Lansinger, J. M. (1967), Auroral zone radio star scintillation measurements and interpretations, pp. 241-260 in Blackband (1967), A68-23083.

Lawrence, R. S., J. L. Jesperson and R. C. Lamb, (1961), Amplitude and angular scintillations of the radio source Cygnus-A observed at Boulder, Colorado, J. Research National Bureau of Standards, 65D, 333-350.

Lawrence, R. S., C. G. Little and H. J. A. Chivers, (1964), A survey of ionospheric effects upon earth-space radio propagation, Proc. IEEE, 52, 4-27.

Leadabrand, R. L., A. G. Larson and J.C. Hodges, (1967), Preliminary results on the wavelength dependence and aspect sensitivity of radar auroral echoes between 50 and 3000 MHz, J. Geophysical Research, 72, 3877-3887.

Leichtman, D.K. (1971), Scintillation margins for UHF satellite links, MITRE WP-4081, The MITRE Corp., Bedford, MA.

Leitinger, R., Editor, (1972), Symposium on the Future Application of Satellite Beacon Measurements, May 29-June 2, 1972, Graz Univ., Graz, Austria, A73-13626.

Levatich, J. L. and T. J. Geli, (1967), Scintillation of INTELSAT 1 VHF satellite signals, Report No. Tech. Memo SDA-10-67, COMSAT Corp., Washington, DC.

Liszka, L. (1963), A study of ionospheric irregularities using satellite transmissions at 54 MHz, Arkiv för Geofysik, 4, 227-246.

Little, C. G. (1951), Diffraction theory of the scintillations of stars on optical and radio wavelengths, Monthly Notices of the Royal Astronomical Society, 111, 289-302.

Little, C.G. and A.C.B. Lovell, (1950), Origin of the fluctuations in the intensity of radio waves from galactic sources, Nature, 165, 423-424.

Little, C. G., G. C. Reid, E. Stiltner and R. P. Merritt, (1962), An experimental investigation of the scintillation of radio stars observed at frequencies of 223 and 456 MHz from a location close to the auroral zone, J. Geophysical Research, 67, 1763-1784.

Liu, C. H. (1966), Cross-correlation functions of spherical waves propagating through a slab containing anisotropic irregularities, J. Atmospheric & Terrestrial Physics, 28, 385-395, A66-27398.

Liu, C. H. and K. C. Yeh, (1966), Gradient instabilities as possible causes of irregularities in the ionosphere, Radio Science, 1, (New Series), 1283-1291, A67-67002#.

Liu, C. H. and K. C. Yeh, (1970), Effects of ionospheric irregularities on stabilities of wave amplitude and phase in space communication, pp. 535-544 in Phase and Frequency Instabilities in Electromagnetic Wave Propagation, K. Davies, Editor, AGARD Conf. Proc. No. 33, NATO Advisory Group for Aerospace Research & Development, N71-22941#.

Lovelace, R. V. E. (1970), Theory and analysis of interplanetary scintillations, Ph.D. Thesis, Cornell Univ., Ithaca, NY, Univ. Microfilms Order No. 71-14, 651.

Lovelace, R. V. E., E. E. Salpeter, L. E. Sharp and D. E. Harris, (1970), Analysis of observations of interplanetary scintillations, Astrophysical J., 159, 1047-1056.

Lyon, J. A., N. J. Skinner and R. W. H. Wright, (1961), Equatorial spread F at Ibadan, Nigeria, J. Atmospheric & Terrestrial Physics, 21, 100-119.

Mallinckrodt, A. J. (1971), Ionospheric scintillation, Interoffice, Memo. Correspondence No. 8300.3.5-50, TRW Systems Group, Redondo Beach, CA.

Matheson, D. N. and L. T. Little, (1971), Radio scintillations due to plasma irregularities with power law spectra: the interplanetary medium. Planetary & Space Science, 19, 1615-1624.

Maynard, L. A. and D. L. Selin, (1971), Simultaneous measurements of ionospheric fading at 254 and 1550 MHz, to be submitted to ASTRA (1971A).

McClure, J. P. (1964A), The height of scintillation-producing irregularities in temperature latitudes, J. Geophysical Research. 69, 2775-2780.

McClure, J. P. (1964B), Polarization measurements during scintillation of radio signals from satellites, J. Geophysical Research, 69, 1445-1447.

McClure, J. P., D. T. Farley, Jr. and R. Cohen, (1970), Ionospheric electron concentration measurements at the magnetic equator, 1964-1966, Report No. ESSA-TR-ERL-186-AL-4, ESSA Research Laboratories, Boulder, CO, N71-29311#.

McClure, J. P. and G. W. Swenson, (1964), Beacon satellite studies of small scale ionospheric inhomogeneities, Report of Dept. of Elec. Engineering, Engineering Experiment Station, Univ. Illinois.

McClure, J. P. and R. F. Woodman, (1972), Radar observations of equatorial Spread F in a region of electrostatic turbulence, J. Geophysical Research, 77, (28), 5617-5621.

Mercier, R. P. (1962), Diffraction by a screen causing large random phase fluctuations, Proc. Cambridge Phil. Society, 58, 382-400.

Meyer-Arendt, J. R. and C. B. Emmanual (1965), Optical scintillation; A survey of the literature, NBS Technical Note 225, National Bureau of Standards, Boulder, CO, AD-614056, Reviewed in Applied Optics, 6, 872.

Michelini, R. D. and M. D. Grossi, (1971), VLBI observations of radio emissions from geostationary satellites, Paper on Contract No. NSR-09-015-079, Paper at 14th Plenary Mtg. COSPAR, Seattle, WA, June 18 - July 2, Smithsonian Astrophysical Observatory, Cambridge, MA, A71-33845#.

Michelini, R. D. and M. D. Grossi, (1972), Very long baseline interferometry observations of radio emissions from geostationary satellites, Space Research XII, pp. 517-525, Academie-Verlag GmbH, Berlin, E. Germany, A73-12270#.

Mikkelsen, I. S. (1971), Knee to total electron content and scintillation boundary, in Geophysical Papers No. R-21, Contract No. F61052-69-C-00119, Danish Meteorological Inst., Geophysics Section, Charlottenlund, N71-33830#.

Mikkelsen, I. S. (1972), Ionospheric research using satellites, Interim Scientific Report 1 Nov. 1971-31 Oct. 1972, Report No. AFCRL-TR-73-0083, Danish Meteorological Inst., Copenhagen, Denmark. N73-23490#.

Millman, G. H. (1967), A survey of tropospheric, ionospheric and extraterrestrial effects on radio propagation between the earth and space vehicles, in Blackband (1967), A68-23070.

Millman, G. H. (1971), Tropospheric effects on space communications, in Tropospheric Radio Wave Propagation, NATO AGARD Conf. Proc. No. AGARD-CP-70-71-Pt-1, General Electric Co., Syracuse, NY, N71-21413#.

Millman, G. H. and R. E. Anderson, (1968), Ionospheric phase fluctuations of satellite transmissions, J. Geophysical Research, 73, 4434-4438, A68-36653#.

Millman, G. H. and R. E. Anderson, (1970), Ionospheric phase fluctuations of satellite transmissions, pp. 545-560 in Davies (1970), General Electric Co., Syracuse, NY, N71-22942.

Millman, G. H., C. D. Bell and R. L. Lietzke, (1969), An analysis of tropospheric and ionospheric refraction effects at mid-latitudes, General Electric Technical Information Series Report No. R69EMH1, General Electric Co., Syracuse, NY.

Millman, G. H. and A. J. Moceyunas, (1965), Observations of ionospheric scintillations by ultra high frequency radar reflections from earth satellites, J. Geophysical Research, 70, 81-88.

Millman, G. H. A. J. Moceyunas, (1966), Observations of ionospheric scintillations by ultra high frequency radar reflections from earth's satellites, in Newman, (1966), N67-29302, A67-30292.

Mitra, S. N. (1949), A radio method of measuring winds in the ionosphere, Proc. IEE, 96, Pt. III, 441-446.

Moorcroft, D. R. and P. A. Forsyth, (1963), On the relation between radio star scintillations and auroral and magnetic activity, J. Geophysical Research, 68, 117-124.

Muchmore, R. B. and A. D. Wheelon, (1955), Line-of-sight propagation phenomena - I Ray treatment, Proc. IRE, 43, 1437-1449.

Muchmore, R. B. and A. D. Wheelon, (1963), Frequency correlation of line-of-sight scintillations, IEEE, Trans. Antennas & Propagation, AP-11, 46-51.

Mueller, E. J. (1970A), Absorption effects on VHF propagation between synchronous satellite and aircraft, Summary Report No. NASA-TM-X-65507, NASA Goddard Space Flight Center, Greenbelt, MD, N71-24914#.

Mueller, E. J. (1970B), Scintillation, polarization and multipath effects on VHF propagation between synchronous satellites and aircraft, Report No. X-490-71-45, NASA Goddard Space Flight Center, Greenbelt, MD.

Mueller, E. J. (1971), Aeronautical satellite system characteristics and propagation factors through 1971, Report No. NASA-TM-X-65511, NASA Goddard Space Flight Center, Greenbelt, MD, N71-24942#.

Mullaney, H. W. (1972), Anomalies and irregularities in the mid-latitude ionosphere, Ph.D. Thesis, Boston Univ., Boston, MA, N73-22270.

Mullen, J. P. (1969), VHF atmospheric studies and communications and navigation systems, pp. 1-3 in AGARD, (1970), N70-32235#.

Mullen, J. P. (1973), Sensitivity of equatorial scintillation to magnetic activity, J. Atmospheric and Terrestrial Physics, In print.

Poularikas, A. D. and T. S. Golden, (1968), A note on the effects of the ionosphere on satellite orbital corrections in near-real time, Report No. X-520-68-366, NASA/Goddard Space Flight Center, Greenbelt, MD.

Poularikas, A. D. and T. S. Golden, (1969), A note on the effects of the ionosphere on satellite orbital corrections in near-real time, IEEE Trans. Aerospace & Electronic Syst., AES-5, 865-867, A69-42549.

Preddey, G. F. (1969), Mid-latitude radio satellite scintillation-the variation with latitude, Planetary & Space Science, 17, 1557-1561, A69-39972.

Preston, R. A., R. Ergas, H. F. Hinteregger, C. A. Knight, D. S. Robertson, I. I. Shapiro, A. R. Whitney, A. E. E. Rogers and T. A. Clark, (1972), Interferometric observations of an artificial satellite, Science, 178, 407-409.

Rafael, M. L. (1969A), Amplitude and phase scintillation of high frequency satellite signals due to ionospheric inhomogeneities, Report No. NASA-CR-106913, on Grant No. NGR-39-009-002, Ionosphere Research Laboratory, Pennsylvania State Univ., University Park, N71-11911#.

Rafael, M. L. (1969B), Amplitude and phase scintillation of high frequency satellite signals due to ionospheric inhomogeneities, Ph.D. Thesis, Pennsylvania State Univ., University Park, N71-36563, Univ. Microfilms Order No. 70-19452.

Rangaswamy, S. and P. E. Schmid, (1971), Measurement of total electron content with a geostationary satellite during the solar eclipse of March 7, 1970. Radio Science, Aug.

Rao, N. N., M. Youakim and K. C. Yeh, (1971), Feasibility study of correction for the excess time delay of transionospheric navigational ranging systems, Report No. SAMSO-TR-71-163 on Contract No. F04701-70-C-0234, Ionospheric Radio Lab., Univ. Illinois, Urbana, AD-729797.

Ratcliffe, J. A. (1956), Some aspects of diffraction theory and their application to the ionosphere, Reports on Progress in Physics, XIX, 188-267, The Physical Society, London, England.

Ratcliffe, J. A. and J. L. Pawsey, (1933), A study of the intensity variations of downcoming wireless waves, Proc. Cambridge Phil. Soc., 29, 301-ff.

Rishbeth, H. and O. K. Garriott, (1969), Introduction to Ionospheric Physics, Academic, New York, Reviewed in Science, 12 June 1970, p. 1336, Also in J. Atmospheric & Terrestrial Physics, 33, p. 301 by S. A. Bowhill.

Rishbeth, H. and D. M. Kelley, (1971), Maps of the vertical F-layer drifts caused by horizontal winds at mid-latitudes, J. Atmospheric & Terrestrial Physics, 33, 539-545, A71-27793.

Rufenach, C. L. (1971A), A radio scintillation method of estimating the small-scale structure in the ionosphere, J. Atmospheric & Terrestrial Physics, 33, 1941-1951.

Rufenach, C. L. (1971B), Radio scintillation observations in the ionosphere and interplanetary medium, Ph.D. Thesis, Dept. of Electrical Engineering, Univ. Colorado, Boulder, Univ. Microfilms Order No. 71-25-870.

Rufenach, C. L. (1972A), Application of satellite radio beacons for measurement of small-scale ionospheric irregularities, Proc. of Symp. on the Future Applications of Satellite Beacon Experiments, Graz, Austria, 29 May - 2 June, NOAA Space Environment Laboratory, Boulder, CO.

Rufenach, C. L. (1972B), A power-law wavenumber spectrum deduced from ionospheric scintillation observations, J. Geophysical Research, 77, 4761-4772.

Ruster, R. (1971), The relative effects of electric fields and atmospheric composition changes on the electron concentration in the mid-latitude F-layer, J. Atmospheric & Terrestrial Physics, 33, 275-280.

Sadobnikova, R. S. (1968), High altitude velocity distribution of ionospheric drift and strength of the electric field in the F2 layer, pp. 186-192 in Isayev, (1968), N71-30091#.

Sailors, D. B. (1970), Effects of scintillation on synchronous satellite communication at 250 MHz, Report No. NELC-TR-1744, Naval Electronics Laboratory Center, San Diego, CA.

Salpeter, E. E. (1967), Interplanetary scintillations: I Theory, Astrophysical J., 147, 433-447.

Schachne, S. H. (1970), Scintillation of Intelsat II F-3 VHF signal, Tech. Memorandum SED-7-70, COMSAT Corp., Washington, DC.

Sessions, W. B. (1972), Amplitude fading of simultaneous trans-ionospheric L-band and VHF signals received at the geomagnetic equator, Report No. X-810-72-282, NASA/Goddard Space Flight Center, Greenbelt, MD.

Sinclair, J. and R. F. Kelleher, (1969), The F-region equatorial irregularity belt as observed from scintillation of satellite transmissions, J. Atmospheric & Terrestrial Physics, 31, 201-206.

Singleton, D. G. (1968A), The occurrence of scintillation-producing irregularities over Australasia, Report No. WRE-TN-APD-14, Weapons Research Establishment, Salisbury, S. Australia, AD-864532.

Singleton, D. G. (1969), The occurrence of scintillation-producing irregularities over Australasia, J. Geophysical Research, 74, 1772-1785.

Singleton, D. G. (1970A), The effect of irregularity shape on radio star and satellite scintillations, J. Atmospheric & Terrestrial Physics, 32, 315-344.

Singleton, D. G. (1970B), Saturation and focusing effects in radio-star and satellite scintillations, J. Atmospheric & Terrestrial Physics, 32, 187-208.

Singleton, D. G. (1970C), Dependence of satellite scintillations on zenith angle and azimuth, J. Atmospheric & Terrestrial Physics, 32, 789-803.

Sire, A. Sh. and V. S. Agalakov, (1971), Variations of the height of the F2 region maximum and temperature in the equatorial latitude, Geomagnetism & Aeronomy, No. 5.

Skinner, N. J. and R. F. Kelleher, (1971), Studies of F-region irregularities at Nairobi I from Spread-F on ionograms, 1964-1970, Annales de Geophysique, 27, 181-194.

Skinner, N. J., R. F. Kelleher, J. B. Hacking and C. W. Benson, (1971), Scintillation fading of signals in the SHF band, Nature, Physical Science, 232, July 5, 19-21, A71-34624.

Slack, F. F. (1967), Scintillation studies using the Early Bird synchronous satellite 136 MHz signal, Report No. AFCRL-67-0655, Air Force Cambridge Research Laboratories, Bedford, MA, AD-665852, N68-20656#.

Slack, F. F. (1968), The ringing irregularities in ionospheric scintillation Report No. AFCRL-68-263, Air Force Cambridge Research Laboratories, Bedford, MA.

Slack, F. F. (1972), Quasiperiodic scintillation in the ionosphere, J. Atmospheric & Terrestrial Physics, 34, 927-939.

Smith, F. G. (1950), Origin of the fluctuations in the intensity of radio waves from galactic sources, Nature, 165, 422-423.

Smith, F. L., III, (1971), Electron content measurements and F-region modeling applied to ionospheric parameter determination, Report No. AFCRL-71-0083, Contract No. F19628-70-C-0035, Dept. of Electrical Engineering, Colorado State Univ., Fort Collins, AD-722042, N71-28426#.

Smith, P. G. (1967A), Atmospheric distortion of signals originating from space sources, IEEE Trans. Aerospace & Electronic Systems, AES-3, 207-216.

Smith, P. G. (1967B), Phase compensation for widely-spaced antenna systems employing coherent signal combinations, IEEE Trans. Aerospace & Electronic Systems, AES-3, 91-106.

Spencer, M. (1955), The shape of irregularities in the upper atmosphere, Proc. Physical Soc., 68B, 493-503.

Sprenger, K. and R. Schminder, (1969), On some relationships between correllation analysis and similar-fade analysis results of drift measurements in the lower ionosphere, J. Atmospheric & Terrestrial Physics, 31, 1085-1098, A69-38557.

Sterling, D. L. (1972), A study of the equatorial F sub 2 region ionosphere, Ph.D. Thesis, Southern Methodist Univ., Dallas, TX, N73-22268.

Strobel, D. F. and M. B. McElroy, (1970), The F-2 layer at middle latitudes, Planetary & Space Science, 18, 1181-1202.

Stuart, G. F. (1972), Characteristics of abrupt scintillation boundary, J. Atmospheric & Terrestrial Physics, 34, 1455-ff.

Tao, K. (1965), Worldwide maps of the occurrence percentage of spread F in years of high and low sunspot numbers, J. Radio Research Lab., 12, 317-ff.

Tatarski, V. I. (1961), Wave Propagation in a Turbulent Medium, McGraw-Hill, New York, Reprinted by Dover, New York.

Taur, R. R. (1973), Ionospheric scintillation at 4 and 6 GHz, COMSAT Technical Review, 3, (1), 145-ff.

Taylor, H. A. (1971), Observed solar geomagnetic control of the ionosphere: implications for reference ionospheres, Report No. NASA-TM-X-65568, NASA Goddard Space Flight Center, Greenbelt, MD, N71-27671#.

Taylor, L. S. (1972), Scintillation of randomized electromagnetic fields, J. Mathematical Physics, 13, 590-595.

Terry, R., B. J. Flaherty and R. E. DuBroff, (1972), A very high frequency radio interferometer for investigating ionospheric disturbances using geostationary satellites, Determination of changes in exospheric electron Content by a comparison of group delay and Faraday rotation, Report No. NASA-CR-127270, Grant No. NGR-14-005-002, Univ. Illinois, Urbana, N72-27345#.

Thomas, J. O. (1959), The distribution of electrons in the ionosphere, Proc. IRE, 47, 162-175.

Tisnado, G. R., R. Woodman and J. Pomalaza, (1970), Statistical study of equatorial scintillations at Ancon. Peru, Internal Report, Instituto Geofisico del Peru, Ancon.

Titheridge, J. E. (1969), On the field alignment of small ionospheric irregularities, J. Atmospheric & Terrestrial Physics, 31, 1439-1444.

Titheridge, J. E. (1971), The diffraction of satellite signals by isolated ionospheric irregularities, J. Atmospheric & Terrestrial Physics, 33, 47-69, A71-244363.

Unger, J. H. W. (1970), Bibliography on atmospheric effects in electromagnetic wave propagation and related subjects, Issue #1, Bell Telephone Laboratories, Propagation Studies Group, Whippany, NJ.

Unger, J. H. W. (1971), Atmospheric effects bibliography, #2, Bell Telephone Laboratories, Propagation Studies Group, Whippany, NJ.

Univ. of Illinois, (1971), Feasibility study for correcting for the excess time delay of transionospheric navigational ranging signals, Report No. SAMSO-TR-71-163 on Contract No. F04701-70-C-0234, Univ. of Illinois, Urbana, AD-729797.

Valley, S. L., Editor, (1965), Handbook of Geophysics and Space Environments, McGraw-Hill, New York, Ch. 17 revision N69-32597#.

Verniani, F., Editor, (1971), Physics of the Upper Atmosphere, Proc. of a Course, 1970, Editrice Compositori International Physics Series, Editrice Compositori, Bologna.

Vestine, E. H. (1947), The geomagnetic field, its description and analysis, Publication No. 580, Carnegie Institution of Washington, Washington, DC.

Vila, P. (1971A), Intertropical F2 ionization during June and July 1966 Radio Science, 6, 689-697, A71-37863.

Vila, P. (1971B), New dynamic aspects of intertropical F2 ionization, Radio Science, Oct. 6, 945-956.

Voelk, H. J. and G. Haerendel. (1970), Striation in ionospheric ion clouds, Part 1, Report No. MPI-PAE/Extraterr-50, Max-Planck-Institut fur Physik und Astrophysik, Munich, W. Germany, N71-31439#.

Voronin, A. L. (1964), Refraction of VHF/UHF waves in the ionosphere, Geomag. & Aeron., 4, 421-426.

Wagner, L. S. (1962), Zenith angle dependence of radio star scintillation, J. Geophysical Research, 67, 4187-4194.

Waldman, H. I. and A. V. DaRosa, (1971), Prognostication of ionospheric electron content, Report No. SAMSO-TR-71-82 on Contract No. F04701-70-C-0233, Stanford Univ., Stanford, CA, AD-731095; AD-731096.

Warwick, J. W. (1964), Radio-star scintillations from ionospheric waves, Radio Science, J. Research NBS, 68D, 179-188.

Weidner, D. K., C. L. Hasseltine and R. E. Smith, (1969), Models of earth's atmosphere, 120 - 1000 km, NASA Space Vehicle Design Criteria (Environment), Report No. NASA SP-8021, NASA Marshall Space Flight Center, Huntsville, AL, N70-12847#.

Wernik, A. W., C. H. Liu, M. Y. Youakim and K. C. Yeh, (1973), A theoretical study of scintillation of transionospheric radio signals, Report No. 50 on Contract No. NGR 14-005-189, Ionosphere Radio Lab., Univ. Illinois, Urbana.

Wernlein, C. E. (1970), A 1540 to 1660 MHz propagation between geostationary satellites and aircraft, Summary Report No. NASA-TM-X-65508, NASA Goddard Space Flight Center, Greenbelt, MD, N71-24913#.

Wheelon, A. D. (1955), Near field corrections to line-of-sight propagation, Proc. IRE, 43, 1459-1466.

Wheelon, A. D. (1959), Radio wave scattering by tropospheric irregularities, J. Res. NBS, Radio Science, 63D, 205-233.

Wheelon, A. D. and R. B. Muchmore, (1955), Line-of-sight propagation phenomena II, Scattered components, Proc. IRE, 43, 1450-1458.

Whitney, H. E. (1969), The definition of scintillation index and its use for characterizing ionospheric effects, pp. 3-11, in Aarons (1970B). N70-3236#.

Whitney, H. E., J. Aarons and D. R. Seemann, (1971), Estimation of the cumulative amplitude probability distribution function of ionospheric scintillations, Report No. AFCRL-71-0525, Air Force Cambridge Research Laboratories, Bedford, MA, AD-736405, N72-22159#.

Whitney, H. E., C. Malik and J. Aarons, (1969), A proposed index for measuring ionospheric scintillation, Planetary & Space Science, 17, 1069-1073.

Whitney, H. E. and W. F. Ring, (1971), Dependency of scintillation fading of oppositely polarized signals, IEEE Trans. Antennas & Propagation, AP-19, 151, Author's reply on p. 152, A71-23522.

Whitten, R. C. and I. G. Poppoff, (1971), Fundamentals of Aeronomy, Wiley, New York.

Wild, J. P. and J. A. Roberts, (1956), The spectrum of radio-star scintillations and the nature of irregularities in the ionosphere, J. Atmospheric & Terrestrial Physics, 8, 55-75.

Wishna, S. (1971), NASA Balloon-aircraft ranging data and voice experiment, Report No. X-752-71-212, NASA Goddard Space Flight Center, Greenbelt, MD.

Yeh, K. C. (1962), Propagation of spherical waves through an ionosphere containing anisotropic irregularities, J. Res. NBS, Radio Propagation, 66D, 621-636.

Yeh, K. C. and C. H. Liu, (1967), Wave propagation in a random medium with anisotropic background, IEEE Trans. Antennas & Propagation, AP-15, 539-542.

Yeh, K. C. and C. H. Liu, (1972A), Propagation and application of waves in the ionosphere, Reviews of Geophysics and Space Physics, 19, 631-709.

Yeh, K. C. and C. H. Liu, (1972B), Theory of Ionospheric Waves, Academic, New York.

Yeh, K. C., D. Simonich, J. Mawdsley and G. F. Preddy, (1968), Scintillation observations at medium latitude geomagnetically conjugate stations, Radio Science, 3, (New Series), 690-697.

Yeh, K. C. and G. W. Swenson, Jr. (1959), The scintillation of radio signals from satellites, J. Geophysical Research, 64, 2281-2286.

Yeh, K. C. and G. W. Swenson, Jr., (1964), F-region irregularities studied by scintillation of signals from satellites, J. Res. NBS, Radio Science, 68D, 881-894.

Yokoi, H., M. Yamada and T. Satoh, (1970A), Attenuation and scintillation of microwaves originating from space sources, Electronics & Communications in Japan, 53, No. 5, pp. 73-81, A71-29390.

Yokoi, H., M. Yamada and T. Satoh, (1970B), Atmospheric attenuation and scintillation of microwaves from outer space, Publications of the Astronomical Society of Japan, 22, 511-524, A71-21421#.

Yoneyama, T. and Y. Mushiake, (1965), Scintillation fading in line-of-sight propagation through a statistically anisotropic turbulent medium, IEEE Trans. Antennas & Propagation AP-13, 476-477.

Yonezawa, T. (1971), The solar-activity and latitudinal characteristics of the seasonal, non-seasonal and semi-annual variations in the peak electron densities of the F2 layer at noon and at midnight in middle and low latitudes, J. Atmospheric & Terrestrial Physics, 33, 889-907.

Zevakina, R. A. and L. N. Lyakhova; Editors, (1971), Ionosphere Disturbances and their Influences on Radio Communications, English Translation of the Russian book, Report No. NASA-TT-F-746, National Aeronautics & Space Administration, Washington, DC, N73-22314#.

APPENDIX A: COORDINATE SYSTEMS FOR IDENTIFYING A POINT ON OR ABOVE EARTH'S SURFACE

A.1 GEOGRAPHIC COORDINATE SYSTEM

Geographic coordinates are coordinates defining a point on the surface of the earth, usually by latitude and longitude. Terrestrial latitude is angular distance from the equator, measured northward or southward through 90° and labeled N or S to indicate the direction of measurement. Terrestrial longitude is the arc of a parallel, or the angle at the pole, between the prime meridian and the meridian of a point on the earth, measured eastward or westward from the prime meridian through 180°, and labeled E or W to indicate the direction of measurement.

Examples of geographic coordinate systems are given in Figures A-1 and A-2.

A.2 GEOMAGNETIC COORDINATE SYSTEM

The geomagnetic coordinate system is a system of spherical coordinates based on the best fit of a centered dipole to the actual magnetic field of the earth. Figure A-1 is a view of the geomagnetic coordinates. The geomagnetic latitudes, with an idealized dipole having its north pole near Thule, Greenland, fail to represent the trajectory of energetic particles and from comparisons of observations at various sites, also fail to represent high-latitude scintillation observations (Allen, 1965; Aarons, Whitney, and Allen, 1971).

A.3 INVARIANT-LATITUDE COORDINATE SYSTEM

The coordinates of the invariant latitude system utilize a dipole field corrected by higher order terms which are obtained by earth's magnetic field. A figure showing the invariant latitude coordinate system for Epoch 1969.75 is presented in Figure A-2. This figure came from ASTRA (1971). Invariant coordinate systems are also discussed by Aarons, Whitney and Allen (1971).

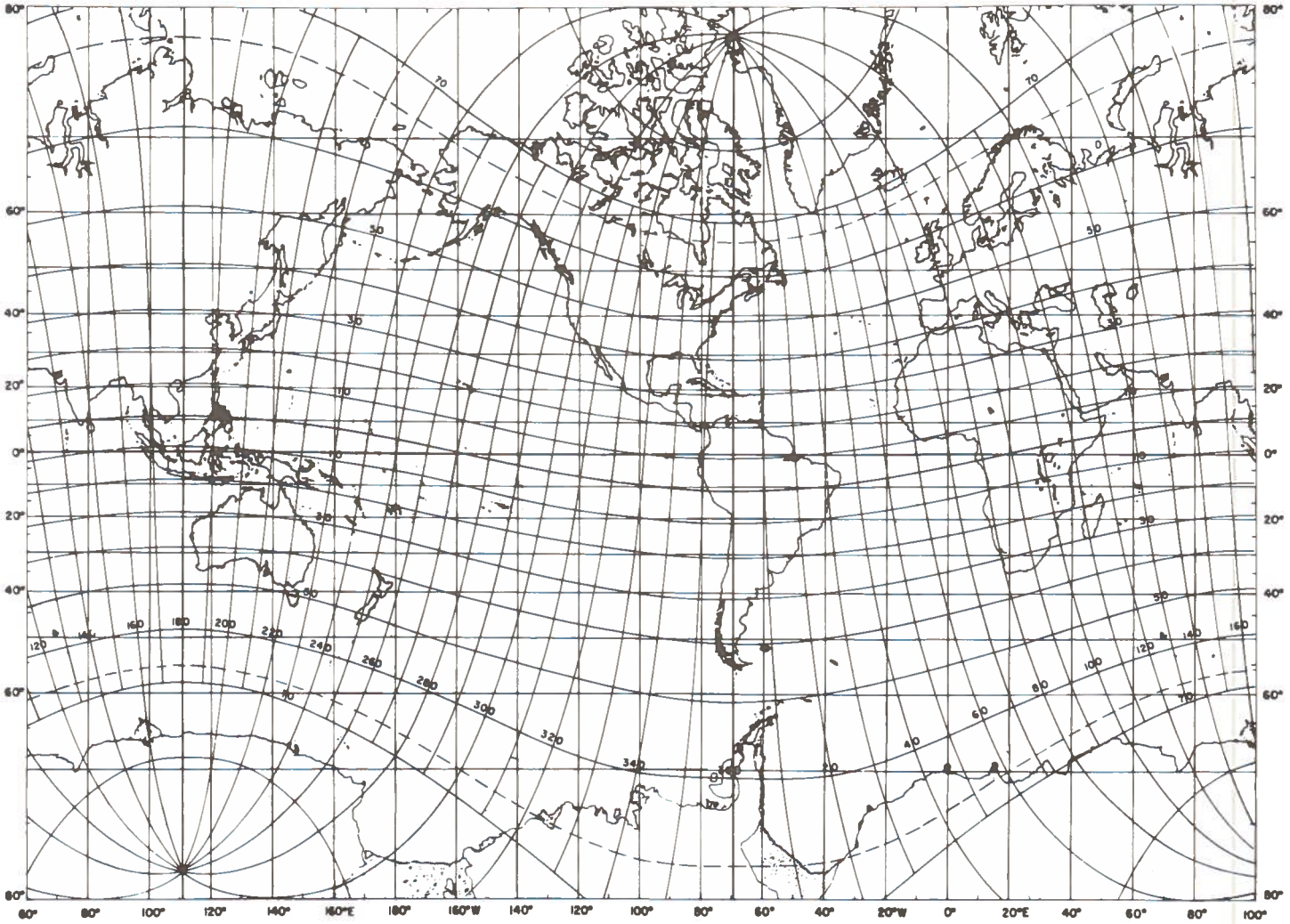

Figure A-1. Geomagnetic Coordinates (Centered Dipole Field) Superimposed on Geographic Mercator Projection, from Chernosky, Fougere, and Hutchinson (1965), After Vestine (1947)

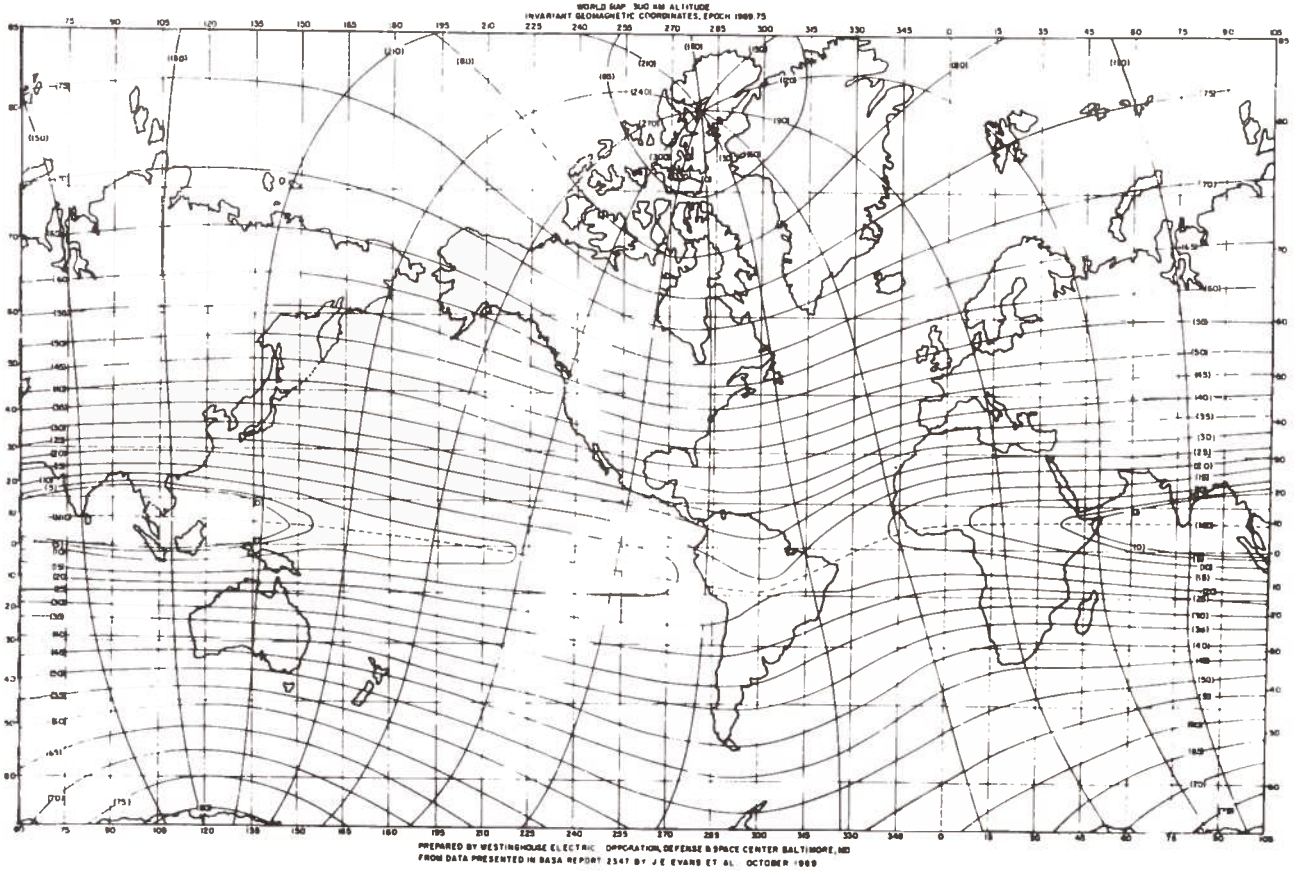

Figure A-2. World Map, 300 km-Altitude, Invariant Coordinate System (Epoch, 1969.75)

A.4 SUMMARY

Invariant latitudes at a standard height of 350 km seem to best order the observations of scintillations. Geomagnetic latitudes, however, are still used on occassion because of the vast amount of material analyzed in this simpler coordinate system; geomagnetic coordinates are a good first approximation to most of the data. (Aarons, Whitney and Allen, 1971).

A.5 REFERENCES

Aarons, J., H. E. Whitney, and R. S. Allen, (1971), Global morphology of ionospheric scintillations, Proc. IEEE, 59, 159-172.

Allen, W. H. Editor, (1965), Dictionary of Technical Terms for Aerospace Use, First Edition, Report No. NASA SP-7, NASA Scientific and Technical Information Division, Washington, DC, (SOD).

ASTRA, (1971) Report of the Fourth Meeting of the ATSRA Panel, Report No. ASTRA IV-WP/45, Application of Space Techniques Relating to Aviation Panel, ICAO, Montreal, Canada.

Chernosky, E. J., P. F. Fougere, and R. O. Hutchinson, (1965), The geomagnetic field, Chapter 11 in Handbook of Geophysics and Space Environments, S. L. Valley, Editor, McGraw-Hill, New York.

Vestine, E. H. (1947), The geomagnetic field, its description and analysis, Publication No. 580, Carnegie Institution of Washington, Washington, DC.

APPENDIX B: INFORMATION ON NASA ATS-5, AND F SATELLITES*

The ATS-5 synchronous satellite, which is spinning, produces a return signal beam which sweeps across the Earth every 783 milliseconds. A signal reception window of approximately 50 milliseconds is available with each rotation.

The visibility of the ATS-5 satellite and the proposed ATS-F satellite can be determined by consulting Figure B-1 which was taken from Clausen, Lerner, Rupp, and Winter (1970). The contours of equal elevation angle are plotted on a geographic grid of the earth. More detailed orbit information can be obtained from the ATS Project Office at NASA Goddard Space Flight Center in Greenbelt, Maryland.

The L-band performance characteristics of the ATS-5 satellite are discussed in great length by Kissel (1970). He considers the parameters affecting propagation measurements such as: orbit geometry, polarization loss, off-beam center allowance, measurement techniques, earth station antenna pointing and earth station noise temperature.

The communications subsystems for the ATS-F and G satellites are considered in detail by Sabelhaus (1971). Various opportunities to use the ATS-F satellites on ionospheric research are considered by Hargreaves (1970) and Schmidt (1970).

B.1 REFERENCES

Clausen, E., T. Lerner, E. Rupp, and H. Winter, (1970) PLACE Final Report, Report No. 6225-95002 on Contract No. NAS 5-21101, Bell Aerospace Co., Buffalo, NY.

Hargreaves, J. K. (1970), ATS-F: observational opportunities, in Future Applications of Satellite Beacon Expt., Dept. of Environmental Sciences, Lancaster Unit., England, N71-37898#.

Kissel, F. J. (1970), L-band performance characteristics of the ATS-5 spacecraft, Report No. X-731-70-51, NASA Goddard Space Flight Center, Greenbelt, MD, N70-30423#.

*Note added in proof. The ATS-F was launched on May 30, 1974 and became ATS-6. See details in Aviation Week and Space Technology (May 27, 1974, pp. 38-42 and photo on cover), (June 10, 1974, p. 14).

Sabelhaus, A. B. (1971), Applications Technology Satellites F and G communications subsystems, Proc. IEEE, 59, 206-212.

Schmidt, G. (1970), Proposal for a receiving equipment suitable for radio signals of the geostationary satellite ATS-F for a determination of the total electron content of the ionosphere, in Future Applications of Satellite Beacon Expt., Max-Planck-Institut fur Aeronomie, Lindau Uber Northeim, W. Germany, N71-37914#.

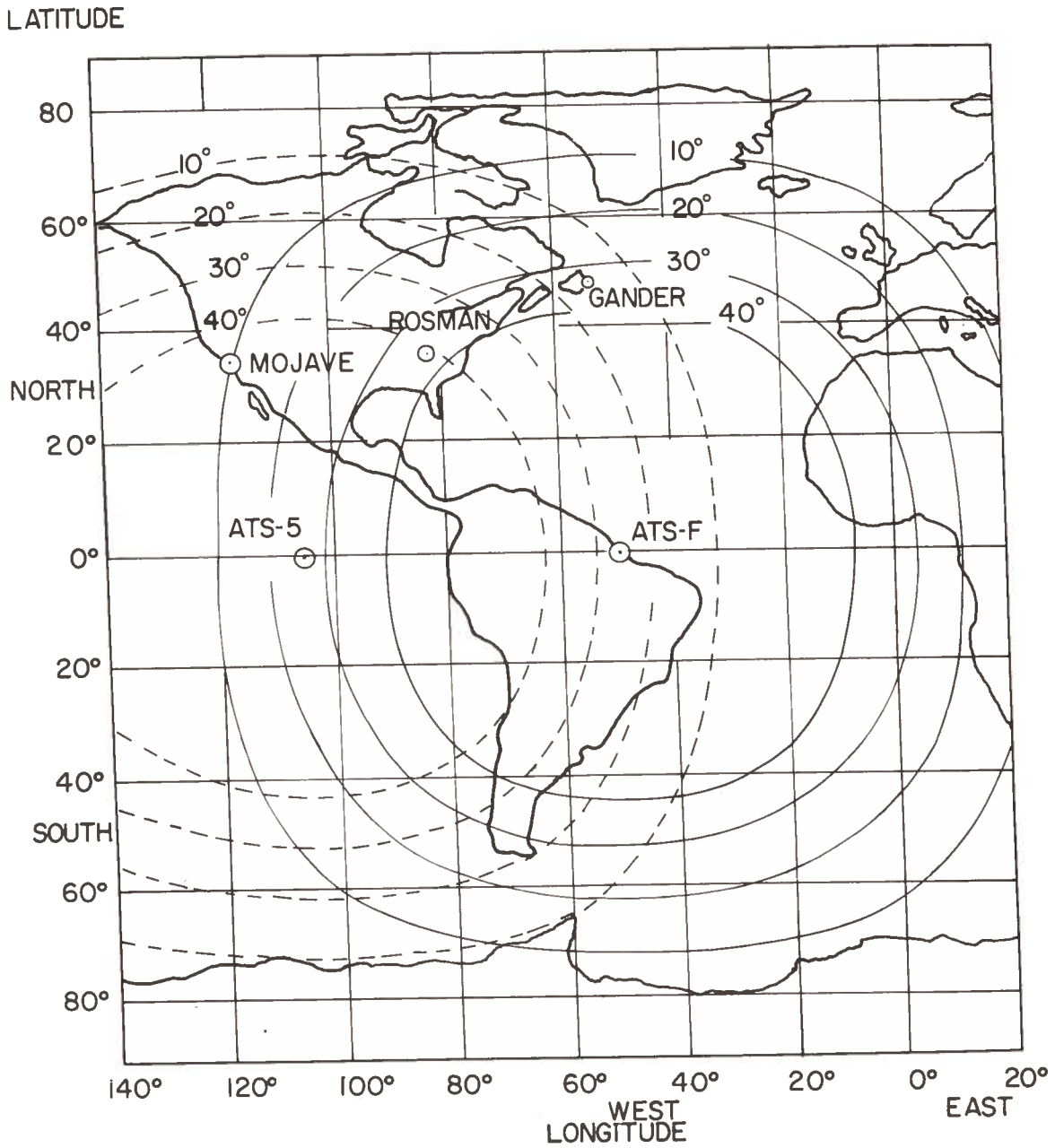

Figure B-1. Visibility Plot of ATS-5 and Proposed ATS-F Satellites. Contours are Lines of Equal Elevation Angle. After Clausen, Lerner, Rupp, and Winter, (1970).

APPENDIX C: DISCUSSION OF RELEVANT STATISTICAL INFORMATION

C.1 PROBABILITY DENSITY FUNCTION

The probability density function for random data describes the probability that the data will assume a value within some defined range at any instant of time. Consider the sample time history record x(t) illustrated in Figure C-1. The probability that x(t) assumes a value within the range x and (x +Δx) may be

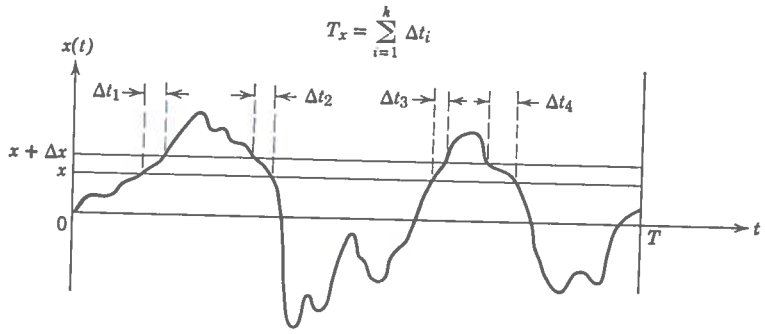

Figure C-1. Probability Measurement

obtained by taking the ratio of T_x/T, where T_x is the total amount of time that x(t) falls inside the range (x, x + Δx) during an observation time T. This ratio will approach an exact probability description as T approaches infinity. In equation form,

$$\text{Prob}\left[x < x(t) \leq x \pm \Delta x\right] = \lim_{T\to\infty} \frac{T_x}{T} \qquad \text{(C-1)}$$

For small Δx, a first-order probability density function p(x) can be defined as follows,

$$\text{Prob}\left[x < x(t) \leq x + \Delta x\right] \approx p(x)\Delta x \qquad \text{(C-2)}$$

More precisely,

$$p(x) = \lim_{\Delta x \to 0} \frac{\text{Prob}[x < x(t) < x+\Delta x]}{x} \lim_{\Delta x \to 0} \lim_{T \to \infty} \frac{1}{T}\left(\frac{T_x}{\Delta x}\right) \qquad \text{(C-3)}$$

The probability density function p(x) is always a real-valued, non-negative function. The above came from Bendat and Piersol (1966).

C.2 PROBABILITY DISTRIBUTION FUNCTION

The probability that the instanteous value x(t) is less than or equal to some value x is defined by P(x), which is equal to the integral of the probability density function from minus infinity to x. This function P(x) is known as the probability distribution function, and should not be confused with the probability density function p(x). Specifically

$$P(x) = \text{Prob}\ [x(t) \leq x] = \int_{-\infty}^{x} p(\xi)d\xi \qquad \text{(C-4)}$$

The distribution function P(x) is bounded by zero and one, since the probability of x(t) being less than $-\infty$ is clearly zero while the probability of x(t) being $+\infty$ is unity (a certainty). The probability that x(t) falls inside any range (x_1, x_2) is given by

$$P(x_2) - P(x_1) = \text{Prob}\left[x_1 < x(t) \leq x_2\right] = \int_{x_1}^{x_2} p(x)\ dx \qquad \text{(C-5)}$$

C.3 SCINTILLATION INDEXES

Many workers have used signals from radio stars and satellites to record on strip charts the changes in amplitude known as scintillations. A scintillation index (S.I.) can indicate the depth of scintillation. Various indexes are described by Briggs and Parkin (1963) and by Bischoff and Chytil (1969). These indexes

vary as to whether the mean or rms value of the amplitude or power of the signal is used to indicate the fluctuations.

The Air Force Cambridge Research Laboratories (AFCRL) and the Joint Satellite Studies Group (JSSG) have adopted a standard method of measurement for ionospheric studies (Whitney, Malik, and Aarons, 1969). The aim of the studies was to describe the morphology of the irregularity structure. Therefore, a simple method had to be utilized to reduce the strip charts. The index adopted is defined as:

$$S.I.\ (\%) = \frac{P_{max} - P_{min}}{P_{max} + P_{min}} \times 100 \qquad (C\text{-}6)$$

where P_{max} is the third peak down from the maximum and P_{min} is the third minimum up from the lowest excursion in the given sample period. Various methods for estimating cumulative probability distributions of ionospheric scintillations are discussed in Aarons, Whitney and Allen (1971) and Whitney, Aarons and Seemann (1971) and Fremouw and Bates (1971). Basically, the AFCRL method utilizes both analog and digital recordings of the same phenomena. From this data standard curves are derived from which to estimate other scintillation data.

C.4 CHANNEL-DELAY SPREAD FUNCTION, $S(\tau)$

Two second order statistics of the received signal amplitude that are of particular importance in characterizing the effects of ionospheric scintillation on the received signal are the channel delay spread functions, $S(\tau)$, also known as the autocorrelation of the signal, and the channel Doppler spread function, $S(f)$, also known as a spectrum plot.

The quantity $S(\tau)$, the channel delay spread function, is a plot of received signal power as a function of the propagation time regardless of its spectral distribution. The multipath spread L which is a measure of the width of $S(\tau)$ and defined as

$$L = \left[\int S^2(\tau)\, d\tau\right]^{-1} , \qquad (C\text{-}7)$$

provides a rough measure of the spread in propagation times of the channel. This function is further described in Green (1968) and CSC (1971).

C.5 CHANNEL-DOPPLER SPREAD FUNCTION, S(f)

The analogous quantity S(f), the channel Doppler spread function, is a plot of received signal power as a function of frequency, regardless of the propagation time of arrival. The Doppler spread B, which is a measure of the width of S(f) and defined as

$$B = \left[\int S^2(f)\, df\right]^{-1} , \qquad (C\text{-}8)$$

provides a rough measure of the frequency interval over which the Doppler shifts of the ionospheric irregularities are spread. This index is further described along with measurement techniques in Green, (1968) and in CSC (1971).

C.6 BIBLIOGRAPHY

Aarons, J., H. E. Whitney, and R. S. Allen, (1971), Global morphology of ionospheric scintillations, Proc. IEEE, 59, 159-172.

Bendat, J. S. and A. G. Piersol, (1966), Measurement and Analysis of Random Data, Wiley, New York.

Bishoff, K. and B. Chytil, (1969), A note on scintillation indicies. Planetary and Space Sciences, 17, 1066-1069.

Briggs, B. H. and I. A. Parkin, (1963), On the variation of radio star and satellite scintillations with zenith angle, J. Atmospheric & Terrestrial Physics, 25, 339-365.

CSC, (1971), An L-band ionospheric scintillation experiment using ATS-G, Report No. 1-2651, Computer Sciences Corp., Falls Church, VA.

Fremouw, E. J. and H. F. Bates, (1971), Worldwide behavior of average VHF-UHF scintillation, Radio Science, 6, 863-869.

Green, P. E., Jr. (1968), Radar Measurements of target scattering properties, Chapter 1 in Radar Astronomy, J. V. Evans and T. Hagfors, Editors, McCraw-Hill, New York.

Whitney, H. E., J. Aarons, and D. R. Seemann, (1971), Estimation of the cumulative amplitude probability distribution function of ionospheric scintillations, Report No. AFCRL-71-0525, Air Force Cambridge Research Laboratories, Bedford, MA.

Whitney, H. E., C. Malik, and J. Aarons, (1969), A proposed index for measuring ionospheric scintillation, Planetary and Space Science, 17, 1069-1073.